universität wien

DISSERTATION

Titel der Dissertation

Effect of the Mycotoxins Beauvericin and Enniatin on Bone under Physiological and Malignant Conditions

angestrebter akademischer Grad

Doktor/in der Naturwissenschaften (Dr. rer.nat.)

Verfasserin / Verfasser:	Mag. Flora Tedjiotsop Feudjio
Matrikel-Number	0648175
Dissertationsgebiet (lt. Studienblatt):	Pharmazie
Betreuerin / Betreuer:	Univ.-Prof. Dr. Oskar Hoffmann

Wien, am 02. Juli 2010

To

my husband and daughter Arouna Ndassa and Awa Nafissa Ndassa,

for your unyielding love, patience and support.

You waited for me all these long years I was away,

so find in this work the fruit of our sacrifices.

Acknowledgements

Holly God, You have always guided my steps, showing me the right way, backing me up and making the best out of the possibilities on my hand. I am deeply thankful.

I am grateful to the Austrian government through the North-South Dialogue Scholarship Program of the Austrian Development Corporation for the financial support. Particularly, I would like to thank Katharina Engels and Elke Stinnig for their assistance during visa application, their moral support and valuable advices.

Univ.-Prof. Dr. Oskar Hoffmann, You offered me the great opportunity to join your group, you facilitated my admission process at the University of Vienna, you cared for me like a father would have, you taught me bone biology and improved my knowledge on computer… More importantly, you supervised this work from the generation of data to the production of the manuscript. I wonder sometimes what I did to deserve such luck and sincerely, I am so very grateful.

Prof. Albert Samé-Ekobo, You facilitated my scholarship application process. Your simplicity, availability and kindness touched me.

Joseph Nguemo and Joseph Le Doux Diffo, you showed me the opportunity to complete a PhD in Austria, not to mention your moral support and availability when I needed you. I am very thankful.

Mum and dad, although you have always been limited with financial possibilities, you taught me that success is possible if one works really hard, you convinced me that there is always a solution to anything, you have always been by my side all along the hard journey and I am so very proud to call myself your daughter.

The enlarged Tedjiotsop circle, I name Mirabelle Tedjiotsop, Jean Nzobou, Kériane Kengni, Sonita Makou, Marie Solange Ngouné, Ange Princesse Donfack, … We have always been together in good and bad days; we have come a very long way. This work is the proof of perseveration and a pattern to follow.

Barbara Berger, Peter Höflich, Barbara Stelzmüller, Waheed Shabbir (Pakistan), Gowri Shankar (India), Parasto Hazemi (Iran), Francesco Ringresi (Italy), Christina Fleg (Spain) Wiltrud Lang, Daniel Danninger, Michael Schnattinger, Babak Ghadiri (Iran), Karin Kirschner and Gerard Angerer. You created a friendly environment favorable to research. You are very easygoing people and that made me feel home.

Dr. Paul Yillia (Sierra Leone), Dr. Rose Ngobelnoun (Cameroon), Anna Agabani (Sudan), Razieh Karimi (Iran), Urska Derganc (Slovenia), Fida Shafi (Palestine), Sadaf Yacub (Pakistan) and Maria Sahar (Pakistan). I would have been lost in Vienna without you. We have shared our cultural differences and through our interesting discussions, I have visited all the corners of the world. You made it easy to cope here far from home and I thank you very much for your kindness.

To my best friends Aimée Teutchou, Blaise Dongmo, Cendrine Yanou, Vedette Dongmo and Samuel Zombou, for these difficult moments we have gone through, and for never forgetting who we are and where we come from.

To all others, who far or close have contributed to this work.

Abstract

Beauvericin (BEA) and enniatins (ENN) are structurally related cyclohexadepsipeptides produced by *Fusarium* that are known to contaminate food and feed. There is compelling evidence that fungal toxins may influence development and activity of osteoclasts (OC) and consequently, may be useful for the treatment of osteoporosis and bone tumors. Thus, this study aimed to characterize pharmacological and toxicological activities of BEA and ENN on bone cells (osteoblasts and osteoclasts), as well as on metastatic (MDA-MB-231 and PC3) and non metastatic (U2OS) cancer cell lines.

BEA inhibited bone resorption by disrupting the resorbing organelle (actin ring) of OC, while ENN did not affect the actin ring structure and inhibited bone resorption directly by reducing the number of TRAP-positive OC. Moreover, BEA did not affect cell viability of mature OC, but induced apoptosis in pre-fusion OC, likely by mechanisms involving ERK1/2 phosphorylation. Interestingly, ENN inhibited OC viability in a Src/Akt dependent manner and induced signal transduction pathways similar to PP2, a reference Src inhibitor. These data suggest that BEA and ENN differentially regulate OC life span and activity.

Inhibition of cell growth, cell viability and induction of apoptosis was observed in MDA-MB-231, PC3 and U2OS. BEA and ENN similarly affected the metastatic (MDA-MB-231 and PC3) and non metastatic cell viability (U2OS), as early as 24 h, with a significant effect observed already at 5 μM drug. Both inhibitors more potently induced apoptosis after 24 h in metastatic cells compared to non metastatic, with ENN being more potent compared to BEA. We studied the signaling pathways leading to proliferation, survival, apoptosis and motility. Interestingly, the metastatic profile did not seem to confer any selective advantage for the effects of both inhibitors at the molecular level. Indeed, while the p38 MAPK pathway remained continuously activated in all cell lines, BEA and ENN inactivated ERK in MDA-MB-231 as opposed to its upregulation in PC3 and U2OS. Moreover, BEA was able to induce PARP cleavage in all cell lines, whereas ENN did so only in PC3. Finally, E-cadherin was upregulated in all cell lines following BEA or ENN treatment.

These data demonstrate the antiresorptive and antitumoral activities of BEA and ENN, and their therapeutic potential in the treatment of OC-induced bone loss, bone cancer and skeletal metastases.

Kurzfassung

Beauvericin (BEA) und Enniatine (ENN) sind strukturell verwandte, sekundäre Metabolite (Cyclohexadepsipeptide) von Fusarium und als Kontamination von Nahrungs-und Futtermitteln beschrieben. Basierend auf Publikationen, daß strukturell verwandte Mykotoxine die Differenzierung und Funktion von Osteoklasten beeinflussen können, stellte sich die Frage, ob diese Substanzklasse zur Behandlung von Knochenerkrankungen eingesetzt gezogen werden kann. Ziel dieser Arbeit war es daher, die pharmakologische und toxikologische Wirkung von BEA und ENN auf Knochenzellen - Osteoblasten und Osteoklasten- und Tumore, die selektiv in den Knochen metastasieren bzw. Knochentumore entwickeln, zu untersuchen. BEA hemmte die Knochenresorption durch eine Zerstörung des Resorptionsapparates des Osteoklasten, des Aktinrings. Im Gegensatz dazu beeinflußte ENN die Struktur des Aktinringes nicht und hemmte die Knochenresorption über eine Verminderung der Differenzierung von Vorstufen zu reifen Osteoklasten. BEA zeigte keinen toxischen Einfluss auf reife Osteoklasten, induzierte jedoch Apoptose bei Osteoklastenvorläufern über Mechanismen, die auf erhöhter Phosphorylierung von ERK1/2 basieren. Im Gegensatz dazu reduzierte ENN die Viabilität von Osteoklasten, dies erfolgte über einen Src/Akt-abhängigen Mechanismus, die ausgelösten Modulation der Signaltransduktionswege waren ähnlich der Wirkung von PP2, einem Standardinhibitor der Src-Kinase. BEA und ENN hemmen somit über unterschiedliche Mechanismen die Lebensspanne und Aktivität von Osteklasten. Anschließend wurde die Wirkung von BEA und ENN auf das Wachstum, Zellviabilität und Apoptoseinduktion von knochenspezifischen Tumortypen untersucht. BEA und ENN hemmten die Viabilität metastasierender Tumorzelllinien (MDA-MB-231 für Mamacarcinom und PC3 für Prostatacarcinom) und nicht metastasierende Tumorzellen (U2OS) in der Konzentration von 5 µM bereits innerhalb von 24 h. Bei längerer Einwirkzeit war die Induktion der Apoptose bei metastasierenden Tumorzellen stärker als bei nicht metastasierenden Zellen, wobei ENN potenter als BEA war. Zur weiteren Charakterisierung wurde die Wirkung der beiden Mykotoxine auf die wichtigsten Signaltransduktionswege von Zellproliferation und Apoptose untersucht. Hier zeigte sich, daß der p38 MAPK-Signaltransduktionsweg in allen Zelllinien aktiviert wurde, der ERK-Weg war in MDA-MB-231 inaktiviert und in PC3- und U2OS-Zellen stimuliert. BEA stimulierte die Spaltung des Apoptosemarker-Enzyms bei allen Zelltypen, ENN hingegen nur bei PC3.

E-Cadherin, einem Marker für Zelladhäsion wurde in allen Zelllinien durch BEA und ENN stimuliert.

In dieser Arbeit konnten die die antiresorptiven und antitumoralen Effekte von BEA und ENN beschrieben und charakterisiert werden, die Ergebnisse zeigen ihr Potential in der Therapie von osteolytischen Knochenerkrankungen, wie Osteoporose, sowie Knochentumore und -metastasen.

Table of contents

Figures

Abbreviations

AP-1	Activator Protein 1
ATCC	American Type Culture Collection
BEA	Beauvericin
BMPs	Bone Morphogenic Proteins
BSA	Bovine Serum Albumin
Cbfa1	Core binding factor alpha1
DAPI	4',6-Diamidino-2-phenylindole
DED	Death Effector Domain
DXA	Dual X-ray Absorptiometry
ENN	Enniatins
ERK	Extracellular signal-Regulated Kinase
FADD	Fas Associated Death Domain
FGF	Fibroblast Growth Factor
GH	Growth Hormone
GSK3	Glycogen Synthase Kinase-3ß
IGFs	Insulin Growth Factors
Ihh	Indian hedgehog
IL	Interleukin
JNK	JUN NH_2-terminal Kinase
LRP5/6	Low-density lipoprotein receptor-Related protein 5/6
MAPK	Mitogen Activated Protein Kinase
M-CSF	Macrophage Colony Stimulating Factor
Mitf	Microphtalmia-associated transcription factor
MMPs	Matrix Metaloproteinases
NFAT2	Nuclear Factor of Activated T cells 2
NFATc1	Nuclear Factor of Activated T cell 1
NFκB	Nuclear Factor kappa-light-chain-enhancer of activated B cells
OPG	Osteoprotegerin
OSCAR	Osteoclast Associated Receptor
Osx	Osterix
PBS	Phosphate Buffer Saline
PDGFs	Platelet-Derived Growth Factors

P/S	Penicillin/Streptomycin
PSA	Prostate Specific Antigen
PTH	Parathyroid Hormone
PTHrP	Parathyroid Hormone-related Protein
PU.1	B-cell transcription modulator
RANK	Receptor Activator of NFκB
RANKL	Receptor Activator of NFκB Ligand
Runx2	Runt-related transcription factor 2
Runx3	Runt-related transcription factor 3
SDS-PAGE	Sodium Dodecyl Sulfate-Polyacrylamide Gel Electrophoresis
TBS	Tris Buffer Saline
TBST	Tris Buffer Saline Tween
TCF/LEF	T Cell specific transcription Factor/Lymphoid Enhancer binding Factor
TGFß	Transforming Growth Factor ß
TNF	Tumor Necrosis Factor
TNFα	Tumor Necrosis Factor alpha
TRAIL	TNF Related Apoptosis Inducing Ligand
TRAF6	TNF Receptor Associated Factor 6
TRAP	Tartrate Resistant Acid Phosphatase
TRADD	TNF Related Associated Death Domain
uPA	Urokinase Plasminogen Activator

1 Introduction

Osteoporosis is a progressive disease of bone; characterized by reduced bone mass, bone fragility, deterioration of bone microarchitecture leading to increase risk of fractures. It occurs when bone formation (by osteoblasts) and resorption (by osteoclasts) are not tightly coupled with regard to quantity, time and space (Zaidi, 2007). Osteoporosis is common in postmenopausal women (postmenopausal osteoporosis), but also occurs in men or can be induced by other disease states (cancer-induced osteoporosis) or some medications (glucocorticoid-induced osteoporosis). We review in this section the physiology of the cells responsible for growth and maintenance of bone (osteoblasts and osteoclasts), as well as the mechanisms of bone metastases, particularly from breast and prostate cancer. Moreover, we review the knowledge about cyclodepsipeptides (particularly beauvericin and enniatins), mycotoxins used in the framework of this study to characterize their roles in bone cells and bone metastases.

1.1 Bone cells

Bone is a highly specialized type of connective tissue, which provides structural support, protective and mechanical functions and plays a critical role in mineral homeostasis. Bones of the body are either long (tibia, femur and humerus) or flat (skull, ileum and mandible); both of which contain cortical and trabecular bone albeit in different concentrations (Bussard et al., 2008). Cortical bone, mainly present in long bone shafts is the compact, dense outer protective layer of mineralized hardened collagen that provides mechanical strength and support to the body. Trabecular or cancellous bone in contrast is predominant in the axial skeleton and at the ends of long bones, has a loosely organized porous matrix and exhibits a greater turnover rate than cortical bone.

The skeleton is made up of three specific cell types, namely the chondrocytes in cartilage, and the osteoblasts and osteoclasts in bone **(**Karsenty**,** 2001**)**. For the purpose of this review, our attention will be focused on bone cells.

1.1.1 Osteoblasts

1.1.1.1 Definition

Osteoblasts are mononucleated cells of mesenchymal origin that are responsible for bone formation. Under light microscopy, they appear as plump cells, approximately 20-30 μm in diameter, lined up on the surface of unmineralized osteoid (Milat and Ng, 2009). Active osteoblasts synthesize and stain positive for alkaline phosphatase, a useful marker for the detection of osteoblasts in culture. After secretion of matrix proteins, the osteoblast loses its synthetic capacity and either becomes a lining cell (resting osteoblast with flat-elongated morphology that lines cancellous and endocortical bone surfaces), or becomes trapped behind an advancing calcification front where it is embedded in bone lacunae as an osteocyte. Lining cells regulate the passage of calcium into and out of the bone, and respond to hormones by making special proteins that activate osteoclasts.

1.1.1.2 Role

Osteoblasts secrete unmineralized material called osteoid, mainly composed of fibers (type I collagen) and non-collagenous components (chondroitin sulfate, osteocalcin, osteonectin, bone sialoprotein and proteoglycans). Moreover, they are responsible for mineralization of this osteoid matrix, a well-orchestrated process in which crystals of calcium phosphate in the form of hydroxyapatite [$3Ca(PO_4)_2(OH)_2$] are produced and laid down in precise amounts in the organic matrix. Mineralization is critical as it provides hardness and strength, preventing bones from inadvertently bending when a force is applied. Osteoblasts play a crucial role in osteoclast differentiation and bone resorption through their expression of key cytokines, the most important of which include the macrophage colony stimulating factor (M-CSF), the receptor activator of NFκB ligand (RANKL) and osteoprotegerin (OPG), a decoy RANK receptor that inhibits bone resorption (Suda, et al., 1999).

1.1.1.3 Transcriptional regulation of osteogenesis

Osteoblasts arise from mesenchymal progenitors cells in the periosteum and the bone marrow. Very few bones, in particular the clavicles and some flat bones of the skull,

develop without a cartilage template, in a process called intramembranous ossification (Hill, et al., 2005). However, in all the other bones, differentiation of mesenchymal cells into proliferating chondrocytes precedes osteoblast differentiation in a three key steps process of endochondral ossification **(**Karsenty**,** 2001**)**: (1) mesenchymal condensation, proliferation of chondrocytes and differentiation into hypertrophic chondrocytes; (2) vascular invasion from the perichondrium or bone collar along with invasion of mesenchymal progenitors (3) that will differentiate into osteoblasts. This highlights the interdependence between chondrocyte hypertrophy and osteoblast differentiation for bone formation to occur (Figure 1).

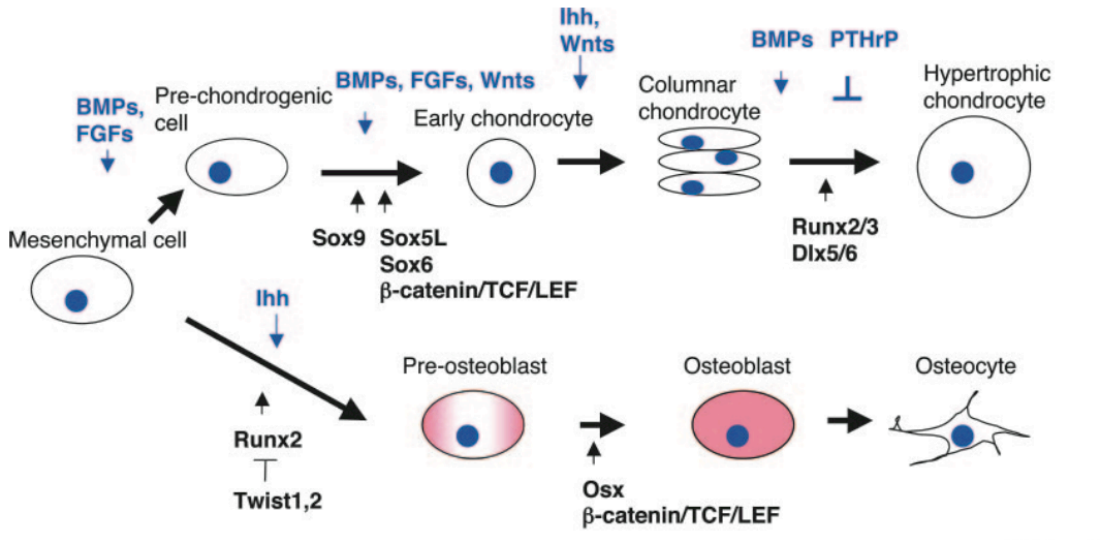

Figure 1. Regulation of chondrocyte and osteoblast differentiation (Kobayashi and Kronenberg, 2005)

Bone morphogenic proteins (BMPs) are the only factors capable of initiating osteoblastogenesis from uncommitted precursors. They induce mesenchymal condensation upon binding to their receptors (BMP receptors type I and II) by phosphorylating their downstream target Smads (1, 5 and 8) (Miyazawa, et al., 2002). Chondrogenesis is mediated by BMPs-dependent expression of Sox9, a high-mobility-group (HMG) domain transcription factor required for chondrocyte lineage commitment (Kobayashi and Kronenberg, 2005). Sox9 plays essential roles in successive steps of chondrocyte differentiation, including mesenchymal condensation, conversion of mesenchymal cells into chondrocytes, proliferation of chondrocytes, and prevents proliferating chondrocytes to differentiate into hypertrophic chondrocytes (Akiyama, et al., 2002; Bi, et al., 1999). Moreover, Sox9 is required for the expression of its two related family members, L-Sox5 and Sox6, both of which are important for normal

chondrocyte function (Smits, et al., 2001). Other signaling molecules such as Indian hedgehog (Ihh), Wnts, ß-catenin, TCf/LEF complex have also been shown to regulate chondrogenesis (Hartmann and Tabin, 2000; St-Jacques, et al., 1999) although individual or combined effects, as well as their molecular mechanism are partially appreciated.

Chondrocyte hypertrophy is a mandatory step during endochondral ossification. Yet, the Cbfa1 transcription factor (or Runx2), one of the mouse homologs of the drosophila runt protein, is induced by BMPs, expressed early in development (embryonic day 12) in chondro-osteoprogenitors present in mesenchymal condensations of the developing skeleton (Ducy, et al., 1997), and acts as the hypertrophic chondrocyte differentiation factor (Inada, et al., 1999; Takeda, et al., 2001). Runx2 and Runx3 are essential for chondrocyte maturation and Runx2 regulates limb growth by organizing chondrocyte maturation and proliferation through the induction of Indian hedgehog (Ihh) expression (Yoshida, et al., 2004). From embryonic day 14, Cbfa1 (or Runx2) expression gradually fades away in the cells of the chondrocyte lineage while it strongly increases in the cells of the osteoblast lineage and constitutes the most specific and earliest commitment marker of the osteoblast lineage (Ducy, et al., 1997).

Runx2 is absolutely required for differentiation to proceed to the osteoblast and to no other lineage (Karsenty, 2001; Kobayashi and Kronenberg, 2005). Runx2 can be activated downstream of smads, or directly following phosphorylation by PTH and FGFs (Zaidi, 2007). Interestingly, Runx2 oeteogenic activity is suppressed by interaction of its DNA binding domain with the Twist box domain of Twist transcription factors (Bialek, et al., 2004). Runx2 binds to the cis-acting elements of osteoblast specific genes, including type I collagen, bone sialoprotein, osteopontin, osteocalcin, and regulate their expression (Ducy and Karsenty, 1995).

Osterix (Osx) is another obligatory signal for osteoblastogenesis, as Osx-deficient mice, similarly to Runx-/-, do not deposit bone (Nakashima, et al., 2002). However, Osx null mice, unlike Runx2-/-, express normal Runx2 levels indicating that Osx acts downstream of Runx2. NFAT2 (Nuclear factor of activated T cells 2) is important for the transcriptional activity of Osx (but not Runx2), as the two of them form a complex that bind to DNA and regulates expression of target genes (Koga, et al., 2005).

Canonical Wnt/ß-catenin signaling is another critical pathway in osteoblastogenesis (Milat and Ng, 2009; Westendorf, et al., 2004). Wnt family members are secreted glycoproteins, defined by sequence homology to drosophila wingless (wg) and the murine int-1 protooncogene. Canonical Wnts (including Wnt4, Wnt5a and Wnt11)

interact with their receptors of the Frizzled family and co-receptors of the LRP5/6 family to stabilize cytoplasmic ß-catenin. Stabilization of ß-catenin occurs through its phosphorylation by the glycogen synthase kinase-3ß (GSK3), its translocation to the nucleus where it binds to transcription factors such as T cell specific transcription factor/Lymphoid enhancer binding factor (TCF/LEF) to regulate transcription of target genes. Consistent with the role of Wnt/ß-catenin in skeletogenesis is the realization that antagonists of Wnt signaling, including Dickkopfs proteins (compete with Wnts for binding to the LRP5/6 receptor), secreted frizzled related proteins and Wnt inhibitory factor 1 (bind directly to Wnts), and sclerostin (product of SOST gene that binds on the LRP5/6 receptor) lead to decreased bone formation and bone mass. Moreover, canonical Wnt/ß-catenin signaling controls a molecular switch that regulates lineage commitment between chondrocytes and osteoblasts, preventing transdifferentiation of osteoblastic cells into chondrocytes (Hill, et al., 2005). There are now clear evidence of interaction between the signaling pathways linked to PTH, BMPs and LRP/Wnt actions leading to bone formation, although data are insufficient to appreciate the relative contribution of each of these pathways (Milat and Ng, 2009).

1.1.1.4 Osteocytes

Osteocytes are retired osteoblasts trapped in the bone lacunae, and represent the most abundant cell type in bone (about ten times more than osteoblasts). They have a star-shaped like morphology and communicate with each other and with other cells via long cytoplasmic extensions that run along tiny canals called canaliculi. Osteocytes do not express alkaline phosphatase, but act as mechanosensors as they sense and respond to changes in fluid flow arising from stress, strain or pressure (Han, et al., 2004). They negatively regulate bone formation through their secretion of sclerostin. Sclerostin is the product of the SOT gene that acts as a master regulatory break molecule on bone formation. In line with this are the observations that loss of function mutations result in high bone mass phenotypes (Balemans, et al., 2001; Brunkow, et al., 2001; Loots, et al., 2005). Sclerostin antagonizes the Wnt/ß-canonical signaling by binding to the extracellular domain of the Wnt co-receptors LRP5 and LRP6, and by disrupting Wnt-induced Frizzled /LRP complex formation (Semenov, et al., 2005).

1.1.1.5 Regulation of osteoblast apoptosis

Apoptosis or programmed cell death, with typical apoptotic features of condensed chromatin and/or nuclear fragmentation, appears less frequently in osteoblasts *in vivo* as compared to osteoclasts (Xing and Boyce, 2005). However, increased osteoblast apoptosis is generally mirrored by decreased bone formation. Human postmenopausal osteoblasts constitutively express Fas receptors, which upon activation by their ligand Fas, induce cell death (Garcia-Moreno, et al., 2004). Osteoblasts do also express functional death receptors for TNF and TRAIL (TNF related apoptosis inducing ligand). Mechanistically (Xing and Boyce, 2005), these death receptors (CD95 for FasL and DR5 for TNF and TRAIL) contain an intracellular death domain that upon activation of the receptor recruits adaptor proteins, such as FADD (Fas-associated death domain) or TRADD (TNF related associated death domain). These adaptor proteins themselves bear a death effector domain (DED) that recruits DED-containing proteins such as procaspase-8. Apoptosis can also be induced by the classical mitochondrial pathway regulated by Bcl-2 family proteins, which involves mitochondrial release of cytochrome c and activation of initiator and executor caspases leading to cleavage of life essential proteins. Some factors including intermittent PTH, IGFs, FGF, TGFß, sex steroids (estrogen and testosterone), IL-6 and leptin exert antiapoptotic effects on osteoblasts. Interestingly, BMP-2, a member of the TGFß family that regulates osteoblast differentiation and bone formation has a novel function of promoting osteoblast apoptosis through a Smad-independent, protein kinase C dependent signaling pathway resulting in cytochrome c release from the mitochondria and activation of caspase 9, 3, 6 and 7 (Hay, et al., 2001). Glucocorticoid therapy leads to bone loss due to impaired intestinal calcium absorption, decreased osteoblastogenesis, increased osteoclast activity and/or life span, and increased apoptosis of osteoblasts and osteocytes (Xing and Boyce, 2005).

1.1.2 Osteoclasts

1.1.2.1 Definition and role

Osteoclasts are large, terminally differentiated multinucleated cells highly specialized in breaking down the mineralized bone matrix. They are located on bone surfaces in the so-called Howship's lacunae or resorption pits. The average osteoclast bears about 5 to

20 nuclei, although osteoclasts with up to 200 nuclei may exist. Their cytoplasm appears homogeneous and foamy in regard to their high concentration of vesicles and vacuoles. They express high levels of Tartrate Resistant Acid Phosphatase (TRAP) and can therefore be identified in culture by staining of this enzyme.

Morphological and functional features of an active osteoclast include adherence to the bone surface, the ability to migrate efficiently toward and along bone surfaces, synthesis and directional secretion of hydrolytic enzymes, acidification of the subosteoclastic bone resorbing compartment and efficient internalization of extracellular bone matrix degradation products (Bruzzaniti and Baron, 2006). At a site of active bone resorption, the osteoclast forms a specialized apical cell membrane, the **ruffled border**, which faces the bone surface and acts as the main resorptive organelle. Another critical component at this apical membrane is the **sealing zone**, an actin reach area surrounding the ruffled border that closely interact with the bone matrix, thus sealing off the subosteoclastic bone-resorbing compartment.

1.1.2.2 Osteoclastogenic cytokines

RANKL is the key osteoclastogenic cytokine expressed by osteoblasts/stromal cells (Yasuda, et al., 1998). However, RANKL is also expressed in high levels in antigen activated T cells and plays a critical role in the pathogenesis of rheumatoid arthritis-induced bone loss (Kong, et al., 1999). Actually, TNFα is the key cytokine mediating the periarticular bone loss of rheumatoid arthritis, promoting osteoclast formation and activation in inflamed joint by stimulating RANKL production by marrow stromal cells, and by directly stimulating differentiation of osteoclasts precursors (Teitelbaum, 2007). TNFα is pivotal to the pathogenesis of inflammatory osteolysis and acts synergistically with RANKL. However, whether TNFα alone can induce osteoclast differentiation is still debatable. Indeed, Lam and colleagues (Lam, et al., 2000) reported that TNFα is incapable of inducing osteoclastogenesis *in vitro* and *in vivo* unless attended by permissive levels of RANKL while Kim and colleagues (Kim, et al., 2005) claimed that the inflammatory cytokine is sufficient to induce osteoclastogenesis in the absence of RANK signaling *in vitro* if attended by TGFß. IL-1 is able to induce RANKL expression by stromal cells and directly stimulates osteoclast precursor differentiation in a p38 MAPK-dependent manner (Wei, et al., 2005). Moreover, IL-1 mediates the osteoclastogenic effect of TNFα and directly promotes the osteoclast phenotype

independently of TNFα in the presence of permissive levels of RANKL (Wei, et al., 2005). M-CSF, also produced by marrow stromal cells is required for macrophage survival and proliferation and more importantly, plays a crucial role in osteoclast differentiation. This fit well with the observation that op/op mice, which lack functional M-CSF, have osteoclast-deficient osteopetrosis (Yoshida, et al., 1990). M-CSF and RANKL are sufficient for osteoclastogenesis, as pure populations of osteoclasts can be generated *in vitro* by cultivating marrow macrophages in the sole presence of these 2 cytokines. RANKL activity is negatively regulated by OPG, a glycoprotein molecule produced by osteoblasts that competes with RANK as a soluble decoy receptor (Simonet, et al., 1997).

1.1.2.3 Regulation of osteoclastogenesis

Osteoclasts originate from multipotent hematopoietic stem cells in the bone marrow (Coccia, et al., 1980; Udagawa, et al., 1990). The earliest known event in osteoclastogenesis is determination of the stem cell precursor (Figure 2), and is induced by the B-cell transcription modulator PU.1 (Tondravi, et al., 1997). At around this point, the cells acquire the c-fms receptor and start to proliferate in response to stimulation of that receptor by M-CSF, a cytokine produced by nearby stromal cells. Consistent with the role of M-CSF in osteoclastogenesis, op/op mice defective in the production of functional M-CSF are severely deficient in mature macrophages and osteoclasts (Yoshida, et al., 1990). Up to this point, B-lymphocytes can still be formed, but the appearance of c-fos and RANK receptor fully commit precursors to an osteoclast lineage (Zaidi, 2007). It is important to point here that RANK receptor is as well expressed on chondrocytes, dendritic cells and mature osteoclasts (Kong, et al., 1999).
Another critical cytokine required for osteoclastogenesis is RANKL, a member of the TNF family, also released by nearby stromal cells. RANKL, a membrane-residing protein on stromal cells binds to its receptor RANK on macrophages and trigger signal transduction cascades leading to the expression of differentiation and survival genes; thus, a genetic defect of any molecule downstream of RANK results in arrest of osteoclastogenesis. Mechanistically (Zaidi, 2007), upon activation, RANK recruits the docking protein TRAF6 (TNF receptor associated factor 6) to its cytoplasmic domain to activate NFκB and all three families of MAP kinases (JNK, ERK1/2 and p38). In line with this is the observation that mice lacking the p50 and p52 subunits of NFκB fail to

generate osteoclasts and are osteopetrotic (Franzoso, et al., 1997). RANKL-induced MAP kinase signaling leads to the activation of AP-1 (activator protein 1), a dimeric complex mainly composed of FOS and JUN. In parallel, the transcription factor NFATc1 (Nuclear factor of activated T cell 1) is activated by the calcium/calmodulin-regulated phosphatase calcineurin; is translocated to the nucleus where it binds consensus sequence on DNA; and together with c-fos, amplifies key osteoclast genes including NFATc1 itself.

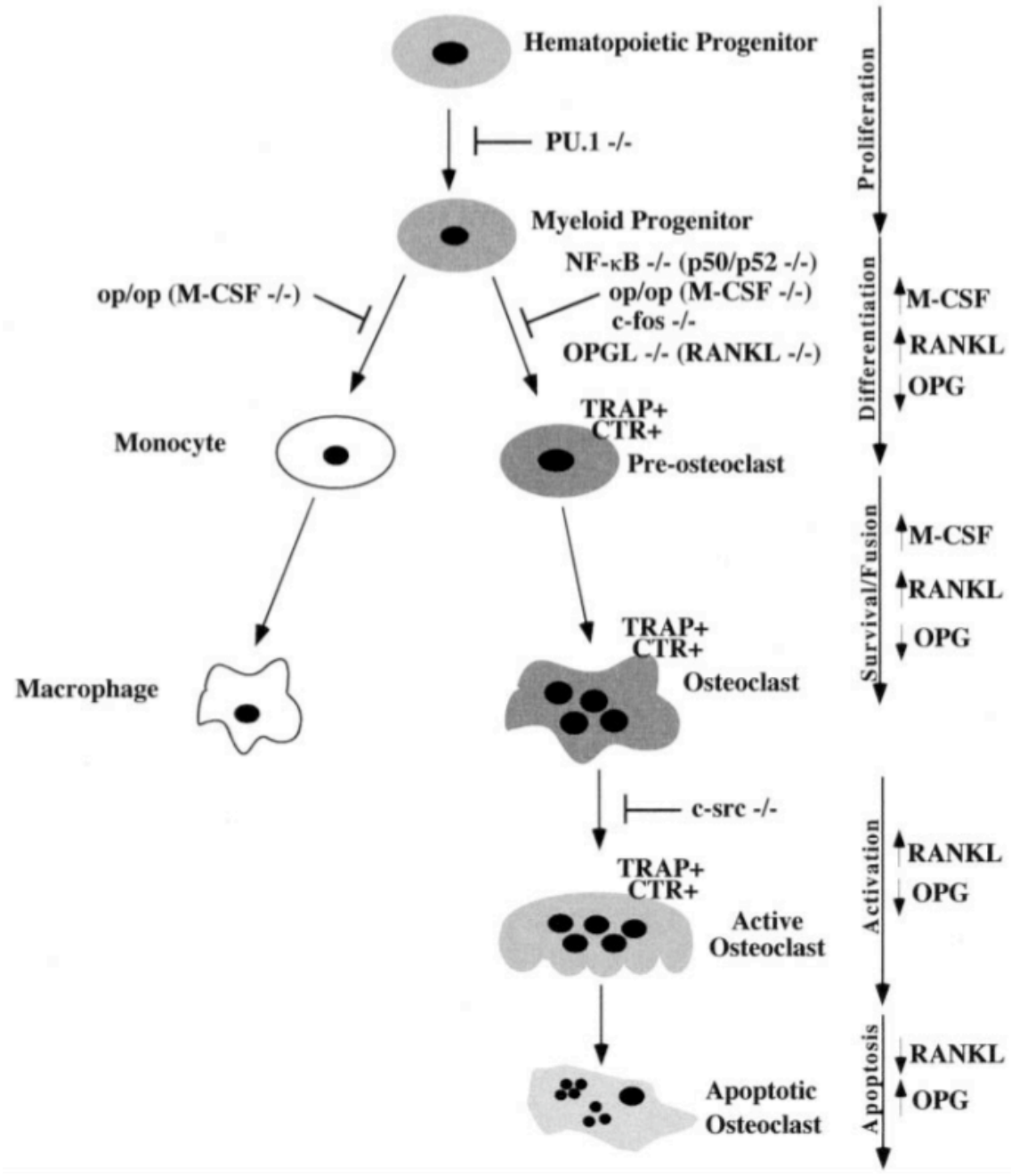

Figure 2. Regulation of osteoclastogenesis (Aubin and Bonnelye, 2000)

c-fos (major component of AP-1) is important for osteoclastogenesis, as c-fos-/- mice lack osteoclasts and are osteopetrotic (Johnson, et al., 1992; Wang, et al., 1992). However, the effects of c-fos are thought to be mediated by NFATc1, as the latter is able to rescue osteoclastogenesis in c-fos-/- precursors (Matsuo, et al., 2004). So NFATc1, the most distal effector, is not only indispensable, but also sufficient for osteoclastogenesis, as its overexpression yields osteoclasts even in the absence of RANKL (Zaidi, 2007).

Microphtalmia-associated transcription factor (Mitf) and Tfe3, both members of the basic/helix-loop-helix/leucine zipper (b-HLH-ZIP) transcription factor subfamily MiT, reside furthest along in the differentiation process and are essential for differentiation of mononuclear precursors (pre-fusion osteoclasts) into multinucleated osteoclasts (Hershey and Fisher, 2004). They directly regulate genes important for osteoclast function such as TRAP, cathepsin K, OSCAR (osteoclast-associated receptor); and may also regulate other transcription factors essential for osteoclastogenesis such as PU.1 and c-Fos by physical interaction (Kobayashi and Kronenberg, 2005).

1.1.2.4 Regulation of bone resorption

Bone is a very dynamic tissue, which is continuously being resorbed and rebuilt. Remodeling is essential in normal physiologic conditions to regulate calcium homeostasis, to repair micro-damaged bone, as well as to shape and sculpture the skeleton during growth. The osteoclast is unique in its ability to do that job. Accordingly, the mature osteoclast must undergo some morphological changes to acquire specific features of an “activated” bone resorbing cell.

At first, the osteoclast attaches to the bone matrix via its vitronectin $\alpha_v ß_3$ receptor with RGD (Arg-Gly-Asp) motifs of matrix proteins. This triggers an “outside-in” signaling characterized by the recruitment of Src at the cell membrane and the tyrosine phosphorylation of a distinct set of proteins, including Pyk2, Cbl, paxillin, cortactin, vinculin, talin, tensin and $p130^{cas}$ (Bruzzaniti and Baron, 2006). This $\alpha_v ß_3$-dependent signaling leads to the formation of complexes that include c-Src, Syk and the Rac-specific guanine nucleotide exchange factor vav-3, and causes adhesion (sealing zone). Once adherent, the osteoclast polarizes (Zaidi, 2007): its bone-apposed ventral membrane invaginates into complex folds to form the ruffled border, the main resorptive organelle. Therefore, the “activated” osteoclast creates an isolated microenvironment between itself and the bone matrix by displaying an apical domain

against the bone surface, carrying secretory (ions and lysozomal enzymes by exocytosis) and absorptive (bone matrix degradation products by endocytosis) functions; and a basolateral domain away from the bone surface, through which cell matrix degraded products are excreted (Bruzzaniti and Baron, 2006).

Protons are synthesized by carbonic anhydrase II ($CO_2 + H20 \rightarrow HCO_3^- + H^+$), packed in Vacuolar ATP-ases vesicles, transported probably via microtubules and inserted into the ruffled border. These protons are then pumped out in the isolated microenvironment and the resulting acidification mobilizes the mineral phase out of the matrix. To prevent intracellular alkalinization that would otherwise occur, this proton secretion is counter-balanced by parallel extrusion of chloride ions through the CIC-7 chloride channel (Teitelbaum, 2007). Chloride ions enter the cell at the basolateral membrane exchanging with bicarbonate (bicarbonate/chloride exchangers), are packed as well in vesicles, transported and released through the ruffled border via the CIC-7 channel in the bone lacunae where they charge-coupled to protons into HCl, bringing the ambient pH to fall to an approximate value of 4.5 (Schlesinger, et al., 1997). This allows acid-optimal lysozomal enzymes such as cathepsin K (released in the bone lacunae) to break down the helical and telopeptides regions of the organic matrix (collagen). Some of these organic and inorganic degradation products are endocytosed in the osteoclast; some are degraded within secondary lysosomes while others are transported through the cell by transcytosis and excreted through the basolateral domain.

Hydroxyapatite dissolution elevates the ambient Ca^{2+} that in turn activates a Ca^{2+} sensor on the osteoclast surface, causing the rapid release of Ca^{2+} from intracellular stores. This rising cytosolic Ca^{2+} acts negatively on resorption, signaling the osteoclast to detach and retract from the bone surface (Zaidi, 2007). The osteoclast then loses the cytoskeletal features characteristic of activation and migrates to the next point on the bone to start anew the cycle (attachment-resorption-migration). With each cycle, the osteoclast leaves on the bone surface a characteristic mark, the so-called “resorption pit” that can be observed as purple lighting spots under the microscope after *in vitro* staining with toluidine blue. Degraded bone matrix products remaining at the site of resorption following osteoclast migration may play a role in the coupling of bone resorption with bone formation during the skeletal remodeling sequence (Bruzzaniti and Baron, 2006).

Bone remodeling appears as a highly coordinated and structured process, where the components perfectly interact with each other. Therefore, any defect in each of the signaling component namely, the vacuolar proton pump V-ATPase (Frattini, et al., 2000; Kornak, et al., 2000; Scimeca, et al., 2000), the chloride channel CIC-7 (Kornak,

et al., 2001), carbonic anhydrase II (Sly, et al., 1983) or cathepsin K (Gelb, et al., 1996) results in altered bone resorption and osteopetrosis. The same holds for Src, Syk and pyk2 (Bruzzaniti and Baron, 2006).

1.1.2.5 Regulation of osteoclast apoptosis

After bone breakdown, the osteoclast undergoes apoptosis. Morphological changes characteristic of osteoclast apoptosis include cell shrinking, chromatin condensation, nuclear fragmentation and strong TRAP staining (Xing and Boyce, 2005). Decreased osteoclast apoptosis usually correlates with increased bone loss as observed in rheumatoid arthritis and glucocorticoid-induced osteoporosis. Although TNFα can induce programmed cell death in a number of cell types upon binding to its death receptor DR5 (Xing and Boyce, 2005), increasing evidence support its role in promoting osteoclast survival rather than death. Indeed, TNFα has been shown to suppress apoptosis in osteoclasts through another signaling pathway involving the activation of the transcription factor NFκB (Van Antwerp, et al., 1996). The anti apoptotic protein Bcl-xL is expressed in osteoclast precursors and its expression is upregulated following treatment with M-CFS alone or in association with RANKL (Woo, et al., 2002). Nevertheless, RANKL alone is not sufficient to prevent apoptosis of osteoclasts precursors. Expression of a truncated Src molecule Src251, lacking the kinase domain induces apoptosis in osteoclasts associated with reduced Akt kinase activity, and provides evidence of a role of Src in osteoclast survival (Xing, et al., 2001). Additionally, Src inhibitors induce osteoclast apoptosis through selective sustained ERK1/2 phosphorylation (Recchia, et al., 2004). Inhibition and activation studies of ERK and NFκB in osteoclasts using adenovirus vectors suggest a role of ERK, but not NFκB in osteoclast survival (Miyazaki, et al., 2000). PTH and 1,25$(OH)_2$ vitamin D3, like many other factors that stimulate bone resorption prevent osteoclast apoptosis, most likely by stimulating expression of RANKL and decreasing expression of OPG by stromal cells (Xing and Boyce, 2005).

1.1.3 Bone homeostasis

1.1.3.1 Effect of parathyroid hormone and vitamin D3

Calcium metabolism is the mechanism by which the body maintains adequate calcium levels. Calcium is the most abundant mineral in the human body. The average adult body contains in total approximately 1 kg, 99 % of which is stored in the skeleton in the form of hydroxyapatite crystals. Normal plasma concentration ranges between 2.2 to 2.6 mmol/l and ionized calcium between 1.1 to 1.4 mmol/l. About 40 % of total blood calcium is bound to plasma proteins, primarily albumin. The remaining 60 % includes ionized calcium plus calcium complexed with phosphate (PO_4) and citrate. The ionized or free calcium is the physiologically active form in the plasma and is the one commonly measured because of its clinical relevance. The regulation of calcium balance is greatly influenced by concentrations of circulating parathyroid hormone (PTH), 1,25-$(OH)_2$-vitamin D3 and to a lesser extent calcitonin (Figure 3).

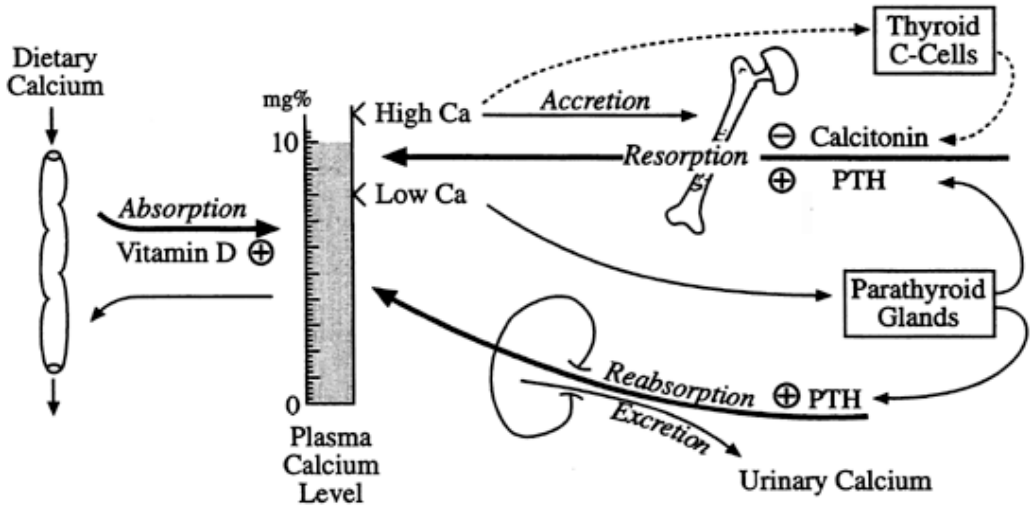

Figure 3. Calcium metabolism

PTH is secreted by parathyroid glands (located behind the thyroid gland) in response to low calcium levels and promotes release of calcium from the bone (thus stimulates bone resorption). PTH also increases plasma calcium by stimulating conversion of 25-OH-vitamin D3 in the kidney in its most active form 1,25-$(OH)_2$-vitamin D3. The latter then promotes dietary calcium intestinal absorption (by increasing the number of calcium binding proteins) and calcium resorption from the kidney. Despite increased calcium absorption, long-term increases in PTH secretion generally result in further bone

resorption by inhibiting osteoblastic function and promoting osteoclastic activity. PTH and vitamin D both function as important regulators of bone growth and bone remodeling. On the other hand, when plasma calcium levels are high, the thyroid parafollicular cells secrete calcitonin, which promotes cellular uptake, renal excretion and bone formation. Calcium metabolism disorders include hypocalcemia, hypercalcemia, osteomalacia and more importantly osteoporosis.

1.1.3.2 Bone disorders

1.1.3.2.1 Bone loss disorders

Bone loss occurs when osteoclastic bone resorption exceeds osteoblastic bone formation. An absolute increase in the rate of bone resorption, with a relative, but insufficient increase in the rate of bone formation, leads to high turnover bone loss (Zaidi, 2007). This bone loss can be generalized (as observed in hypogonadism, thyrotoxicosis, hyperparathyroidism and disease of cytokine excess), or localized in focal osteolysis as observed in skeletal metastases, Paget's bone disease, rheumatoid arthritis and periodontitis. Opposed to the hyper-resorption that defines high-turnover disorders, bone resorption can slow down *per se* and lag behind resorption, leading to low turnover osteoporosis, as is the case in aging, disuse, glucocorticoids and calcineurin inhibitors (Zaidi, 2007).

Osteoporosis is the most prominent disorder of the skeleton. It is defined by the World Health Organization (WHO) as bone mineral density 2.5 standard deviations below average peak bone mass of a young sex matched healthy person, as measured by Dual X-ray Absorptiometry (DXA). Osteoporosis is most common in women after menopause where it is termed postmenopausal osteoporosis, but may develop in men and premenopausal women in the presence of particular hormonal disorders or other chronic diseases (rheumatoid arthritis, Paget's disease of bone), or as a result of some medication, specifically glucocorticoids. Risks factors for osteoporosis include gender (female), advanced age, small skeletal frame, family history, low diet calcium and vitamin D, medication (glucocorticoids, anti-convulsants), low sex steroids (estrogen, testosterone), excessive alcohol, smoking and inactive lifestyle. Other bone disorders include osteogenesis imperfecta (or brittle bone disease which is a genetic disorder in people born with defective connective tissue or without the ability to make it, usually

because of a deficiency of type-I collagen), osteosarcoma (primary malignancy of bone) and bone metastases.

Glucocorticoids, a key component in the management of many inflammatory disorders, present adverse effects particularly on bone. They increase bone resorption, inhibit bone formation and have indirect action on bone by decreasing intestinal calcium absorption, modifying vitamin D metabolism, sustaining a marked hypercalciuria with variable changes in plasma PTH levels (Manelli and Giustina, 2000; Tamura, et al., 2004).

Rheumatoid arthritis is a chronic, systemic autoimmune inflammatory disorder that principally affects the synovial lining of joints. This inflammatory process (characterized by pain, swelling and stiffness) targets the articular cartilage, the bone at the joint margins, as well as periarticular cartilage and subchondral bone (Goldring, 2003). Pro-inflammatory cytokines, particularly TNFα, IL-1 and IL-6, play critical roles in the pathogenesis of rheumatoid arthritis and are usually raised in the joint and blood of patients with rheumatoid arthritis (Brennan and McInnes, 2008; Christodoulou and Choy, 2006; Goldring, 2003). Consistent with this is the successful targeting of these cytokines as therapeutic intervention in the management of rheumatoid arthritis. These cytokines are produced by activated T cells, macrophages and fibroblasts present in the joint. IL-1 and TNFα, both upregulate RANKL expression in bone lining and stromal cells. Moreover, RANKL is expressed on T cells and fibroblasts within the synovial inflammatory tissue of patients with rheumatoid arthritis and its expression is upregulated by proinflammatory cytokines (Schett, et al., 2005). TNFα and RANKL act synergistically to enhance osteoclast differentiation and regulate osteoclast-induced focal bone loss (Goldring, 2003). Moreover, TNFα and IL-1 induce cartilage remodeling by stimulating the production of matrix metaloproteinases (MMPs) by chondrocytes.

Paget's disease of bone, also called osteitis deformans is a chronic disorder, characterized by focal areas of increased bone turnover resulting in enlarged and deformed bones. The disease is named after the British surgeon James Paget who first described it in 1877. The origin of the disease is unknown although viral (paramyxoviruses), genetic (mutations in Sequestosome 1 gene) and environmental causes have been implicated, as well as the deficiency of dietary calcium and repetitive mechanical loading of the skeleton (Ralston, et al., 2008). The pathogenesis of Paget's disease involves 3 stages (Ralston, et al., 2008): The first step (**lytic phase**) is characterized by marked osteolysis at localized areas with abnormally increased

osteoclast number and nuclei (up to 100 as compared to 5-10 nuclei in normal osteoclasts), resulting in a bone turnover rate up to 20 times more rapid than normal. This significant increase in bone resorption leads to a rapid compensatory increase in bone formation (**mixed phase**) by osteoblasts, which are increased in number, but morphologically normal. The new bone deposition is accelerated and disorganized in a haphazard pattern rather than the normal linear pattern, making it mechanically weaker, more bulky, less compact, more vascular and liable to pathological fracture and deformity. In the final phase (**sclerotic phase**), bone formation exceeds bone resorption resulting in a disorganized woven bone allowing bone marrow space to be infiltrated by excessive fibrous connective tissue and blood vessels, leading to a hypervascular bone state. Eventually the hypercellularity may diminish leaving a dense "pagetic bone" known as the burnt-out Paget disease.

1.1.3.2.2 Osteopetroses

Osteopetrosis also known as marble bone disease or Albers-Schonberg disease is an inherited disorder, characterized by increased bone density due to poor bone removal. Despite the high bone mass phenotype observed, bones are generally brittle, fragile and therefore susceptible to fracture. The damage can be severe enough to disturb tooth eruption, cause marrow cavity obliteration, nerve entrapment, growth retardation, blindness and deafness (Zaidi, 2007). Osteopetrosis can be due to absence (impaired osteoclastogenesis) or dysfunctional osteoclasts. The latter case is more common with osteoclasts usually in normal if not elevated number, but showing defects in resorption components like deficiency in vacuolar H^+-ATPase, chloride channel CIC-7 or cathepsin K genes. In humans, the most severe form is the infantile malignant autosomal recessive osteopetrosis arising from mutations in genes encoding components of the acidification machinery, namely the α_3-subunit of the vacuolar proton pump, the chloride channel CIC-7 or carbonic anhydrase II (Frattini, et al., 2000; Kornak, et al., 2000; Kornak, et al., 2001; Sly, et al., 1983). A less severe form is observed in pycnodysostosis, a disease of dwarfism and fragile bones that results from cathepsin K mutation (Gelb, et al., 1996). There is no cure for most types of osteopetroses; but the malignant form in which carbonic anhydrase II is missing can be treated by bone marrow transplant. Other alternatives are the use of 1,25-dihydroxy vitamin D and recombinant human interferon gamma to induce osteoclast bone resorption.

1.1.3.3 Treatment of bone loss disorders

Antiresorptive agents for osteoporosis are the state-of-the-art therapy, aiming to restore bone density by decreasing bone remodeling. Their mechanism of action is to inhibit bone resorption by inhibiting osteoclast generation and/or activity and by inducing osteoclast apoptosis. Bisphosphonates (including alendronate, ibandronate, risodronate and etidronate) are by far the most widely used treatment for osteoporosis, tumor osteolysis, humoral hypercalcemia, multiple myeloma and Paget's disease of bone (Zaidi, 2007). They competitively bind to the geranyl pyrophosphate pocket of farnesyl pyrophosphate synthase to inhibit the mevalonate pathway of cholesterol biosynthesis in osteoclasts, which in turn lead to impaired prenylation of important small GTP-binding proteins such as Rho, and to subsequent changes in the cytoskeletal function that promotes osteoclast apoptosis (Mundy, 2002). Calcitonin transiently inhibits osteoclast activity without decreasing osteoblast collagen synthesis (Stepan, et al., 2003). Other antiresorptive therapies include calcium plus vitamin D and selective estrogen receptor modulators (raloxifene) (Vestergaard, 2005).

Anabolic drugs are being increasingly used nowadays. They directly stimulate bone formation and improve bone quality and bone mass. Teriparide, the recombinant human parathyroid hormone (1-34), administered intermittently improves bone density, features of bone turnover and reduces fracture incidence, but also significantly improves bone microarchitectural and geometric properties (Girotra, et al., 2006). Strontium ranelate, another anabolic agent also inhibits bone resorption (Girotra, et al., 2006; Zaidi, 2007). Growth hormone (GH) and insuline-like growth factor (IGF-1) are being investigated as potential anabolic agents given their critical role for acquisition and maintenance of bone mass, although their ubiquitous effect on many organ systems constitute a serious drawback (Girotra, et al., 2006).

1.2 Bone metastases

Metastasis occurs when cancer cells break away from their primary tumour, invade the blood stream or lymph vessels and travel to distant organs and tissues where they settle in and start growing. Even after metastasis, the cancer is still named after the part of the body (tissue) it has started. In order to explain the bias observation that some organs have larger number of secondary tumours while others have relatively few, three major theories have been put forward (Liotta, 2001):

- The "**Growth factor theory**" holds that tumour cells leave the blood and lymphatic vessels to the same extent at all organs, but multiply only in those organs that have the appropriate growth factors.
- The "**Adhesion molecule theory**" proposes that the endothelial cells that line blood vessels in target organs express adhesion molecules that cause circulating tumour cells to stop and invade those organs.
- The "**Chemokine theory**" implies that organ-specific attractant molecules enter the circulation, stimulating tumour cells to invade the walls of blood vessels and enter the organs.

Although there is evidence to support all three theories, the mediator molecules (whether they be growth factors, adhesion molecules or chemoattractants) have remained unknown until Müller *et al.* (Muller, et al., 2001) identified chemokines (CXCL12 and CCL21) in first destination target organs (lymph nodes, bone marrow and lungs) and chemokine receptors (respectively CXCR4 and CCR7) on human breast cancer cells, providing molecular support for the chemoattraction theory.

Metastasis is a highly organized, non-random, organ-selective and numerous sequential step process. Different cancers tend to spread to different sites; however, bone is the third most common site of metastasis after the lungs and liver (Bagi, 2005). Bone metastasis is different, much prevalent and morbid than primary bone cancer, a cancer that starts in the bone. Carcinomas of the breast, lung and prostate commonly metastasize to the bone (Mundy, 2002), with the axial skeleton seeded more than the appendicular skeleton partly due to the persistence of red bone marrow in the former (Tofe, et al., 1975). The appearance of skeletal metastases indicates a negative prognostic sign that marks the stage when the disease is rarely curable and the treatment mainly palliative (Bagi, 2005). Manifestations of metastatic bone disease include pathological fractures, pain, cranial nerve palsies, spinal cord compression, bone marrow suppression and hypercalcemia of malignancy.

1.2.1 Rules that direct cancer spread to the skeleton

The skeleton is one of the most preferred sites of metastasis of malignant tumours. Over 60 % of patients with nonosseous primary malignant neoplasms present abnormal bone scans (Tofe, et al., 1975) and particularly, breast, lung and prostate cancer constitute the major source of all metastases to bone (Tofe, et al., 1975; Tomita, et al., 2008). Indeed, up to 70 % of patients with advanced breast or prostate cancer, and approximately 15 to

30 % of patients with carcinoma of the lung, colon, stomach, bladder, uterus, rectum, thyroid or kidney develop bone metastases (Roodman, 2004). Moreover, the thorax (54 %), vertebra (52 %) and pelvis (38 %) are mostly involved when compared to the skull (22 %) (Tofe, et al., 1975).

Primary tumour cells invade their surrounding normal tissue by producing proteolytic enzymes, which degrade the walls of small blood vessels in the normal tissue or of those induced by the tumour, allowing the cancer cell to enter the circulation and travel to distant organ sites (Liotta and Kohn, 2001). (1) One of the critical determinants of the site of metastasis is blood flow from the primary site (breast or prostate) to the skeleton (Bagi, 2005). Blood flow is high in areas of red marrow, accounting for the predilection of metastases for those sites (Roodman, 2004). This is consistent with the "**mechanical**" hypothesis proposed by James Ewing in 1929 stipulating that patterns of blood flow carrying cells from the primary tumour entirely account for the unequal dissemination of metastases, and the first organ encountered in the circulation (lung) would harbor the greatest number (Fidler and Poste, 2008). However, there are other highly vascularized organs (kidneys, spleen) to which tumour cells rarely metastasize, implying that other factors are involved (Mundy, 2002). (2) More to the point, the Batson's vertebral venous plexus of high-volume and low-pressure vertebral veins plays a pivotal role in the dissemination of breast and prostate cancer to the axial skeleton (Bagi, 2005). The Batson's venous system; a thin walled, valveless network of veins within and surrounding the vertebral column and extending from cranium to pelvis; directly connects primary tumour sites (breast or prostate) with the skeleton, bypassing the liver and lungs. The sluggish blood flow in this plexus is more conducive to tumour survival and facilitates extravasation of tumour cells from the circulation. (3) Last but not the least, aggregates of tumour cells and other blood cells (lymphocytes, platelets) eventually form emboli (Figure 4) that can be easily trapped in capillary beds within the bone (Bagi, 2005). Once the tumour cell embolus reaches the skeleton, they have a high probability of survival in the highly favorable bone microenvironment. This is supported by the "**seed and soil**" hypothesis proposed by Stephen Paget in 1889 stating: "when a plant goes to seed, its seeds are carried out in all directions; but they can only live and grow if they fall in congenial soil" (Fidler and Poste, 2008). This highlights the tightly intimate relationship (crosstalk) that the cancer cell (seed) must entertain with its environment (soil) in order for a metastasis to be established.

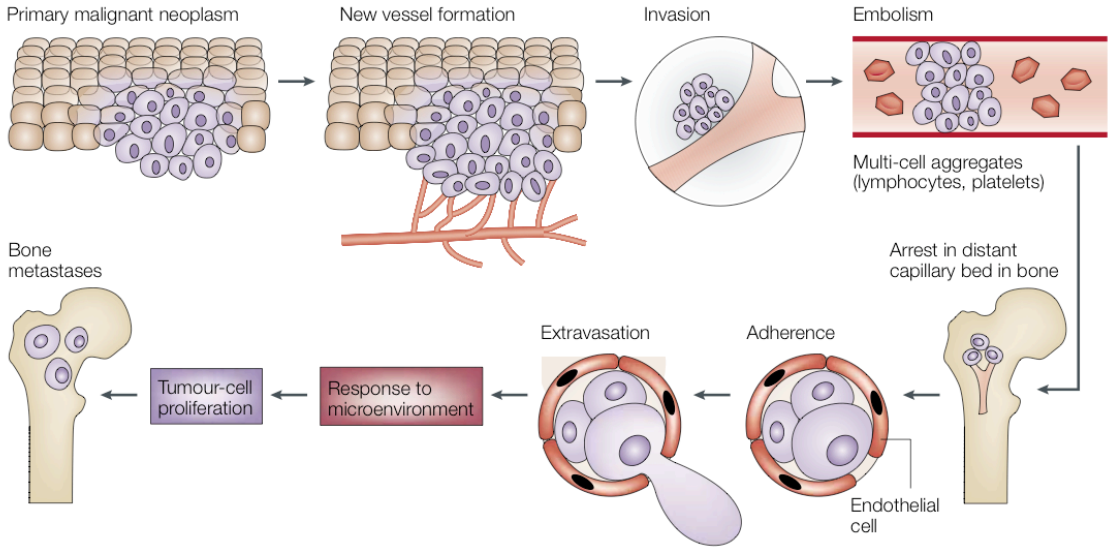

Figure 4. Steps involved in tumour cell metastasis from the primary site to the skeleton (Mundy, 2002)

The tumour cells must possess the capacity to migrate across the sinusoid wall of the blood vessel, invade the marrow stroma, build their own blood supply and travel to the endosteal bone surface to stimulate the activity of osteoclasts or osteoblasts, thereby determining whether the following bone metastasis is osteolytic or osteoblastic (Mundy, 2002).

1.2.2 Bone microenvironment, interaction between cancer and bone cells: the vicious cycle

Bone is the first site of androgen-independent prostate, and second site (after lungs) of estrogen-independent breast cancer progression (Bagi, 2005). As a matter of fact, the bone microenvironment, as well as the interaction between bone and cancer cells plays a crucial role in the development and progression of skeletal metastases. In normal physiological conditions, bone remodeling is tightly regulated; with bone resorption coupled to bone formation to ensure that the amount of old bone resorbed equals the amount of new bone deposited. However, colonization of the skeleton by tumour cells (mainly from breast and prostate) disturbs this equilibrium, leading to dramatic changes in bone resorption (lytic tumours), bone formation (blastic tumours) or both (mixed tumours).

The bone matrix harbors many growth factors that are released in the bone marrow cavity following osteoclastic activity. These growth factors include IGF-1, TGFß, FGFs

and PDGFs. IGF-1, the most abundant growth factor stored in bone promotes tumour cell proliferation, chemotaxis and survival whereas TGFß and Ca^{2+}, also stored in large amount in bone, stimulate cancer cell production of PTHrP (Mundy, 2002; Yoneda and Hiraga, 2005). PTHrP then signals in osteoblasts/stromal cells through binding on PTH receptors to increase production of RANKL, a cytokine that plays a central role in osteoclast differentiation and activation (Yoneda and Hiraga, 2005). This consequently leads to increased osteoclastic bone resorption, with released of growth factors that feed back to tumour cells to further stimulate growth and metastasis, creating a "**vicious cycle**" (Bagi, 2005; Mundy, 2002; Yoneda and Hiraga, 2005): resorbed bone releases TGFß and IGF-1, thereby stimulating cancer cell growth and further production of PTHrP, which in turn causes more bone resorption, release of growth factors and subsequent stimulation of tumour cell proliferation. Therefore, osteoclastic activity transforms the bone milieu into a "**fertile soil**" by triggering release of bone stored growth factors and mineral components that support cancer cell growth, establishment and progression of metastases (Figure 5).

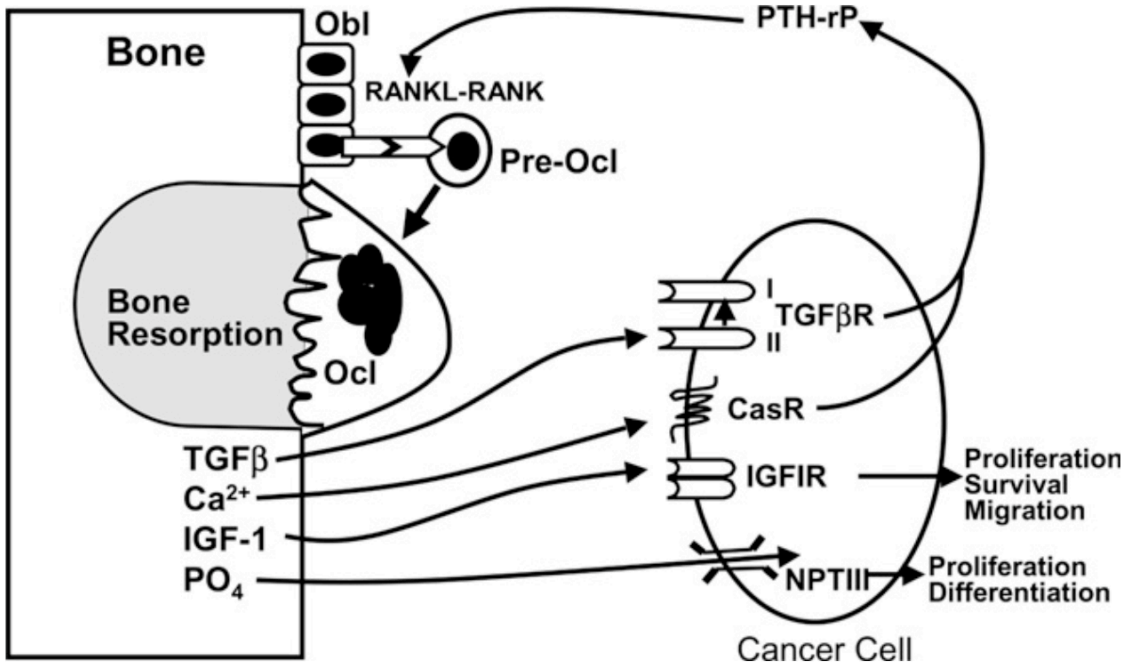

Figure 5. Communication between bone cells and cancer cells in bone metastasis (Yoneda and Hiraga, 2005)

Although being a fertile milieu confers the bone a very attractable target for metastasis, this feature in itself is not sufficient, and in order for metastasis to occur, tumour cells must possess unique biological properties or molecular signatures. In this regard, they

should be able to overproduce PTHrP, activate matrix metalloproteinases (MMP-2, MMP-9), downregulate E-cadherin, express elevated levels of integrins, osteopontin, bone sialoprotein and chemokine receptors (CXCR4, CCR7) (Yoneda and Hiraga, 2005).

1.2.3 Pathophysiology of bone metastases

Once in the local bone microenvironment, tumour cells closely interact with bone cells (osteoblasts and osteoclasts), as well as hematopoeitic and stromal cells to deregulate the normal bone remodeling mechanisms. Depending on the effect of tumour-secreted factors on bone resorption or bone formation, two major metastatic phenotypes have been described (Bagi, 2005; Mundy, 2002). The **osteolytic phenotype** is caused by osteoclast-activating factors that boost out bone resorption while the **osteoblastic phenotype** results from osteoblast-activating factors that stimulate osteoblast proliferation, differentiation and bone formation. Breast cancer metastasizing to bone usually causes osteolytic metastases whereas prostate cancer results in osteoblastic metastases. However, the concept of bone metastases as being either osteolytic or osteoblastic is somewhat overrated, as up to 25 % of patients with bone metastases from breast cancer also show blastic lesions that are similar to those with metastatic prostate cancer, and some patients with prostate cancer have lytic lesions that are comparable to those seen in metastatic breast cancer patients (Mundy, 2002). This has given rise to an additional phenotype, the so-called **mixed tumours**. Interestingly, lytic and destructive lesions are predominant with reduced osteoblast activity in the case of metastatic breast tumour, as opposed to predominant blastic lesions associated with resorptive components in metastatic prostate tumour. Yet, some types of metastases, particularly from myeloma, cause solely osteolytic bone lesions (Bagi, 2005; Mundy, 2002). Osteolytic lesions are associated with massive bone destruction leading to pain, pathological fractures and disability, seriously affecting cancer patient quality of live and worsening the prognosis. Although osteoblastic metastasis is less harmful to bone morphology and has lesser impact on bone health as compared to lytic tumours, it is very unlikely that the newly randomly deposited bone with woven internal structure (rather than linear) fulfills any mechanical function in the skeleton (Bagi, 2005).

1.2.3.1 Mechanism of osteolytic metastases

Bone resorption through the action of osteoclasts is likely to be the main mechanism in the early stages of bone metastasis, and is probably the main mechanism by which osteolysis (particularly in breast and prostate cancer) progresses (Bagi, 2005). The peptide PTHrP released by breast tumour cells is the main mediator of osteoclast activation (Bagi, 2005; Mundy, 2002). This is in line with the findings that breast cancer cells that have metastasized to the bone produce elevated levels of PTHrP than do those remained in the primary site or those who have metastasized to soft tissues (Mundy, 2002). More to the point, the resulting osteolysis was shown to be blocked by neutralizing antibodies against PTHrP. PTHrP stimulates production of RANKL by Osteoblasts/stromal cells, which in turn binds to its receptor RANK on osteoclasts and osteoclasts precursors to enhance osteoclast differentiation and bone resorption. If it is now widely accepted that cancer cells by themselves do not have the ability to resorb the bone, they do however produce the osteoclastogenic cytokine RANKL, and whether or not this particular RANKL produced by tumour cells is sufficient to activate osteolysis is still a matter of debate (Mundy, 2002). Other osteoclastogenic factors produced by cancer cells include TNFα and ß, IL-1, 6, 8 and 11, estrogen receptors, PTH receptors, as well as TGFα and ß (Bagi, 2005; Mundy, 2002). Osteoclasts are pivotal in the pathogenesis of tumour-associated osteolysis, as they are directly responsible for focal bone loss at metastatic sites, as well as the release of bone stored growth factors (IGF-1, TGFß, FGFs, PDGF, BMPs) into the local environment that feed back to stimulate tumour cell growth. Other causes of cancer-associated bone loss may be deprivation of sex steroids, disuse or immobilization, use of cytotoxic cancer therapies, radiation therapy and use of palliative therapies such as glucocorticoids.

1.2.3.2 Mechanism of osteoblastic metastases

Osteoblastic lesions occur most commonly in prostate cancer and result from a direct stimulation of osteblast proliferation and bone formation by tumour-secreted factors. One of the best well-characterized mediators is the growth factor endothelin-1 (Bagi, 2005; Mundy, 2002). Other factors include IGFs, TGFß, FGFs, BMPs, uPA, PSA and the B isoform of PDGF.

1.3 Cyclodepsipeptides

Depsipeptides are a group of natural or synthetic compounds having sequences of amino and hydroxy carboxylic acid residues (usually alpha-amino and alpha hydroxy acids), commonly but not necessarily regularly alternating and joined by amide and ester bonds. In cyclodepsipeptides, the residues are connected in a ring.

Cyclodepsipeptides have been isolated from bacteria, actinomycetes and fungi. The recent years have witnessed a tremendous effort in the identification of these compounds, mostly motivated by the large scope of their biological activities and therapeutic opportunities. They are lipophilic ionophores, which are readily incorporated into cell membranes, forming cation selective pores that allow ions to pass through (Firakova, et al., 2007; Lemmens-Gruber, et al., 2009). In this regard, they greatly influence cell membrane permeability and action potential. Additionally, their antibiotic, insecticidal, anthelmintic, antimicrobial, phytotoxic, antimalarial and cytotoxic properties are established (Firakova, et al., 2007; Lemmens-Gruber, et al., 2009). It is believed that the cyclic structure of the depsipeptide is essential for the biological activity, as their linear homologues are inactive (Lemmens-Gruber, et al., 2009).

Beauvericin and enniatins are well-described, structurally related cyclohexadepsipeptides (six residues connected in a ring) mycotoxins produced by *Fusarium* (Audhya and Russell, 1974; Doel, et al., 1978; Gupta, et al., 1991; Logrieco, et al., 1998; Logrieco, et al., 2002), *Beauveria* (Hamill, et al., 1969; Suzuki, et al., 1977), *Paecylomyces* (Bernardini, et al., 1975) and *Polypovirus* (Doel, et al., 1978). They occur in food contaminated grain samples (corn, wheat, barley, feed) (Logrieco, et al., 2002; Jestoi, et al., 2004; Uhlig, et al., 2004). However, the health risk for the population following exposure to these toxins is still unclear and may be underestimated as to date, there have been no convincing data to shed light on the topic. They have been proven to be phytopathogenic, endowed with antibiotic, insecticidal (Grove and Pople, 1980; Guadet, et al., 1989; Gupta, et al., 1991), hydrophobic (Tomoda, et al., 1992), and ionophoric properties (Kamyar, et al., 2004; Kouri, et al., 2003; Kouri, et al., 2005), and have been reported to inhibit acyl-CoA: cholesterol transferase (Tomoda, et al., 1992), the enzyme that catalyzes the conversion of cellular cholesterol and long chain fatty acyl-CoA into cholesteryl ester.

1.3.1 Beauvericin

Beauvericin was first isolated in the fungus *Beauveria bassiana* (Hamill, et al., 1969), but is also produced by several other fungi including *Fusarium*, and is active against Gram-positive bacteria and mycobacteria (Castlebury et al., 1999; Fotso and Smith, 2003). Chemically (Figure 6), beauvericin is a cyclic hexadepsipeptide with alternating methyl-phenylalanyl and hydroxyl-iso-valeryl residues.

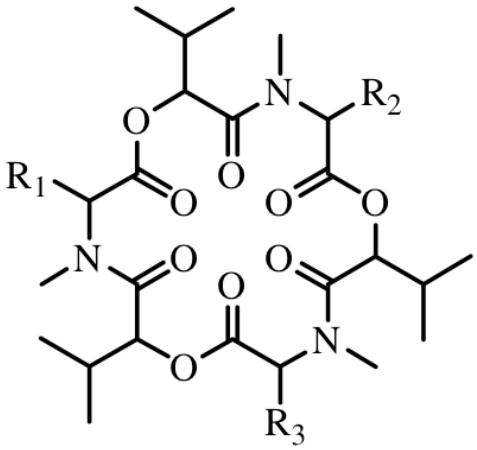

Compound	
Beauvericin	R_1=R_2=R_3= -$CH_2C_6H_5$
Enniatin A	R_1=R_2=R_3= -$CH(CH_3)CH_2CH_3$
Enniatin A1	R_1=R_2= -$CH(CH_3)CH_2CH_3$, R_3= -$CH(CH_3)_2$
Enniatin B	R_1=R_2=R_3= -$CH(CH_3)_2$
Enniatin B1	R_1=R_2= -$CH(CH_3)_2$, R_3= -$CH(CH_3)CH_2CH_3$

Figure 6. Chemical structure of beauvericin and enniatins (Uhlig, et al., 2004)

Beauvericin is not mutagenic (Fotso and Smith, 2003), but rather cytotoxic to several mammalian cell line models, including the murine P815 mastocytoma cells, Yac-1 lymphoma cells and EL-4 thymoma cells (Ojcius, et al., 1991); the rat mast cell like RBL-1 cells, the simian fibroblastoid CV-1 cells and the human IARC/BL 41 cells (from Burkitt's lymphoma), HeLa cells (from cervical carcinoma) and Hep G2 cells (from hepatoma) (Logrieco, et al., 2002; Macchia, et al., 1995); the human monocytic cells U-937 and promyelocytic leukemia cells HL-60 both of myeloid origin (Calo, et al., 2004); the human lymphoblastic leukemia cells (CCRF-CEM) (Jow, et al., 2004)

and the porcine kidney PK15 cells (Klaric, et al., 2008). In particular, beauvericin induces programmed cell death similar to apoptosis, and causes cytolysis accompanied by internucleosomal DNA fragmentation into 200 bp (Macchia, et al., 1995; Ojcius, et al., 1991). Beauvericin induced cytotoxicity has been shown to be mediated by increased intracellular Ca^{2+} calcium influx, either from internal stores (Jow, et al., 2004; Ojcius, et al., 1991), or by extracellular Ca^{2+} influx via the plasma membrane prior to the increased intracellular Ca^{2+} apoptotic effect (Tang, et al., 2005).

1.3.2 Enniatins

Enniatins are secondary metabolites produced predominantly by the fungi *Fusarium* during an enzymatic reaction catalyzed by enniatin Synthetase. Their anthelminthic, anti-HIV-1 and antimalarial activities have been reported (Firakova, et al., 2007; Lemmens-Gruber, et al., 2009). Likewise beauvericin, enniatin was found not to be mutagenic at toxic concentrations (Behm et al., 2009). Interestingly, enniatins have been shown to act as potent inhibitors of drug efflux pumps (ATP-binding cassette transporters), thereby holding promise for the management of multidrug resistance that usually occurs in bacterial resistance or cancer therapy due to pumping of chemotherapeutics out of the cells (Firakova, et al., 2007). Dornetshuber *et al*. (Dornetshuber, et al., 2007) have reported slight, but significant tumor-promoting effect after short term exposure (up to 8 hours) of human mammalian cells to nanomolar concentrations of enniatin, as compared to its apoptotic-inducing effect at low micromolar concentrations already after 24 hours treatment.

1.4 Scope of the study

Bone loss occurs when bone resorption by osteoclasts uncouples from bone deposition by osteoblasts, either temporally or spatially. In low turnover bone loss, bone formation slows down and lags behind bone resorption, condition that prevails in aging, disuse and glucocorticoids medication. However, in high turnover bone loss, bone resorption dominates and can be generalized as observed in hyperparathyroidism, sex steroids deprivation (estrogens and androgens) and thyrotoxicosis; or localized in focal osteolysis observed in rheumatoid arthritis, Paget disease of bone, periodontitis and skeletal metastases. These disorders are associated with bone pain, pathological fractures, hypercalcemia and disability; seriously compromising bone health and

severely affecting a patient's quality of life. The past decade has witnessed remarkable advances in our understanding of the pathogenesis of these bone disorders. It is now clear that the osteoclast is the principal culprit of these conditions, and therefore represents the first choice therapeutic target. Biphosphonates are by far the gold standard for the management of bone loss, as they directly inhibit osteoclast activity and survival. However, their therapeutic use is narrowed by frequent side effects like on the oesophagus and rare but serious side effects like osteonecrosis of the jaw, calling for new medications.

Cyclodepsipeptides are mycotoxins with an immense spectrum of biological activities, ranging from ionophoric, antibiotic, insecticidal, phytotoxic, anthelminthic and antimalarial to cytotoxic. Recently, cyclodepsipeptides dextruxins were reported to inhibit bone resorption without affecting osteoclast differentiation and survival (Nakagawa, et al., 2003), bringing evidence for the first time that cyclodepsipeptides could actually affect bone resorbing cells, and consequently raising the need of screening other cyclodepsipeptides for their antiresorptive effects. Beauvericin and enniatins, their related homologues, have been proven cytotoxic to several mammalian cell lines models and tumour cells. However, their effect on bone cells, namely osteoblasts and osteoclasts, remains yet to be elucidated. Given the effect of dextruxins on osteoclasts, it is anticipated that beauvericin and enniatins might exhibit these inhibitory properties as well.

Increased osteoclast activity is observed during osteolytic tumour metastasis. The crosstalk between tumour cells and bone cells (osteoblasts and osteoclasts) in the bone microenvironment, the so-called vicious cycle, is determinant for the establishment and progression of metastasis. As bone resorption is likely to be the main mechanism in the early stages of bone metastasis, and probably the main mechanism by which osteolysis, particularly from breast and prostate cancer patient progresses (Bagi, 2005), an effect of beauvericin and enniatins on osteoclasts is therefore likely to impact on the tumour cell itself in the local bone milieu. As a consequence, it was also of interest to examine the direct effect of beauvericin and enniatins on tumour cells that have the ability to metastasize to the bone.

The aim of this study was to characterize pharmacological and toxicological effects of two structurally related cyclohexadepsipeptides mycotoxins beauvericin and enniatins on bone cells (osteoblasts and osteoclasts), as well as on cancer cell lines (MDA-MB-231, PC3 and U2OS).

More specifically, this study aimed to:

- examine the effect of beauvericin and enniatins on osteoclast differentiation, cytoskeleton, activity, survival and apoptosis;
- evaluate the effect of beauvericin and enniatins on cell viability and apoptosis of osteoclast precursors (osteoblasts and RAW 264.7);
- establish the signal transduction pathways affected in RAW 264.7 and coculture-derived osteoclasts following exposure to beauvericin and enniatins;
- investigate the effect of beauvericin and enniatins on the proliferation, viability and apoptosis of metastatic breast (MDA-MB-231) and prostate (PC3) cancer cell lines, as well as on a primary tumour of bone cell line (U2OS);
- elucidate the molecular signaling pathways of beauvericin and enniatins in these metastatic and non metastatic cell lines.

1.5 Presentation of the thesis

This work is subdivided in 4 main sections: an introduction with aim and objectives (behind) followed by a materials and methods section. The outcome of the experimental work is presented in 2 parts (manuscript 1 and manuscript 2). Each manuscript is a complete paper formated according to Biochemical Pharmacology Journal with figures located at the end just before the references. The last section is the summary and conclusion.
The bibliography section of this thesis contains complete references of the citations in the introduction section.

2 Materials and methods

2.1 Materials

2.1.1 Commonly used solutions and buffers

a) PBS without Ca^{2+}/Mg^{2+} 10X: 2.00 g KCl, 2.00 g KH_2PO_4, 80.00 g NaCl, 27.07 g $Na_2PO_4.2H_2O$, 1000 ml distilled H_2O. Mixed to dissolve, this solution is diluted 1:10 with distilled H_2O, sterile filtrated before use and stored at 4 °C.

b) PBS with Ca^{2+}/Mg^{2+} 10X: 1.00 g $CaCl_2$ (anhydrous), 2.00 g KCl, 2.00 g KH_2PO_4, 1.00 g $MgCl_2.6H_2O$, 14.34 g $Na_2HPO_4.2H_2O$, 80.00 g NaCl, 1000 ml distilled H_2O. Mixed to dissolve, this solution is stored at 4 °C. Dilute 1:10 with distilled H_2O and adjust the pH to 7.2 using NaOH 5N before use.

c) TBS 10X: 24.20 g Tris base, 80.00 g NaCl, 1000 ml distilled H_2O. Mixed to dissolve, this solution is immediately diluted 1:10 with distilled H_2O for the preparation of TBS 1X and the pH adjusted to 7.6 using 37 % HCl. To prepare TBST 0.1 % and 0.3 %, 1 liter of TBS 1X is diluted with 1 ml and 3 ml of Tween 20 respectively.

d) Running buffer 10X: 286.50 g glycerin, 60.50 g Tris base, 40.00 g SDS, 2000 ml distilled H_2O. Mixed to dissolve, this solution is stored at room temperature. Dilute 1:10 with distilled H_2O and adjust the pH to 8.9 before use.

e) Transfer buffer: 36.00 g glycerin, 7.53 g Tris base, 4000 ml distilled H_2O. Mix to dissolve and adjust the pH to 8.3. This solution is stored overnight at 4 °C, then completed with 1000 ml methanol and stored at 4 °C.

f) Sample buffer 4X: 6.06 g Tris base, 9.45 g glycerin, 6.00 g SDS, 0.20 g bromophenol blue, 0.11 g EDTA, 50 ml distilled H_2O. Mixed to dissolve, this solution is stored at –20 °C.

g) Stripping buffer 1X: 9.31 g Tris HCl, mix to dissolve with 800 ml distilled H_2O, adjust the pH to 6.8 using NaOH 5N, add 20.00 g SDS, mix and adjust the

volume to 1000 ml with distilled H_2O. This solution is stored at 4 °C and always supplemented with ß-mercaptoethanol (700.00 µl ß-mercaptoethanol in 100 ml stripping buffer) before use.

h) Lower Tris buffer: 18.17 g Tris base, mix to dissolve with 800 ml distilled H_2O, adjust the pH to 8.8 using 37 % HCl, add 4.00 g SDS and complete the volume to 100 ml with distilled H_2O. This solution is sterile filtrated using a folded filter paper and stored at 4 °C.

i) Upper Tris buffer: 6.06 g Tris base, mix to dissolve with 800 ml distilled H_2O, adjust the pH to 6.8 using 37 % HCl, add 4.00 g SDS and complete the volume to 100 ml with distilled H_2O. This solution is sterile filtrated using a folded filter paper and stored at 4 °C.

j) Ponceau red solution 0.2 %: 0.20 g ponceau S, 3.00 g Trichloro acetic acid, 100 ml distilled H_2O. Mixed to dissolve, this solution is stored at room temperature.

k) NaN_3 solution 500X: 0.10 g NaN_3, 1 ml distilled H_2O. Mixed to dissolve, this solution is stored at 4 °C.

l) Lysis buffer 1.50 ml: 1.50 ml Frackelton lysis buffer, 75.00 µl NaF (1 M), 7.50 µl Aprotinin (2 mg/ml), 15.00 µl Leupeptin (1 mg/ml), 1.50 µl Pepstatin (1 mg/ml), 15.00 µl Orthovanadate (200 mM), 15.00 µl PMSF (100 mM). Mix to dissolve. This solution is prepared immediately before use.

m) Blocking solution 5 % non fat dry milk: 1.25 g dry milk (fix milk), 25 ml TBST 0.1 %. Mix to dissolve at +80 °C. This solution is prepared immediately before use.

n) Trypsin/EDTA 10X: 0.25 g trypsin (1:250), 0.20 g EDTA, 10 ml PBS without Ca^{2+}/Mg^{2+} 1X. Mix to dissolve. This solution is sterile filtrated and stored at – 20 °C. Dilute 1:10 with sterile PBS without Ca^{2+}/Mg^{2+} 1X before use.

o) Toluidine blue staining solution 1 %: 1.00 g sodium borate, 1.00 g toluidine blue O, 100 ml distilled H_2O. Mix to dissolve and store at room temperature.

2.1.2 Gel for electrophoresis

a) Running gel 10 %: 1430 µl H_2O, 880 µl Lower Tris buffer, 1170 µl acrylamide, 1.05 µl TEMED, 17.50 µl APS. Mixed to dissolve, this solution is used immediately for one gel of a Bio-Rad Minigel system (Mini-Protean II).

b) Stacking gel 10 %: 945 µl H_2O, 375 µl Upper Tris buffer, 195 µl acrylamide, 2.04 µl TEMED, 15 µl APS. Mixed to dissolve, this solution is used immediately for one gel of a Bio-Rad Minigel system (Mini-Protean II).

2.1.3 Tartrate resistant acid phosphatase (TRAP) staining solution

a) TRAP buffer: 0.11 g Na-acetate, add 20 ml of distilled H_20, adjust the pH to 5 using HCl 1M, add 0.046 g Na-tartrate. Mix to dissolve.

b) Naphtol solution: 0.005 g naphtol AS-MX phosphate, 500 µl N,N-dimethyl formamide. Mix to dissolve.

c) Staining solution: 9 ml TRAP buffer, 90 µl naphtol solution, 5.40 mg fast red violet salt. Mix to dissolve by sonicating 5 minutes in ultrasound bath.

2.1.4 Equipments and supply

2.1.4.1 Equipments

Equipments	**Company name**
Autoclave	Tomy SX–300E, Tomy Kogyo Co..LTD, Japan
Bone saw	Isomet Low Speed Saw, Buehler, USA
Centrifuges	Hermle Z323K, Hermle, Germany SORVALL® RT7, Minnesota, USA

Cell counter + analyzer	Casy®1 Model DT Schärfe system, Germany
Computers	Power Macintosh, Windows 2000 or XP
Digital camera	Coolpix 995, Nikon, Japan
Digitalization table	KT-0405-A, Wacom, Japan
Electrophoresis mould	Protean® II xi Slab Cell, Bio-Rad, USA
ELISA-reader	Labsystems Multiskan MS, Labsystems, Finland
Eppendorf centrifuge	Eppendorf centrifuge 5415 C, Eppendorf, Germany
Eppendorf thermomixer	Eppendorf Thermomixer 5436, Eppendorf, Germany
Fluorescence microscope	Optiphot2-UD, Nikon, Japan
Hemocytometer	IVO, Germany
Ice machine	Scotsman AF–10, Germany
Incubators	Hera Cell 240, Kendro®, Germany Modell 500, Memmert, Germany
Inverted microscopes	Diaphot 300, Nikon, Japan TMS, Nikon, Japan
Laminar air flow	Ehret Reinraum Technic, Germany
Light source for microscope	KL 1500 Electronic, Schott, North America
Magnetic stirer	Ikamag® RCT, Germany
Microscope	Olympus BX51, Japan
pH-Meter	713 pH Meter, Metrohm, Switzerland
Saw blades	Diamond wafering blades/series 15 HC Diamond, Buehler, USA
Scales	LC 621 P, Sartorius, Austria MC 210 P, Sartorius, Austria
Shaker	Swip, Edmund Bühler, Germany
Shaking incubator	GFL® 3032, Burgwedel, Germany
Sterilizer	WTC Binder, Germany
Ultrasound bath	Transsonic T 570, Elma, Germany

Ultra pure water system	Milli-QUF PLUS, Millipore
Video camera	DXC-ISIAP, Sony, Japan
Vortex	Vortex Genie 2™, Bender & Hobein AG, Zurich, Switzerland
Water baths	GFL® 1086/1092, Burgwedel, Germany
Water purification system	Milli-RO 5 PLUS, Millipore

2.1.4.2 Supply

Supply	Company name
Centrifuge tubes 15 and 50 ml, cell scrapers	Sterilin, Bibby Sterilin Ltd., UK; 3010 Costar, Cambridge, USA
Coverslips (22 x 22 mm) and microscope slides (76 x 26 mm)	Menzel-Glaser, Germany
Cryogenic vials	Falcon, Becton Dickinson, USA
Eppendorf tubes	Eppendorf, Germany
Glass pipettes 5, 10, 20 and 25 ml	Silber Brand, Germany
Injection needles $27G^{3/4}$ 0.4x19 $N^{r}20$	Becton Dickinson, Ireland
Nitrocellulose membrane 0.45 µm and gel blotting filter paper	Whatman Schleicher & Schull, Dassel, Germany
Plastic pipettes 1, 5, 10 and 25 ml	Costar, Corning Incorporated, USA
Polystyrene round-bottom tubes 5 ml	BD Falccon™, USA
Silicon	GE Bayer Silicones, USA
Syringes 1, 5 and 10 ml	Terumo Europe, Belgium
Tissue culture plates-6, 12, 24, 48, 96-well plates	Costar, USA; Falcon, USA; Greiner Bio-one, Germany; Iwaki, Japan; Nunc, Denmark
Tissue culture dishes-2, 5 and 10 cm	Iwaki, Japan; Sterilin, UK
Amersham Hyperfilm™ ECL	GE Healthcare, Japan

2.1.5 Cells, culture media, sera

- Osteoblasts were isolated from the calvariae of new-born mice (1 to 2 days old);

- Bone marrow cells were extracted from the femora and tibiae of 6 to 8 weeks old mice;
- The monocyte-macrophage cell line RAW 264.7 was obtained from American Type Culture Collection (ATCC) (Manassas, VA, USA);
- The metastatic breast cancer MDA-MB-231, the metastatic prostate cancer PC3 and the osteosarcoma cell line U2OS were also obtained from the ATCC;
- α-MEM (Alpha modification of the minimum essential medium) was purchased from Gibco, Invitrogen, UK;
- α-MEM containing 2 mmol/l glutamax was from Gibco, Invitrogen, UK;
- Fetal calf serum (FCS) was from Sigma-Aldrich Chemie GmbH, Taufkirchen, Germany.

2.1.6 Test substances

The substances used were 2 cyclohexadepsipeptides, beauvericin (#B-7510) and enniatins (#E-3643), both produced as a desiccate by Sigma Aldrich Chemie, Taufkirchen, Germany.
Enniatins (ENN) had a purity of approximately 96 %, a molecular weight of 681.5 g/mol and was composed of 3 % enniatin A, 20 % enniatin A_1, 19 % enniatin B and 54 % enniatin B_1. Beauvericin (BEA) was of 99 % purity with a molecular weight of 784 g/mol. The concentrations used ranged from 0.01 μM to 10 μM. The substances were dissolved in absolute ethanol to make stock solutions at 0.1 mM, 1 mM and 10 mM. The substances are light sensitive; therefore, the desiccates were stored dark at 4 °C and the stock solutions at – 80 °C.

2.2 Methods

2.2.1 Cell culture and maintenance

- Primary osteoblasts (OB) were maintained in α-MEM supplemented with 10 % heat inactivated FCS (Sigma, lot 114k3395), 100 U/ml penicillin (Life Technologies Inc. Grand Island, USA) and 100 μg/ml streptomycin (Life Technologies Inc. Grand Island, USA);

- RAW 264.7 cells were cultured in α-MEM containing glutamax (2 mmol/l) enriched with 10 % heat inactivated FCS, 100 U/ml penicillin, 100 µg/ml streptomycin, in the presence or absence of 50 ng/ml rm RANKL (R&D systems, Minneapolis, MN, USA);
- Bone marrow cells were isolated from femora and tibiae, and cocultured with osteoblasts in α-MEM enriched with 10 % FCS, 100 U/ml penicillin, 100 µg/ml streptomycin, 1 µM PGE_2 (#14010, Cayman Chemical, USA) and 1 nM 1,25 $(OH)_2$ vitamin D_3 (#R0 21-5535, Hoffmann-La Roche AG, Basel, Switzerland);
- Cancer cells (MDA-MB-231, PC3 and U2OS) were grown in α-MEM supplemented with 10 % heat inactivated FCS, 100 U/ml penicillin and 100 µg/ml streptomycin.

All cells were maintained at 37 °C in a humidified atmosphere of 5 % CO_2 in air. The cells were refreshed every 2 or 3 days with new medium according to the specific requirements of each cell line.

2.2.2 Splitting

Cells were grown on tissue culture dishes until confluency. Confluent cells were washed (with 37 °C warm PBS without ca^{2+}/Mg^{2+}) and detached from the culture dishes by enzymatic digestion using 37 °C warm 1X trypsin/EDTA or otherwise mentioned. Following enzymatic digestion, cells were collected in centrifuge tubes and spun down at 1500 rpm for 5 min at 4 °C. The pellet was resuspended in culture medium and the cells seeded and allowed to proliferate onto new culture dishes with splitting rates of 1:4.

2.2.3 Freezing

Following enzymatic digestion, cells were pelleted, resuspended in new medium, and counted using the Casy® cell counter + analyzer system. The counted cells were pelleted again and resuspended in a defined volume of freezing medium (50 % heat inactivated FCS, 40 % α-MEM and 10 % DMSO). About 4 millions cells in 1.5 ml freezing medium were aliquoted in cryogenic vials. The latter were immediately placed in freezing containers (Nalgene, USA) with isopropanol and stored for overnight at –80 °C

to allow freezing at a constant rate of -1 °C/min. These vials were later transferred in liquid nitrogen tanks for long term storage.

2.2.4 Primary osteoblast isolation

Primary OB were isolated by sequential collagenase IV (#C9891, Sigma-Aldrich St. Louis, MO, USA)/dispase II (#165859, Boehringer Mannheim, IN, USA) digestion of calvariae from 1 to 2 days old mice. The calvariae were extracted, washed in cold PBS without Ca^{2+}/Mg^{2+} and transferred in a 50 ml centrifuge tube with cold PBS without Ca^{2+}/Mg^{2+}. Thereafter, calvariae were digested four times for 10 min each and the last time for 20 min with enzyme solution (0.1 % collagenase IV, 0.2 % dispase II, α-MEM free of serum and antibiotics) in a shaking incubator at 37 °C, 200 rpm. The supernatant of the first digestion step (fraction I) was discarded, and the 4 other fractions were pulled together in a fresh centrifuge tube and pelleted at 1500 rpm, 4 °C for 10 min. The cells were resuspended in α-MEM containing 10 % heat inactivated FCS, 100 U/ml penicillin, 100 µg/ml streptomycin, and seeded in 10 cm tissue culture dishes (cells from 10 calvariae in one dish). After 24 hours, the cells were refreshed with new medium and cultured until confluency (one more day). The cells were then splitted, cultured until confluency again (2 days) and frozen.

2.2.5 Preparation of mouse osteoclasts-like cells from bone marrow

6 to 8 weeks old mice were killed by cervical dislocation and their femora and tibiae were aseptically isolated and placed in a 10 cm dish with either sterile PBS without Ca^{2+}/Mg^{2+} or an old culture medium. The muscles were removed under sterile conditions and the marrow cavity was flushed out with α-MEM containing 10 % FCS for bone marrow, using a G27 hypodermic needle and a 1 ml syringe. The cells were homogenized, transferred in a 50 ml centrifuge tube and pelleted at 1500 rpm for 5 min at 4 °C. The bone marrow cells were then resuspended and cocultured (cells from one femur bone in 12 wells of a 48-well plate) with primary osteoblasts isolated from 1 to 2 days old mice calvariae (1 million osteoblasts in 12 wells of a 48-well plate) on either bone slices (for pit assays and attachment on bone surface), coverslips (for attachment on glass surface) and/or on culture dishes (for attachment on plastic surface). The cells were submitted to osteoclastogenic conditions (1 µM PGE_2 and 1 nM 1,25 $(OH)_2$

vitamin D_3), together with the pharmacological compound (BEA or ENN) and maintained in culture for 5 to 6 days at 37 °C and 5 % CO_2. The cells were refreshed every 2 days with new medium and after culture, they were submitted to TRAP staining for trapping of multinucleated cells with 3 or more nuclei.

2.2.6 Preparation of rabbit osteoclasts

Osteoclasts (OC) were isolated from long bones of 5 days-old New Zealand white rabbits. They were transferred onto plastics, coverslips or bone specimens and first incubated for 2 hours in α-MEM (with 10 % FCS heat inactivated, 100 U/ml penicillin and 100 µg/ml streptomycin), then rinsed to remove most of the contaminating cells and thereafter incubated for 24 hours in the presence or absence of different concentrations of the test compounds.

2.2.7 Preparation of bovine bone slices

Bovine bone was previously isolated from cattle, dried for 24 hours at 50 °C and stored in cooling conditions (4 °C). Bone was cut into slices of 300-350 µm thickness using a low speed Isomet saw with diamond blade. The slices were further cut into small pieces of equal square (4 mm x 4 mm) that could fit neatly 4 by 4 in a well of 48-well plate. Thereafter, the bone slices were sonicated 3 times for 5 min each in distilled water and one time for 5 min in 70 % ethanol. Under the laminar air flow, the bone slices were tagged (scratch with the pencil) on one side, and each side was UV-radiated for 15 minutes. The bones were then glued on sterile silicone, 4 per well in a 48-well plate, the marked side down, and preincubated for at least 2 hours or overnight in α-MEM with 10 % heat inactivated FCS, 100 U/ml penicillin and 100 µg/ml streptomycin (0.5 ml total volume per well) at 37 °C, 5 % CO_2.

2.2.8 Measurement of bone resorption

Bone marrow cells (1 femur bone for 12 wells of a 48-well plate) were cocultured with OB (1 million cells for 12 wells of a 48-well plate) on bone slices (4/well) under osteoclastogenic conditions (1 µM PGE_2 and 1 nM 1,25 $(OH)_2$ vitamin D_3) for 5 to 6 days in the presence of the pharmacological compound (BEA or ENN). At the end of the culture, the bone slices were removed from the wells and given in polystyrene tubes

with 70 % isopropanol (not more than 8 bones slices per tube). The bones slices were then sonicated for 15 min to ensure complete washing of adherent cells and rests of silicone, then dried on a clean towel paper and incubated 1/well in a 24-well plate, with 700 µl of 1 % toluidine blue each for 4 min on a shaker at room temperature. Staining with toluidine blue made it possible to see the resorption areas under the microscope. Afterwards, the bone slices were rinsed in 3 changes of distilled water, dried and stored in a 96-well plate (1/well) until pit area measurement. The areas of osteoclast resorption lacunae were visualized using an Olympus BX51 microscope with a 5x magnification under oblique light. 2 pictures per bone slice were taken with the camera (intelligent exposure) of the Cell * F computer program (one at the left upper corner and the other at the right lower corner). The 2 pictures were further combined in one picture on which pit areas were traced and analyzed using the digitalization table and pen of the Cell * F. For each bone slice, the software automatically calculated the sum of all pits areas and the total bone surface on which pits areas were traced. These results were then copied in Microsoft Excel which gave us the percentage of resorption /bone slice.

$$\% \text{ resorbed area} = \frac{\text{total area of pits}}{\text{total area of bone slice}} * 100$$

2.2.9 TRAP staining of osteoclasts

Cells cultured on plastic surfaces or on coverslips were washed with 37 °C warm PBS with Ca^{2+}/Mg^{2+}, fixed with 3.7 % formaldehyde (Sigma-Aldrich Chemie GmbH, Steinheim, Germany) for 3 and 10 min, washed with PBS again and stored at 4 °C in PBS with Ca^{2+}/Mg^{2+} containing Sodium azide to prevent infection. Thereafter, the cells were incubated with the TRAP buffer for 30 min at 37 °C, 5 % CO_2. Following incubation in alcohol/acetone solution (v/v) for 30 seconds at room temperature, the cells were freed for 2 min to allow dehydration. The cells were then incubated for 5 to 10 min with the staining solution at 37 °C, 5 % CO_2 and the staining was stopped by washing the cells in 3 changes of distilled water. Stained cells were visualized under an inverted microscope, magnification 10x, and multinucleated cells with 3 or more nuclei were counted. The cells were stored at 4 °C for further investigations.

2.2.10 Growth inhibition assay

MDA-MB-231 ($15x10^4$ cells/well), PC3 ($23x10^4$ cells/well) and U2OS ($7x10^4$ cells/well) were seeded in triplicates in 6-well plates and allowed to attach for 2 days. Cells were then treated with the vehicle (absolute ethanol) or drug in increasing concentrations for 24 and 48 hours. Before treatment, cells of 3 wells (each well handled separately) were enzymatically detached, collected and counted using the Casy cell counter. The average count at this step was considered as the starting time 0 cell density for all vehicle and treated groups. At different time points, cells were enzymatically detached, collected, counted and the average cell density per treated group (n=3 wells/group) was compared to the average cell density of the vehicle group at that specific time point. The data are presented as mean ± SEM.

2.2.11 Cell viability assay

The MTS-test was used to determine the number of viable cells in culture. This method involves the CellTiter 96®AQueous One Solution Reagent (#G3580, Promega, Madison, WI, USA) composed of 1.90 mg/ml MTS and 300 µM PES in Dulbecco's buffered saline, pH 6.0. OB ($2x10^4$ cells/well), RAW 264.7 ($4x10^4$ cells/well), MDA-MB-231 ($37x10^3$ cells/well), PC3 ($37x10^3$ cells/well) and U2OS ($25x10^3$) were seeded in 96-well plate, 8 wells per groups, and allowed to attach for at least 1 hour. Thereafter, cells were submitted to the vehicle or drug in increasing concentrations for 6 to 48 hours. Before termination, the cells were incubated with 20 µl of the CellTiter reagent for 2 hours and the absorbance was read at 490 nm with a Multiskan plate reader. The data were collected using Delta Soft3 software and the results are presented as a proportion of viable cells in the presence of pharmacological compound compared to the vehicle group.

2.2.12 Cytoskeleton staining and apoptosis

OB, OC and RAW 264.7 cells on coverslips were fixed with 3.7 % formaldehyde in PBS for 3 and 10 min, incubated with Alexa Fluor 488 conjugated phalloidin (0.165 µM in PBS) (#A12379, Molecular Probes, Invitrogen) for 30 min at room temperature followed by the DAPI reagent (0.1 µg/ml in PBS) (Sigma-Aldrich) for 10 min at 37 °C

and 5 % CO_2. MDA-MB-231, PC3 and U2OS on coverslips were fixed for 3 and 10 min with 3.7 % formaldehyde in PBS at room temperature, and then incubated with 0.1 µg/ml of the DAPI reagent in PBS for 15 min at 37 °C, 5 % CO_2. The coverslips were mounted onto microscope glass slides using fluorosave embedding medium, sealed with Fixogum rubber cement (Marabuwerke GmbH & Co.KG, Germany) and stored at 4 °C. Stained coverslips were examined under a fluorescence microscope using the triple band filter set DAPI/FITC/TRITC and a 40x objective with immersion oil. The cytoskeleton was examined on the basis of cell shape and F-actin organization using phalloidin labeling, while apoptotic cells were identified based on the condensation of chromatin and fragmentation of nuclei (apoptotic bodies) with DAPI staining.

2.2.13 Study of cell transduction signaling

2.2.13.1 Principle of ECL western blotting detection of proteins

Enhanced chemiluminescence (ECL) western blotting is a light emitting, non-radioactive method for detection of immobilized specific antigens, directly or indirectly with Horseradish peroxidase (HRP) labeled antibodies. Enhanced chemiluminescence is achieved by performing the oxidation of luminol (substrate in the ECL detection reagent) by the HRP (conjugated on the secondary antibody) in the presence of chemical enhancers such as phenols. The oxidized luminol then decays to the ground state by emitting a light with maximal intensity between 5 and 20 min and a half-life of approximately 60 min. The maximum light emission is at a wavelength of 428 nm and can be detected by a short exposure to blue-light sensitive autoradiograghic film (Hyperfilm ECL).
This technique is widely used to detect and identify proteins that have been previously resolved on SDS-PAGE (sodium dodecyl sulfate polyacrylamide gel electrophoresis) and blotted onto a membrane.

2.2.13.2 Cell culture and lysis

RAW 264.7 cells were cultured on 6-well plates (Iwaki) in presence or absence of 50 ng/ml rm RANKL for 5 to 6 days. The role of the cytokine was to allow differentiation of the monocyte-macrophage cell line into multinucleated cells. Following culture, cells were treated with the vehicle (ice cold absolute ethanol) or with the pharmacological

compound (1 μM BEA or 10 μM ENN) for different time points (1 min, 15 min, 1h, 2h), then washed 3 times with ice cold PBS and submitted to lysis. Cells were lysed in lysis buffer (50 mM NaCl, 10 mM Tris-base, 1 % Triton X-100, pH 7.05) containing proteases and phosphatases inhibitors (50 mM NaF, 10 μg/ml Aprotinin, 10 μg/ml Leupeptin, 1 μg/ml Pepstatin, 2 mM Orthovanadate, 1mM PMSF), using 100 μl lysis buffer for 2 wells and cell scrapers to detached the cells from the wells. Lysed cells were then transferred into eppendorf tubes, sonicated on ice for 1 min to shear the DNA, vortexed every 2 min for 15 min and centrifuged at 4 °C, 15000 rpm for 15 min. The supernatant was collected and 5 μl of cell lysate was used for the protein assay while the rest was stored at –80 °C for further analyses.

2.2.13.3 Protein assay

The total sample protein content was assayed in a Greiner 96-well plate using the Bio-Rad DC protein assay reagents kit (reagents A, B and S) (Bio-Rad Laboratories, Hercules, CA, USA). 5 μl of sample (cell lysate or BSA standard at different concentrations) was incubated with 25 μl solution A' (mixture of reagent A + reagent S: for 1000 μl of reagent A, we needed 20 μl reagent S to obtain the solution A') and 200 μl reagent B. The plate was then gently vortexed and incubated for 15 min at room temperature. The absorbance was read at wavelength 690 nm, using a Labsystems Multiskan MS plate reader and data were processed using Delta Soft 3 software. Therefore, the standard curve was plotted automatically and the protein concentrations were read directly. Results are expressed as μg protein/μl cell lysate and represent the mean values from 2 replicates.

2.2.13.4 Electrophoresis

About 30 μg of proteins per sample were resolved on 10 % SDS-PAGE. The running gel was prepared and poured into a Bio-Rad mini-gel mould. The system was left at room temperature for at least 1 hour or overnight, to allow polymerization. Following, the stacking gel was prepared and overlaid on the running gel. The comb was inserted in there, to pre-set the wells into which the samples will be further deposited, and left at room temperature for 1 hour to allow polymerization. At the same time, the samples were being prepared by mixing with 1X and 4X sample buffers, cooking at 95 °C for 5

min, followed by a quick centrifugation. After polymerization of the stacking gel, the comb was gently removed and the wells washed 3 times with 1X running buffer. The system was then transferred in an electrophoresis tank (Mini Protean II Electrophoresis Cell) with 1X running buffer for running of the electrophoresis. Equal volumes of samples corresponding to equal amounts of proteins (30 μg/sample) were loaded into the wells. The cell lysate of a reference cancer cell line (A-431) was used as control for sufficient protein separation, as well as a molecular weight marker containing standard proteins with known molecular weights (SeeBlue Plus2 Prestained Standard, #LC5925, Invitrogen; or PageRuler Prestained Protein Ladder, #SM0671, Fermentas). The SDS included in the samples linearized the proteins, and conferred to them a negative charge. Therefore, they were allowed to migrate across the gel towards the anode only according to their weight. A current of 350 mV with a potential difference of 25 mA was applied until all samples reached the running gel. Thereafter, the proteins were submitted to a new current of 350 mV with a potential difference of 35 mA and migrated all along the running gel. The electrophoresis was termed finished when all samples had resolved until the level of the appropriate molecular weight markers.

2.2.13.5 Transfer of proteins to nitrocellulose membrane

Following electrophoresis, the gel with Proteins was carefully removed from the electrophoresis plates and immediately given on a filter paper, then covered with the nitrocellulose membrane and again with a second filter paper (creating a sandwich). The whole system was placed into a transfer tank (Mini Protean II Electrophoresis Transfer Cell) containing a magnetic stir bar and a cold transfer buffer was added. The proteins were transferred from the gel to the nitrocellulose membrane in cooling conditions, under a current of 100 V and 350 mA, on mixing with a magnetic stirrer for 1 hour. Thereafter, the nitrocellulose membrane was carefully marked with a pencil and stained with 0.20 % ponceau red to check for successful protein transfer and localization of proteins bands.

2.2.13.6 Membrane blocking and antibody incubation

The nitrocellulose membrane was rinsed 3 times with sterile water (to wash away the ponceau staining) and washed 5 min in TBS 1X (Tris buffer saline 1X) at room temperature on shaking. The blot was then incubated with the blocking solution (5 %

non fat dry milk in 0.1 % TBST) for 1 hour at room temperature on shaking. This step had the benefit to block non-specific sites of the antibody on the membrane. Following the blocking step, the blot was washed 3 times for 5 min each in 0.1 % TBST (Tris buffer saline tween 20) on shaking, and incubated for overnight at 4 °C with the primary antibody diluted 1:1000 (or otherwise stated) in 0.1 % TBST. Thereafter, the blot was washed 3 times for 5 min each in 0.1 % TBST on shaking, and incubated for 1 hour with the secondary antibody (anti-rabbit or anti-mouse IgG HRP conjugate) diluted 1:5000 in 0.1 % TBST at room temperature. The detection was performed with an enhanced chemoluminescence detection kit. The membranes were stripped off bound antibodies after ECL detection and reprobed several times. It is important to point that during washing steps, the volume of wash buffer was as large as to completely submerge the blot and at any time, the blot was not allowed to dry out.

The primary antibodies used were anti phospho Src-Tyr416 (1:1000, rabbit polyclonal, #2101, 60 kDa), anti phospho Akt-Ser 473 (1:1000, rabbit monoclonal, #4060, 60 kDa), anti phospho NF-κB p65-Ser536 (1:1000, rabbit monoclonal, #3033, 65 kDa), anti phospho-p38 MAPK Thr180/Tyr182 (1:1000, rabbit polyclonal, #9211, 43 kDa), anti caspase 3 (1:1000, rabbit polyclonal, #9662, 35 kDa) and anti cleaved PARP (1:1000, rabbit polyclonal, #9544, 89 kDa) from Cell Signaling, Inc (Beverly, MA, USA). Anti phospho p-44/42 MAPK Thr202/Tyr204 (1:1000, mouse monoclonal, #9106, 44/42 kDa) was from New England Biolabs, Inc (Ipswich, MA, USA). Anti E-cadherin (1:2500, mouse monoclonal, #C20820, 120 kDa), anti FAK (1:1000, mouse monoclonal, #F15020, 125 kDa) and anti STAT3 (1:2500, mouse monoclonal, #S21320, 92 kDa) were purchased from Transduction Laboratories (Lexington, KY, USA). Anti PI3 kinase α (333) (1:1000, rabbit polyclonal, #sc-423, 85 kDa) was from Santa Cruz Biotechnology, Inc (Santa Cruz, CA, USA) and anti ß-actin (1:2000, mouse monoclonal, #A-2228, 42 kDa) from Sigma (St. Louis, MO, USA). The secondary antibodies anti-mouse IgG HRP-conjugate (#W4021) and anti-rabbit IgG HRP-conjugate (#W4011) were from Promega (Madison, WI, USA).

2.2.13.7 ECL detection of proteins

Following incubation with the secondary antibody, the membrane was washed 3 times for 5 min each in 0.1 % TBST on shaking at room temperature. The membrane was further washed 2 times for 5 min each in TBS 1X to allow complete removal of the tween 20 from the membrane, as the latter could interfere with ECL reagents and

increase the background. The detection solution was prepared by mixing v/v detection reagent 1 and detection reagent 2 (both from GE Healthcare, UK), and the volume of this solution was calculated by multiplying the surface of the nitrocellulose membrane (in cm^2) by 0.125 ml. Therefore, the blot was incubated with the detection solution for 1 min at room temperature, then wrapped in a saran wrap and placed in the x-ray film cassette. The film was developed in the dark room under x-ray light and red safe light for short time period (20 seconds to 20 minutes) and following detection, the film was aligned with the blot to allow identification of molecular weight markers.

2.2.13.8 Stripping and reprobing

The complete removal of primary and secondary antibodies from the membrane had been made possible by stripping. After each ECL detection, the membrane was stored wet at 4 °C wrapped in a saran wrap. To perform the stripping, the membrane was washed 4 times for 5 min each in 0.1 % TBST at room temperature on shaking, followed by incubation for 30 min in the stripping buffer (containing ß-mercaptoethanol) at 50 °C and 100 rpm. Thereafter, the blot was washed 6 times for 5 min each in 0.1 % TBST at room temperature on shaking, and then blocked again in 5 % non fat dry milk before reprobing with another antibody.

2.2.13.9 Statistical analysis

Data were analysed using one factor ANOVA (analysis of variance) incorporated in the StatView statistical program. All experiments were repeated at least 3 times. Statistical differences between groups were determined by Fisher's LSD test. Significant differences are presented as *$p<0.05$, **$p<0.01$, ***$p<0.001$ compared to the control groups.

3 Achievement of the study

3.1 Manuscript 1: Structurally related cyclodepsipeptides beauvericin and enniatins differentially regulate bone resorption and osteoclast survival

F. Tedjiotsop Feudjio[a], S. Forsdahl[b], J. Nguemo Djiometio[a], R. Lemmens-Gruber[a], O. Hoffmann[a,*]

[a] Department of Pharmacology and Toxicology, University of Vienna, Althanstrasse 14, A-1090 Vienna, Austria

[b] Department of Pharmacy, Faculty of Health Sciences, University of Tromsø, Norway

* Correspondence: Professor Oskar Hoffmann, Department of Pharmacology and Toxicology, University of Vienna, Althanstrasse 14, A-1090 Vienna, Austria

Tel.: +43-1-4277-55340; fax: +43-1-4277-55390

E-mail: oskar.hoffmann@univie.ac.at

Abstract

Beauvericin (BEA) and enniatins (ENN) are structurally related cyclohexadepsipeptides, produced by several strains of the *fungi* genus *Fusarium*, *Beauveria*, *Polyporus* and *Paecilomyces* that are known to contaminate food and feed. There is compelling evidence that fungal toxins may influence development and activity of osteoclasts (OC) and consequently, may be useful for the treatment of osteoporosis and bone tumours. To evaluate their effects on OC, we: 1- cocultured murine bone marrow cells with primary calvarial osteoblasts (OB) to generate OC, 2- assessed OC differentiation and viability using TRAP staining, 3- performed pit analyses of bovine bone slices, and 4- stained the cytoskeleton with alexa fluor 488 conjugated phalloidin. BEA inhibited bone resorption by disrupting the resorbing organelle (actin ring) of OC while ENN did not affect the actin ring structure and inhibited bone resorption directly by reducing the number of TRAP-positive OC. Moreover, BEA did not affect cell viability of mature OC, but induced apoptosis in OC likely by mechanisms involving ERK1/2 phosphorylation. Interestingly, ENN inhibited OC viability in a Src/Akt dependent manner and induced signal transduction pathways similar to that of PP2, a reference Src inhibitor. These results illustrate that BEA and ENN differentially regulate OC life span and activity. Therefore they could be potential candidates for the treatment of OC-induced bone loss used either alone or in combination.

Key words: apoptosis, cyclohexadepsipeptides, ERK1/2, resorption, Src/Akt, viability

1. Introduction

Osteoclasts (OC) are multinucleated cells of the monocyte-macrophage lineage whose main and specific function is to regulate mineral homeostasis by resorbing the extensive surface of mainly trabecular bone [1,2]. For the proper development and maintenance of bone size, shape and integrity, the bone deposition (by OB) should be tightly balanced quantitatively, spatially and temporally with the bone resorption (by OC). A net increase in the rate of bone resorption with an insufficient increase in the rate of bone formation inevitably leads to osteoporosis with an increase risk of bone fractures, a state that is associated to many metabolic diseases; including Paget's bone disease, various arthritis, diabetes mellitus [3]; and tumor osteolysis. Therefore, an identification of pharmacological compounds that could regulate bone cell generation and function

would be of great interest in the understanding and control of metabolic and metastatic bone diseases.

Beauvericin (BEA) and enniatins (ENN) are well-known cyclohexadepsipeptide mycotoxins produced by *Fusarium* [4-8], *Beauveria* [9,10], *paecilomyces* [11] and *polypovirus* species [5]. They occur in fungi-contaminated grain samples at concentrations up to several mg/kg [8,12,13] and their toxicity to humans and animals may be underestimated, as to date there are no convincing evidence on the topic. However, they have been proven to be phytopathogenic, endowed with antibiotic [14,15], insecticidal [6,16,17], hydrophobic [18], ionophoric [19-21] and non mutagenic [22,15] properties, and have been reported to inhibit acyl-CoA: cholesterol transferase [18], the enzyme that catalyzes the conversion of cellular cholesterol and long chain fatty acyl-CoA to cholesteryl ester. Moreover, BEA is cytotoxic to several mammalian cell line models, including the murine P815 mastocytoma cells, Yac-1 lymphoma cells and EL-4 thymoma cells [23]; the rat mast cell like RBL-1 cells, the simian fibroblastoid CV-1 cells and the human IARC/BL 41 cells (from Burkitt's lymphoma), HeLa cells (from cervical carcinoma) and Hep G2 cells (from hepatoma) [24,25], the human monocytic lymphoma cells U-937 and promyelocytic leukemia cells HL-60 both of myeloid origin [26], the human lymphoblastic leukemia cells (CCRF-CEM) [27] and the porcine kidney PK15 cells [28]. In particular, BEA induces programmed cell death similar to apoptosis and causes cytolysis accompanied by internucleosomal DNA fragmentation into 200 bp [23,25]. BEA induced cytotoxicity has been shown to be mediated by increased intracellular Ca^{2+} influx, either from internal stores [23,27], or by extracellular Ca^{2+} influx via the plasma membrane prior to the increased intracellular Ca^{2+} apoptotic effect [29]. ENN is cytotoxic to human cancer cells [30] and acts as potent inhibitor of drug efflux pumps [31,32].

Despite this huge amount of available information, their effect on the bone tissue is still far from being appreciated. Nakagawa *et al*. [33] reported that destruxins, related cyclodepsipeptides, inhibit bone resorption without affecting OC differentiation and survival, therefore raising the need of screening other cyclodepsipeptides, particularly BEA and ENN, for their antiresorptive effects. Thus in this study, we address the effect of two mycotoxins BEA and ENN on mouse bone cells OB and OC, and on the OC precursor cell line RAW 264.7 cells.

2. Materials and methods

2.1. Animals and cells

The animals used were BALB/c mice and New Zealand white rabbits. The cells used were OB isolated from newborn (1- to 2-days-old) mice; bone marrow cells extracted from femora and tibiae of at least 8-weeks-old mice or 5 days old rabbits, as well as the monocyte-macrophage cell line RAW 264.7. Cell cultures were maintained in a humidified atmosphere of 37 °C and 5 % CO_2 in air.

2.2. Drugs

The substances used were 2 cyclohexadepsipeptides, BEA (#B-7510) and ENN (#E-3643), both purchased as a desiccate from Sigma-Aldrich Chemie (Taufkirchen, Germany). ENN had a purity of approximately 96 %, a molecular weight of 681.5 g/mol and was composed of 3 % enniatin A, 20 % enniatin A_1, 19 % enniatin B and 54 % enniatin B_1. BEA was of 99 % purity with a molecular weight of 784 g/mol. The concentrations used ranged from 0.01 μM to 10 μM. The substances were dissolved in absolute ethanol to make stock solutions at 0.1 mM, 1 mM and 10 mM. The compounds are light sensitive; therefore, desiccates were stored dark at 4 °C and the stock solutions at – 80 °C.

2.3. Chemicals

Recombinant murine mouse RANKL was purchased from R&D systems (Minneapolis, MN, USA). The CellTiter96® AQ_{ueous} One Solution Cell Proliferation reagents were from Promega (#G3580, Madison, WI, USA). ECL western blotting detection reagents were provided by Amersham Pharmacia Biotech (Aylesburg, UK). FluorSave™ reagent was from Calbiochem (San Diego, USA). Alexa-488-conjugated Phalloidin was purchased from Molecular probes (#A12379, Leiden, Netherlands). DAPI (4,6-diamino-2-phenyl-indoldihydrochloride), ponceau red, toluidine blue, naphtol AS-MX-phosphate, fast red violet salt and collagenase type IV (#C9891) were purchased from Sigma-Aldrich (St. Louis, MO, USA). 37 % acrylamide, TEMED and DC protein assay reagent kit (reagents A, B and S) were from Bio-Rad (Hercules, CA, USA). The primary antibodies anti-phospho Akt-Ser473 (rabbit monoclonal, #4060, 60 kDa), anti-

Akt (rabbit polyclonal, #9272, 60 kDa), anti-phospho Src-Tyr416 (rabbit polyclonal, #2101, 60 kDa), anti-phospho NF-κB p65-Ser536 (rabbit monoclonal, #3033, 65 kDa), anti-Non phospho Src-Tyr416 (mouse monoclonal, #2102, 60 kDa), anti-phospho-p38 MAPK Thr180/Tyr182 (rabbit polyclonal, #9211, 43 kDa), anti-p38 MAPK (rabbit polyclonal, #9212, 43 kDa) were from Cell Signaling, Inc (Beverly, MA, USA). Anti-phospho p-44/42 MAPK Thr202/Tyr204 (mouse monoclonal, #9106, 44/42 kDa) was purchased from New England Biolabs, Inc (Ipswich, MA, USA). Anti-PI3 kinase α (333) (rabbit polyclonal, #sc-423, 85 kDa) was purchased from Santa Cruz Biotechnology, Inc (Santa Cruz, CA, USA) and anti-ß-actin (mouse monoclonal, #A-2228, 42 kDa) from Sigma (St. Louis, MO, USA). The secondary antibodies anti-mouse IgG HRP-conjugate (# W4021) and anti-rabbit IgG HRP-conjugate (#W4011) were from Promega (Madison, WI, USA).

2.4. Preparation of osteoblasts

Primary cultures of mouse OB cells were obtained by sequential collagenase/dispase digestion from calvariae of newborn mice. OB were passaged once, grown till confluency again and then stored in liquid nitrogen until experiments were performed. Mouse OB were seeded at a density of $2x10^6$ cells/60 cm^2 in α-modification of the minimal essential medium (α-MEM) supplemented with 10 % heat inactivated FCS (Sigma-Aldrich Chemie GmbH, Taufkirchen, Germany), 100 U/ml penicillin (Life Technologies Inc. Grand Island, USA), and 100 µg/ml streptomycin (Life Technologies Inc. Grand Island, USA) and grown until confluency (approx. 3 - 4 days).

2.5. Preparation of mouse osteoclasts

Bone marrow cells from the femora and tibiae of 6- to 8-weeks-old mice were cultured (density of approx. 500 000 cells/cm^2) together with primary OB isolated from calvariae of newborn mice (density of 30 000 cells/cm^2) on plastics, coverslips or bone slices, under osteoclastogenic conditions (1 nM 1,25-$(OH)_2$-Vitamin D_3 (Hoffmann-La Roche, Basel, Switzerland) and 1 µM PGE_2 (Cayman, USA)) in α-MEM containing 10 % FCS, 100 U/ml penicillin, and 100 µg/ml streptomycin. For differentiation studies, different concentrations of BEA, ENN, or the vehicle (absolute ethanol, final concentration in cultures 1 ‰ v/v) were applied immediately (day 0) and/or at day 2 and 4 with medium

change. Pre-fusion OC were prepared by incubating OB and bone marrow cells together for 4 days under osteclastogenic conditions with one medium refreshment at day 2. For viability experiments [33], primary precursors (OB and bone marrow cells) were cocultured and allowed to differentiate within 5 days into multinucleated OC. Afterwards, the OB layer was carefully removed by washing with warm phosphate-buffered saline (PBS) without Ca^{2+}/Mg^{2+} and the remaining OC culture of about 95 % purity was incubated with 1-10 µM BEA or ENN for 2, 6 and 12 hours.

2.6. Preparation of rabbit osteoclasts

OC were isolated from the long bones of 5 days-old New Zealand white rabbits. They were transferred onto plastics, coverslips or bone specimens and first incubated for 2 hours in α-MEM (with 10 % FCS, 100 U/ml penicillin and 100 µg/ml streptomycin), then rinsed to remove most of the contaminating cells and thereafter incubated for 24 hours in the presence or absence of different concentrations of the test compounds.

2.7. Tartrate Resistant Acid Phosphatase (TRAP) staining

After treatment, cells on coverslips or plastics were fixed with 3.7 % formaldehyde (Sigma-Aldrich, St. Louis, MO, USA) in PBS for 13 min at room temperature, and incubated in the TRAP buffer containing 40 mM sodium acetate (pH 5) and 10 mM sodium tartrate for 30 min at 37 °C, 5 % CO_2. Thereafter, cells were permeabilized with ethanol/acetone (v/v) and stained for activity of TRAP with a solution containing dimethyl formamide, naphthol AS-MX phosphate and fast red violet salt for 5 to 10 min. TRAP-positive multinucleated cells with 3 or more nuclei were counted.

2.8. Toluidine blue staining

Attached OC were removed from bone slices by 15 min sonication in 70 % isopropanol, stained with 0.1 % toluidine blue, washed in distilled water, and stored dry until pit area measurement. The areas of OC resorption lacunae were measured using a Nikon Optiphot microscope with a 10x/0.30 NA objective under oblique illumination. Six photographs per bone slice were taken randomly, digitized using Adobe Photoshop and processed using NIH-Image 6.0 and Microsoft Excel.

2.9. Cell viability assay

The MTS-test (CellTiter 96®AQ_{ueous} One Solution Reagent) was used to determine the number of viable cells in culture. The test was performed by seeding 50 µl suspension of OB at a density of $2x10^4$/well or RAW 264.7 cells at $4x10^4$/well (maintained in α-MEM with 2 mmol/l glutamax, 10 % heat inactivated FCS, 100 U/ml penicillin and 100 µg/ml streptomycin) in a 96-well culture plate (Iwaki, Asahi Techno Glass, Japan). The cells were first incubated for 1 hour to allow attachment on the plastic surface. Thereafter, another 50 µl medium containing different concentrations of the test compounds were added to each well and the cells were incubated for another 6 to 24 hours. 15 µl of the CellTiter reagent was added in each well for the last 2 hours of incubation and the absorbance was read at 490 nm with a Labsystems Multiskan MS plate reader (Labsystems Mult 45139, Finland). The data were collected using Delta Soft3 software. The results are presented as a proportion of viable cells in the presence of BEA or ENN compared to untreated cells (vehicle group).

2.10. Cytoskeleton staining and apoptosis

(OB and bone marrow cells), rabbit OC, OB (2 millions/6-well plate) and RAW 264.7 cells (4 millions/6-well plate) were seeded on coverslips and incubated for 24 hours. Afterwards, the cells were treated with the vehicle or with the pharmacological compound (BEA or ENN) for 6, 12 or 24 hours. Pre-fusion OC obtained at day 4, were further incubated for 24 hours with BEA or ENN. After treatment, the cells (coverslips) were fixed with 3.7 % formaldehyde in PBS for 13 min, incubated with Alexa 488-conjugated phalloidin (0.165 µM) in PBS for 30 min at room temperature followed by the DAPI reagent (0.1 µg/ml) for 10 minu at 37 °C, 5 % CO_2. The coverslips were mounted onto microscopes glass slides (Menzel-Glaser, Germany) using fluorosave embedding medium, sealed with Fixogum rubber cement (Marabuwerke GmbH & Co.KG, Germany) and stored at 4 °C. Stained coverslips were examined under a fluorescence microscope (Optiphot2-UD, Nikon, Japan) using the triple band filterset DAPI/FITC/TRITC and a 40x objective with immersion oil. The cytoskeleton was examined on the basis of cell shape and F-actin organization using the phalloidin labeling, and apoptotic cells were identified based on nuclear fragmentation (apoptotic bodies) and condensation of chromatin (DAPI staining).

2.11. Western Blotting experiments

Mouse OC from primary precursors (OB and bone marrow cells) or OC derived from the monocyte-macrophage cell line RAW 264.7 stimulated with rmRANKL, were treated with the vehicle, BEA (1 μM) or ENN (10 μM) in starvation medium (containing only 0.5 % heat inactivated FCS) at different time points 0, 1, 15, 60 and 120 min. In some experiments, cells were treated with the reference Src kinase inhibitor PP2 (Alexis Biochemicals, Lausen, Switzerland) or the reference MAPK inhibitor PD98059 (Calbiochem, San Diego, USA) prior to the addition of BEA or ENN respectively. After treatment, cells were washed several times with ice-cold PBS and lysed in lysis buffer (50 mM NaCl, 10 mM Tris-base, 1 % Triton X-100, pH 7.05) containing several inhibitors of proteases and phosphatases (50 mM NaF, 10 μg/ml Aprotinin, 10 μg/ml Leupeptin, 1 μg/ml Pepstatin, 2 mM Orthovanadate, 1mM PMSF). About 30 μg of proteins per sample were resolved on 10 % SDS-PAGE according to their molecular weight, electrotransferred onto a 0.45 μm nitrocellulose membrane (Whatman GmbH, Dassel, Germany), blocked for one hour in 5 % non fat dry milk in Tris Buffer Saline Tween 0.1 % (TBST) and incubated overnight at 4 °C with the primary antibody (1:1000 in TBST 0.1 %). Afterwards, the proteins were incubated for one hour with the secondary antibody (HRP-conjugated anti-mouse or anti-rabbit) (1:5000 in TBST 0.1 %) and the detection was performed with an enhanced chemoluminescence detection kit. The membranes were stripped and reprobed several times.

2.11. Statistical significance

The data were processed using one factor ANOVA (analysis of variance) incorporated in the StatView statistical program. All experiments were repeated at least 3 times. Statistical differences between groups were determined by Fisher's LSD test. Significant differences are presented as *$p<0.05$, **$p<0.01$, ***$p<0.001$ versus untreated groups (vehicle).

3. Results

3.1. BEA and ENN inhibit OC differentiation and bone resorption

In our first series of experiments, we found that BEA and ENN inhibit OC differentiation and bone resorption. Primary precursors (OB and bone marrow cells) were seeded on bone slices and treated with BEA or ENN in increasing concentrations (0.1-10 μM). We observed a dose-dependent inhibition of bone resorption by BEA and ENN (Fig.1). However, BEA was more potent as compared to ENN given that the inhibition of bone resorption with 0.1 μM BEA was significantly reduced versus control ($p<0.01$) compared to that of ENN 0.1 μM (Fig.1). These results were confirmed in rabbit OC where BEA and ENN also inhibited bone resorption dose-dependently (Fig. 2) and again, 0.01 μM BEA was more potent in inhibiting bone resorption compared to ENN 0.01 μM. Next, we sought to determine the effect of these 2 compounds on different stages of OC differentiation and consequently on bone resorption. In a coculture system, OB stimulated with vitamin D3 and PGE2 produce several factors including M-CSF and RANKL, which allow bone marrow cells to differentiate within 4 days into pre- fusion OC and to terminally differentiate after 5 days in multinucleated OC with bone resorbing activity. We carried our coculture system (OB and bone marrow cells) on bone slices and treated starting from day 0, from day 2 or from day 4. At lower concentration (0.1 μM), BEA did not inhibit bone resorption (addition from day 4) (Fig. 3A) as compared to the control. However, the same concentration of BEA (0.1 μM) significantly inhibited bone resorption when added from day 0 ($p<0.05$) or from day 2, by inhibiting differentiation of bone marrow cells into OC precursors. From 1-10 μM BEA, we observed a dose-dependent and time-dependent inhibition of bone resorption, confirming the fact that BEA does not only inhibit bone resorption *per se*, but also inhibits differentiation of bone marrow cells in bone resorbing cells (Fig. 3A). With regard to ENN, a lower concentration (0.1 μM) did not significantly affect OC differentiation (when added from day 0 or from day 2), nor did it affect bone resorption (when added from day 4) (Fig. 3B). The moderate concentration 1 μM inhibited OC differentiation (when added from day 0) ($p<0.001$) without affecting bone resorption. Finally, at 10 μM, both, differentiation in OC and bone resorption were significantly inhibited ($p<0.001$). Taken together, these data suggest that BEA and ENN dose-dependently inhibit OC differentiation and bone resorption. However, at moderate concentrations (1 μM), BEA affects both OC differentiation from bone marrow

precursors and bone resorption, while ENN only affects OC differentiation from bone marrow precursors, but not bone resorption *per se*.

3.2. BEA and ENN inhibit differentiation of bone marrow precursors, but not of pre-fusion OC, into TRAP-positive multinucleated OC

To further confirm the effects of both compounds on OC differentiation, we cultured primary precursors (OB and bone marrow cells) on coverslips and allowed them to differentiate into multinucleated OC upon increasing concentrations (0.1-10 μM) of BEA or ENN. The TRAP-staining was performed at the end of the culture (Fig. 4A) and we observed a dose-dependent inhibition of TRAP+ cells, showing a significant effect already at 1 μM with BEA ($p<0.001$) and 10 μM with ENN ($p<0.001$). However, these concentrations were higher than those that inhibited bone resorption in the pit assay conditions (Fig. 1). Indeed, we observed inhibition of bone resorption at 10 times much lower concentrations, 0.1 μM for BEA and 1 μM for ENN. To evaluate the effect of the compounds on pre-fusion OC, we cocultured primary precursors (OB and bone marrow cells) for 4 days to allow them to differentiate in pre-fusion OC (Fig. 4B). We then treated these pre-fusion OC with 1 and 10 μM BEA or ENN for 24 hours, followed by TRAP staining. Interestingly, at 1 μM, BEA and ENN did not affect differentiation into multinucleated OC. However, at 10 μM, they inhibited OC differentiation ($p<0.001$), with BEA being more potent compared to ENN ($p<0.05$). Taken together, these results suggest that first: BEA and ENN inhibit OC differentiation from bone marrow precursors dose-dependently (Fig. 4A), second: At concentrations equal and lower than 1 μM, BEA and ENN have no effect on OC differentiation from pre-fusion OC (Fig. 4B), third: At 1 μM, BEA affects bone resorption from pre-fusion OC (Fig. 3A, addition BEA 1 μM from day 4), but not OC differentiation (Fig. 4B) while at the same concentration (1 μM) ENN has no effect both on bone resorption (Fig. 3B, addition ENN 1 μM from day 4) and OC differentiation (Fig. 4B).

3.3. Effects of BEA and ENN on the cytoskeleton and apoptosis of OC

Polarization of OC is an essential step in the initiation of bone resorption with actin ring being the essential organelle of a resorbing OC. We next evaluated whether or not an effect of BEA or ENN on actin ring formation could be responsible for the inhibition of bone resorption. We cocultured precursors on coverslips for 4 days and then performed

the treatment with 1-10 μM BEA or ENN for 24 hours, followed by phalloidin and DAPI nucleic acid staining. 9.3 % of OC in the control group (Fig. 5B) showed a well-developed actin ring (Fig. 5Aa) with no sign of apoptosis (fragmentation and/or condensation of nuclei). At 1 μM BEA, the number of OC bearing an actin ring (4.7 % OC with actin ring, Fig. 5B) was reduced by half compared to the control and the actin ring was more present as dense patches spread around the cell (Fig. 5Ab). At the same concentration (1 μM), ENN increased the number of OC with well-defined actin ring (Fig. 5Ac) to 12.4 % (Fig. 5B). However, there was no significant differences in the number of apoptotic cells in both BEA 1 μM and ENN 1 μM as compared to the control (Fig. 5C). At a higher concentration (10 μM), the cytoskeleton was not organized as an actin ring in BEA treated-OC (Fig. 5B, $p<0.05$ compared to the control). In ENN treated-OC, the actin appeared as dense patches around the cells and throughout the cytoplasm with slightly reduced OC number bearing an actin ring (7.1 % OC with actin ring, Fig. 5B). Interestingly, at this higher concentration (10 μM), BEA significantly induced apoptosis ($p<0.05$ compared to the untreated control and to ENN 10 μM) whereas ENN had no effect (Fig. 5C). Collectively, these data suggest that BEA primarily affects bone resorption by disrupting the resorbing organelle (actin ring) of OC and later on, due to the reduction of TRAP+ multinucleated cells, while ENN has no effect on the actin ring structure and therefore affects bone resorption due to the reduction of TRAP+ multinucleated OC. Moreover, BEA is apoptotic at higher concentrations (10 μM) whereas ENN is not at all apoptotic.

3.4. ENN, but not BEA, affects OC viability

At this stage, it was interesting for us to determine the effects of our drugs on OC viability. The experiment was performed as described in the materials and methods section. After 2 and 6 hours, neither BEA, nor ENN affected OC viability (Fig. 6A). Surprisingly, after 12 hours incubation, ENN dose-dependently decreased OC viability by half as compared to the control ($p<0.01$ and $p<0.001$ respectively for 1 μM and 10 μM ENN) while BEA had no effect at all. Taken together, these data suggest that ENN, but not BEA affects the OC viability.

3.5. BEA and ENN have more effect on the viability of RAW 264.7 cells than OB

At this point, it was necessary to assess the effect of the cyclodepsipeptides on the viability of OB to make sure that the inhibiting effect observed in OC derived from cocultures was not coming from OB. To do so, we submitted OB to increasing concentrations (0.1-10 μM) of BEA or ENN for 6 to 24 hours and the cell survival rate was determined by the MTS-test method. BEA and ENN affected OB viability (Fig. 6B) only at a higher concentration (10 μM) and at all time points (6-24 hours), but with a more significant effect of BEA ($p<0.001$) than ENN ($p<0.01$ at 6 and 24 h, $p<0.05$ at 12 h) when compared to the control. RAW 264.7 is a monocyte-macrophage cell line that can differentiate in OC upon stimulation with RANKL and is therefore considered to be an OC precursor. We assessed the effect of BEA and ENN on the viability of these RAW 264.7 cells and both compounds exerted significant inhibitory effects, even at a lower concentration (0.1 μM) and at all time points; again with BEA being more potent (Fig. 6B). Moreover, RAW 264.7 cells were more sensitive to both BEA and ENN when compared to OB.

3.6. BEA and ENN induced apoptosis in RAW 264.7 cells and OB

To characterize BEA and ENN-induced growth inhibition, morphological changes of OC precursors (OB and RAW 264.7 cells) were examined using the DAPI staining. The nuclear morphology of the control and treated cells was compared on the basis of nuclear fragmentation and condensation of chromatin. At lower concentrations (0.1 and 1 μM), neither BEA, nor ENN induced apoptosis in RAW 264.7 cells or OB as compared to the control (Fig. 7). However, at a higher concentration (10 μM), BEA significantly induced apoptosis in RAW 264.7 cells ($p<0.001$ at all time points) and in OB ($p<0.05$ at 6 h, $p<0.001$ at 12 and 24 h). At the same concentration (10 μM), ENN also significantly induced apoptosis in RAW 264.7 cells ($p<0.001$ at 12 and 24 h), but at a lower extent in OB ($p<0.05$ at 12 and 24 h). To summarize, BEA and ENN induced apoptosis in RAW 264.7 cells and in OB only at higher concentrations, with more effect on RAW 264.7 cells as compared to OB and with a more apoptotic effect of BEA as compared to ENN.

3.7. Signal transduction of BEA and ENN

3.7.1. Using RAW 264.7 cells

To understand the molecular mechanisms underlying such biological responses, we first used the monocyte-macrophage cell line RAW 264.7 as an OC model. RAW 264.7 cells were cultured for 6 days in the presence of 50 ng/ml rmRANKL to generate OC (Fig. 8). The latter were then treated with BEA 1 μM (Fig. 8A) or ENN 10 μM (Fig. 8B) for different time points, lysed, resolved on SDS-PAGE and the western blot was performed to target phosphorylated and total proteins. Actin served as control for equal loading. The MAPK pathway has been implicated in cell proliferation, differentiation and survival. In BEA treated RAW 264.7-derived OC, the MAPK pathway was affected with activation of ERK1/2 and p38 MAPK. Moreover, we observed a slight upregulation of Akt. On the other hand, ENN affected the MAPK pathway by a dephosphorylation of ERK1/2 at 1 and 15 min of treatment, followed by its rephosphorylation after 1 and 2 hours. Akt and p38 MAPK were upregulated with time, unlike Src that was downregulated. Taken together, these data suggest that BEA and ENN both affect the MAPK and Akt pathways in RAW 264.7-derived OC.

3.7.2. Using a Coculture system

To clarify these findings, we used the coculture system as described in materials and methods. Fig. 9 (A and D) shows the signal transduction pathways of BEA 1 μM in coculture-derived OC. We observed a time-dependent upregulation of Src with maximal levels after 1 and 2 hours. This result was confirmed by the reference Src inhibitor PP2, which prevented upregulation of Src when applied 15 min or 1 hour prior to the treatment with BEA. PI3 kinase was affected neither by BEA, nor when PP2 was applied before BEA implicating that PI3 kinase is either upstream of Src, or is independent of the Src pathway. Akt was downregulated after 1 and 15 min treatment with BEA and upregulated again after 1 and 2 hours. Interestingly, PP2 prevented upregulation of phospho Akt when applied 1 hour prior to BEA treatment indicating that Akt is downstream of Src. BEA affected the MAPK pathway by upregulating p38 MAPK and slightly upregulating phospho ERK1/2. Surprisingly, PP2 did not prevent upregulation of neither ERK1/2, nor p38 MAPK indicating that BEA activates the MAPK pathway in a Src-independent manner. Finally, the NFκB pathway was

downregulated by BEA and was not affected by a pretreatment with PP2 indicating that BEA downregulates NFκB independently of Src. To summarize, BEA acts as a Src activator, promotes a Src-dependent activation of Akt, upregulates the MAPK pathway independently of Src and downregulates the NFκB pathway independently of Src.

Fig. 9 (B and E) shows the signal transduction pathways of ENN 10 μM in coculture-derived OC. Likewise BEA; ENN affected the MAPK pathway by upregulating both ERK1/2 and p38 MAPK. Interestingly, the reference MAPK/ERK kinase (MEK) inhibitor PD98059 alone did not affect ERK1/2. This could be due to our experimental setting which involved starvation of the cells 15 min prior to and during treatment. Moreover, PD98059 did not prevent up-regulation of the MAPK pathway by ENN, indicating that ENN affects the MAPK pathway in a MEK-independent manner. Again, we observed no change in PI3 kinase levels neither with ENN alone, nor when following pretreatment with PD98059. Therefore, PI3 kinase is upstream or independent of the MAPK pathway. On the other hand, ENN downregulated Src more efficiently after 15 min, and when applied prior to ENN, PD98059 did not prevent ENN from downregulating Src. Akt levels increased after 1 and 15 min treatment with ENN and decreased again after 1 and 2 hours. PD98059 had no effect on Akt and did not prevent ENN from upregulating Akt after 1 and 15 min. Finally, ENN downregulated NFκB after 1 and 2 hours and the MEK inhibitor PD98059 did not affect the regulation of NFκB when applied before ENN. In a previous study, Recchia *et al*. [34] used potent and selective c-Src inhibitors (pyrrolopyrimidine derivatives) to investigate the functional and molecular consequences of inhibited c-Src tyrosine kinase activity in OC, and reported that these small pyrrolopyrimidine derivatives impaired OC function and induced cell damage suggesting apoptosis *in vivo* and *in vitro* by mechanisms likely involving selective sustained ERK1/2 phosphorylation. The fact that ENN both downregulated Src and phosphorylated ERK1/2, led us to hypothesize that ENN might be a Src inhibitor. To address this hypothesis, we used PP2, a reference Src inhibitor along side with ENN in the same experimental conditions (Fig. 9C). As expected, PP2, just like ENN, inhibited Src and Akt, upregulated the MAPK pathway and downregulated the NFκB pathway. Altogether, ENN that behaves like a Src kinase inhibitor, upregulates the MAPK pathway independently of MEK and finally downregulates the NFκB pathway in a MEK-independent manner.

4. Discussion

In this study, we observed that first: BEA and ENN dose-dependently inhibited OC differentiation (Fig. 4A) and bone resorption (Fig. 1) from bone marrow precursors, second: at concentrations equal to 1 µM, BEA affected both OC differentiation from bone marrow precursors and bone resorption (Fig. 3A) while ENN affected only OC differentiation from bone marrow precursors, but not bone resorption *per se* (Fig. 3B), third: at concentrations equal and lower than 1 µM, BEA and ENN had no effect on OC differentiation from pre-fusion OC (Fig. 4B), fourth: at 1 µM, BEA affected bone resorption from pre-fusion OC (Fig. 3A, addition BEA 1 µM from day 4), but not OC differentiation (Fig. 4B) while at the same concentration (1 µM) ENN had no effect both in bone resorption (Fig. 3B, addition ENN 1 µM from day 4) and OC differentiation (Fig. 4B) from pre-fusion OC. It was obvious that BEA and ENN might both affect bone resorption through different mechanisms. With regard to ENN, the effect on OC differentiation was correlating with an effect on bone resorption suggesting that ENN may inhibit bone resorption directly by reducing the number of TRAP+ multinucleated cells. Opposed to ENN, the behaviour of BEA was puzzling. Indeed, OC differentiation was not affected at concentrations (BEA 1 µM, Fig. 4B) that inhibited pit formation (Fig. 3A, addition BEA 1 µM from day 4). This phenomenon has been previously reported in related cyclodepsipeptides dextruxins [33]**,** where the latter were found to inhibit pit formation without affecting OC differentiation and survival. Moreover, the authors concluded that dextruxins inhibited bone resorption by specifically affecting the bone-resorbing function (actin rings) of OC. To verify that BEA might be acting by the same mechanism, we performed the cytoskeleton staining of OC treated with BEA or ENN. We confirmed that BEA, like dextruxins [33] primarily affected bone resorption by disrupting the resorbing organelles (actin rings) of OC and later on due to the reduction of TRAP+ multinucleated cells, while ENN had no effect on the actin ring structures and therefore affected bone resorption by directly reducing the number of TRAP multinucleated OC.

The DAPI staining of BEA (10 µM) treated OC presented signs of apoptosis with fragmentation and/or condensation of nuclei. This result is consistent with previous studies where BEA has been reported to be cytotoxic to several mammalian cell line models [23-28]. Moreover, BEA was shown to induce programmed cell death similar to apoptosis and to cause cytolysis accompanied with internucleosomal DNA fragmentation into 200 bp [23,25]. Interestingly, ENN treated-OC presented no

significant signs of apoptosis as compared to the control. However, in 2007, Dornetshuber *et al*. [30] reported that while short-term exposure (up to 8 hours) to ENN at nanomolar concentrations slightly, but significantly stimulated cell proliferation, it showed profound apoptosis-inducing effects, especially against various human cancer cell types at low micromolar concentrations (already after 24 hours of treatment). In our experimental setting, we used micro molar concentrations (1-10 μM) and comparable exposure time (24 hours). Features specific to the different cells lines we have used could explain the discrepancy of our results. Furthermore, we performed the apoptosis experiments using pre-fusion OC and not fully mature OC. Therefore we cannot exclude the possibility that ENN can induce apoptosis in mature OC.

In addition to their similar effects on bone resorption, BEA, calcitonin (a powerful inhibitor of OC activity that exerts a rapid, transient, and reversible inhibition of bone resorption [35]) and dextruxins were found to have another common feature. Indeed, in our series of experiments, we observed that the viability of OC was not affected at all by BEA, one more feature that brings it closer to dextruxins, which are related cyclodepsipeptides previously reported to have no effect on the survival of OC [33]. Unlike BEA and dextruxins, ENN dose-dependently inhibited OC viability after 12 hours. However, the reversibility of the effects of BEA or ENN on bone resorption has not been investigated in this study.

The effects of both mycotoxins, especially ENN, on the induction of apoptosis and reduction of cell viability of OB were not as striking as on RAW 264.7 cells. Osteoporosis is a disease of the bone tissue that results from an imbalance between osteoclastic bone resorption and osteoblastic bone formation. If normal function is to be regained, substances of therapeutic interest should have little or no effect on OB. In this regard, Plotkin *et al*. [36] reported that the therapeutic efficacy of bisphosphonates or calcitonin in diseases such as glucocorticoid-induced osteoporosis might be due, at least in part, to their ability to prevent osteocyte and OB apoptosis. However, it has recently been demonstrated [37] that higher concentrations of alendronate and zoledronate were cytotoxic for OB, decreasing cell viability after 72 h, and this is consistent with our observations. The sensitivity of RAW 264.7 cells to BEA or ENN further supports the observation that these mycotoxins have an effect on OC precursors and are consistent with the observations of Tomoda *et al*. [18] who reported BEA and ENN to exert cytotoxic activities in J774 macrophages and to inhibit acyl-CoA: cholesterol transferase (ACAT) activity with BEA being the most potent inhibitor of microbial origin.

We have investigated the molecular signal transduction pathways of BEA and ENN in RAW 264.7 cells stimulated with the RANK-ligand to differentiate in OC, and in OC generated from cocultures. The proto-oncogene c-Src plays an essential role in bone remodeling, as deletion of the c-Src gene in transgenic mice by homologous recombination leads to osteopetrosis and impaired OC function [38]. Src can be activated downstream from RANK [39], a member of the tumor necrosis factor receptor superfamily that is involved in OC formation and survival, as well as in OC and dendritic cell function [40-43].

We have demonstrated that ENN reduced Src phosphorylation both in RAW 264.7 and coculture derived OC, which was consistent with the inhibition of bone resorption observed with this substance. The role of c-Src in OC differentiation has been controversial. It has been demonstrated that the number of TRAP+ OC was as higher in the Src-/- mice as in the wild type, although these OC were dysfunctional and unable to resorb the bone [44]. However, a reduction of TRAP+ cells following Src inhibition has been recently reported [34], indicating a novel role of c-Src in modulating OC differentiation. ENN inhibited bone resorption by reducing the number of TRAP+ OC rather than affecting the bone resorbing organelles (actin rings). The downregulation of c-Src observed here is in agreement with previous observations [34] and further supports a role of c-Src in OC differentiation. Opposed to ENN, BEA upregulated Src in OC. PP2, a reference Src inhibitor, prevented BEA from upregulating Src, confirming that BEA inhibits bone resorption independently of Src.

Expression of a c-Src molecule truncated at amino acid 251 (Src251), lacking the kinase domain, induces osteopetrosis in wild type and $Src^{+/-}$ mice and worsens osteopetrosis in $Src^{-/-}$ mice by a novel mechanism not seen in $Src^{-/-}$ mice, consisting in an increase in OC apoptosis [45]. Expression of this Src251 molecule was associated with decreased Akt kinase activity and decreased OC survival in response to the RANK-ligand. In our study, ENN dose-dependently inhibited OC survival, correlating with down regulation of Src and Akt while BEA did not affect OC survival likely due to the Src/Akt up-regulation.

P38 MAPK is required for inducing OC differentiation, but without affecting neither the survival, nor the bone resorbing function of OC induced by RANKL [46]. However, c-Src inhibition slightly stabilizes p38 MAPK as suggested by the reduction of phospho-p38 in control versus inhibitor-treated OC [34]. These cyclodepsipeptides have in here been proven to phosphorylate p38 MAPK in OC, although independently of Src and their effects on cell survival.

The activation of the transcription factor NF-κB seems to play a crucial role in OC differentiation. This transcription factor is present as a complex with the inhibitory subunit IκB in unstimulated cells. Activation of NF-κB is controlled by sequential phosphorylation, ubiquitination, and degradation of its inhibitory subunit, IκB. Yet, ERK and NF-κB regulate different aspects of OC activation: ERK is responsible for OC survival whereas NF-κB regulates OC activation for bone resorption [47]. BEA and ENN both downregulated NF-κB, consistent with their inhibition of bone resorption. BEA did not affect the viability of OC, although we noticed a slight phosphorylation of ERK1/2. Meanwhile, BEA induced apoptosis in OC. A role of ERK1/2 in cell death has been previously reported. ERK1/2 activation mediates apoptosis after DNA damage in a p53 independent manner [48]. Moreover, small pyrollopyrimidine derivatives impair OC function and induce cell damage suggestive of apoptosis *in vivo* and *in vitro* by mechanisms involving selective sustained ERK1/2 phosphorylation [34]. Therefore, we believe that the phosphorylation of ERK1/2 following BEA treatment in OC, mediated apoptosis observed in this cells rather than their survival. ENN also upregulated ERK1/2, but without inducing apoptosis in OC. However, this up-regulation of ERK1/2 may not mediate cell survival considering that ENN has been proven to inhibit cell survival. Interestingly, the reference MEK inhibitor PD98059 failed to prevent upregulation of ERK1/2 when applied before ENN suggesting that ENN upregulated ERK1/2 independently of MEK. Further analyses should be carried out to characterize the origin of this upregulation of ERK1/2 in ENN treated OC.

A very striking finding of this study has been the effect of ENN in OC. We have provided evidence that ENN may actually be a Src kinase inhibitor. Indeed, in the same experimental setting, ENN just like PP2 inhibited Src and Akt phosphorylation, upregulated the MAPK pathway and downregulated the NFκB pathway. There is no doubt that the molecular signaling pathways of ENN and PP2 in OC are similar. However, the role of ENN as a Src kinase inhibitor has to be further characterized. In particular, *in vitro* kinase assays have to be performed to confirm these observations and thereafter to determine its potency.

In conclusion, we have shown that the 2 mycotoxins BEA and ENN, although structurally related, differentially regulate OC life span. BEA specifically inhibits bone resorption and induces apoptosis in pre-fusion OC by a mechanism probably involving upregulation of ERK1/2 while ENN specifically inhibits OC survival in a Src/Akt dependent manner. These 2 cyclodepsipeptides could therefore be

potential candidates for osteoporotic therapies where they could be used alone or in combination.

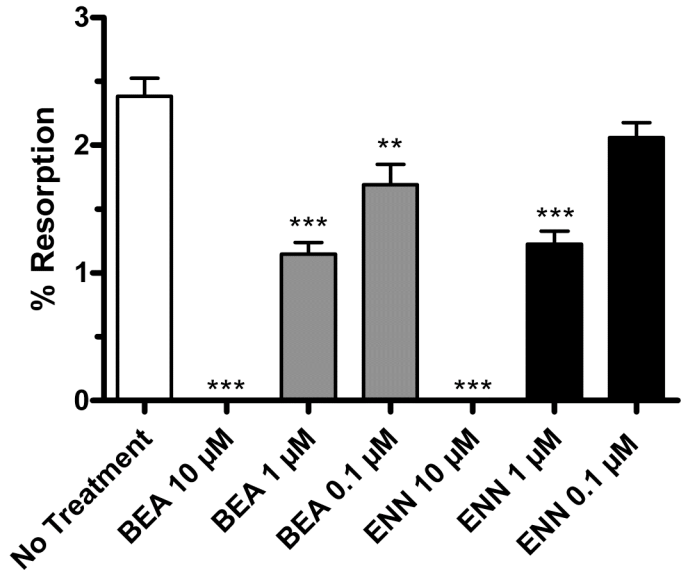

Fig. 1. Dose-dependent inhibition of bone resorption with BEA or ENN in mouse-OC. Bone marrow cells from femora and tibiae of 6- to 8-weeks-old mice were cocultured for 5 days with primary OB from newborn mice on bone slices in 48-well plates. Cells were treated immediately with the vehicle (No Treatment) or BEA or ENN in increasing concentrations. After culture, bone slices were stained with 1 % toluidine blue for pit area measurement. Data are expressed as the mean ± SEM of at least 8 bone slices, *P<0.05; **P<0.01; ***P<0.001 compared with the No Treatment group.

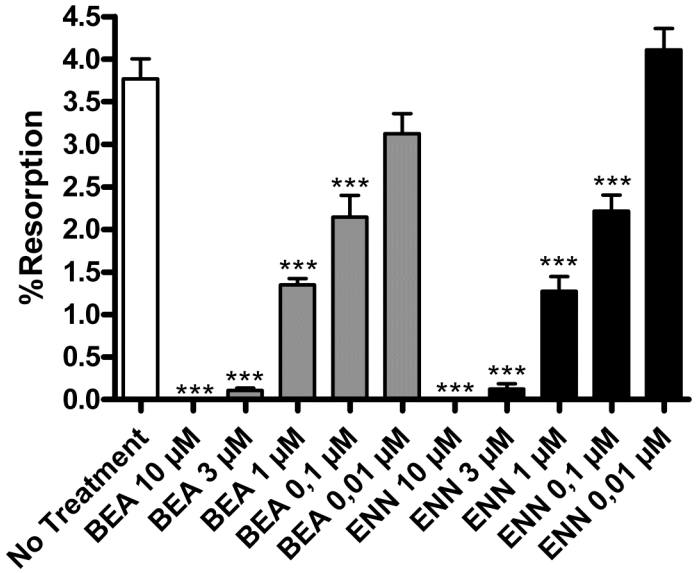

Fig. 2. Dose-dependent inhibition of bone resorption with BEA or ENN in rabbit-OC. OC were isolated from long bones of 5 days-old New Zealand white rabbits and cultured in 48-well plates, on bone slices for 24 hours, in the presence of the vehicle (No Treatment) or BEA or ENN in increasing concentrations. After culture, bone slices were stained with 1 % toluidine blue for pit area measurement. Data are expressed as the mean ± SEM of at least 8 bone slices, *P<0.05; **P<0.01; ***P<0.001 compared with the No Treatment group.

A

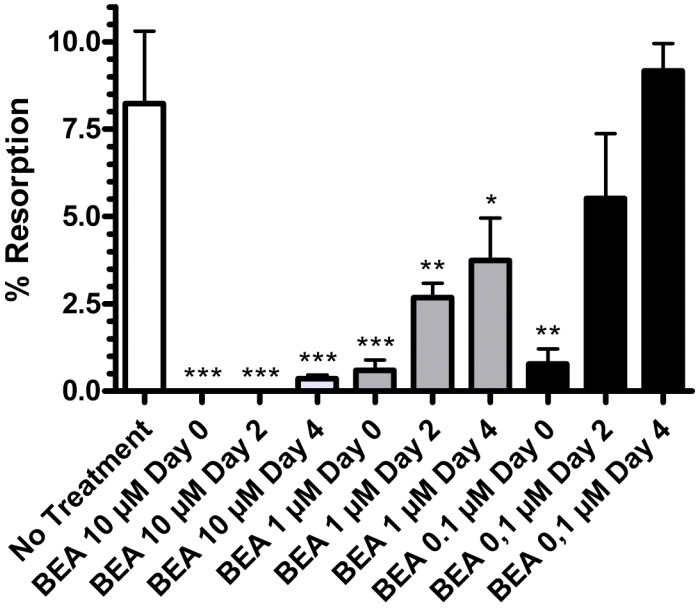

B

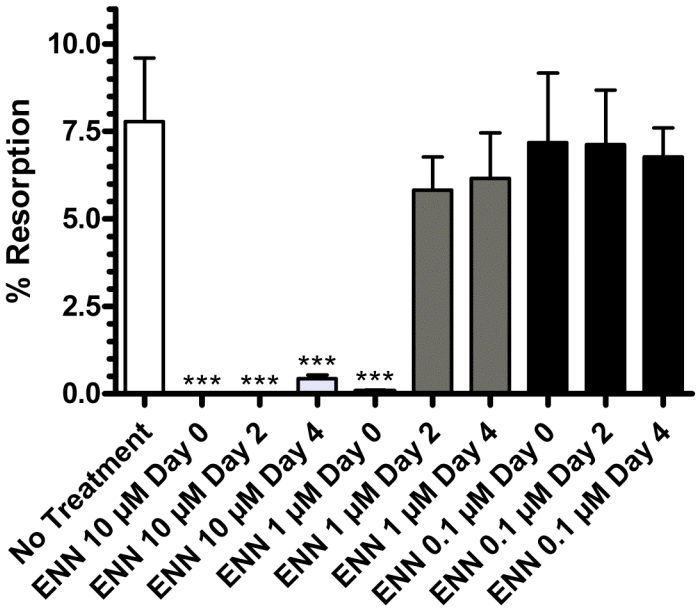

Fig. 3. Dose-dependent and time-dependent inhibition of bone resorption with BEA or ENN in mouse-OC. Bone marrow cells from femora and tibiae of 6- to 8-weeks-old mice were cocultured with primary OB from newborn mice on bone slices in 48-well plates for 5 days. Cells were treated with the vehicle (No Treatment) or BEA (A) or ENN (B)in increasing concentrations from day 0, day 2 and/or day 4. After culture, bone slices were stained with 1 % toluidine blue for pit area measurement. Data are expressed as the mean ± SEM of at least 8 bone slices, *P<0.05; **P<0.01; ***P<0.001 compared with the No Treatment group.

A

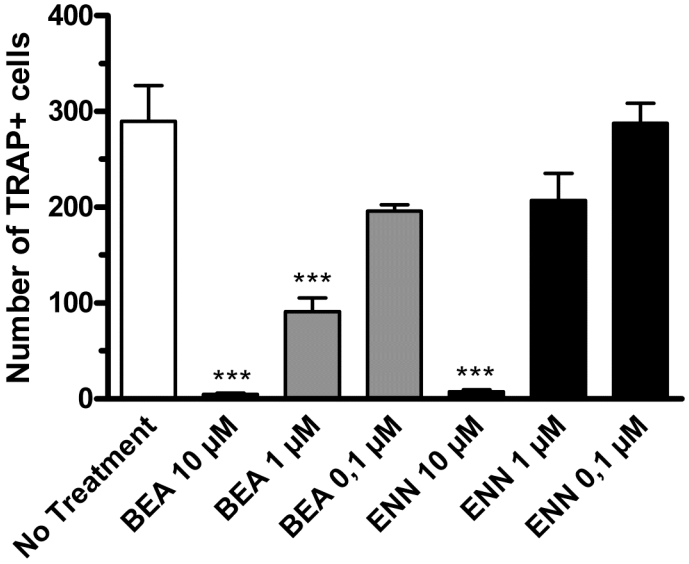

B

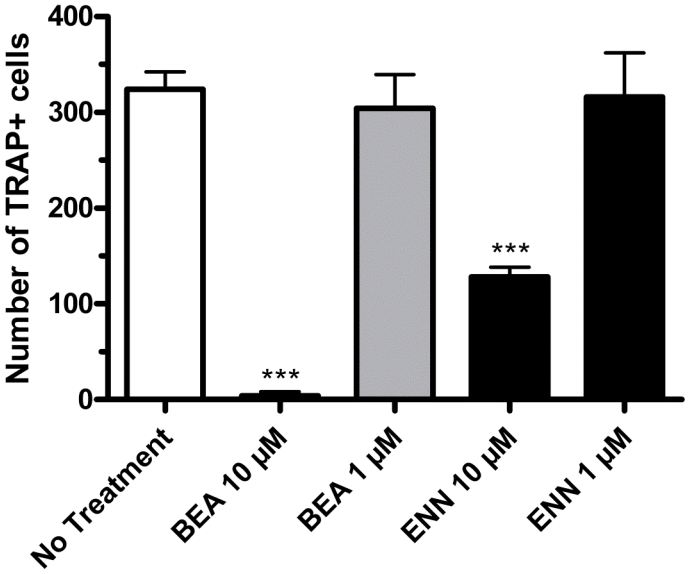

Fig. 4. BEA and ENN dose-dependently inhibit OC differentiation from bone marrow precursors, but not from pre-fusion OC. Bone marrow cells from femora and tibiae of 6- to 8-weeks-old mice were cocultured with primary OB from newborn mice on coverslips in 6-well plates for 5 days. Cells were treated immediately (A) or at day 4 (B) with the vehicle (No Treatment) or BEA or ENN in increasing concentrations. After culture, cells were fixed with 3.7 % formaldehyde in PBS followed by TRAP staining. TRAP-positive multinucleated cells with 3 or more nuclei were counted. Data are expressed as the mean ± SEM of at least 3 coverslips, *P<0.05; **P<0.01; ***P<0.001 compared with the No Treatment group.

A

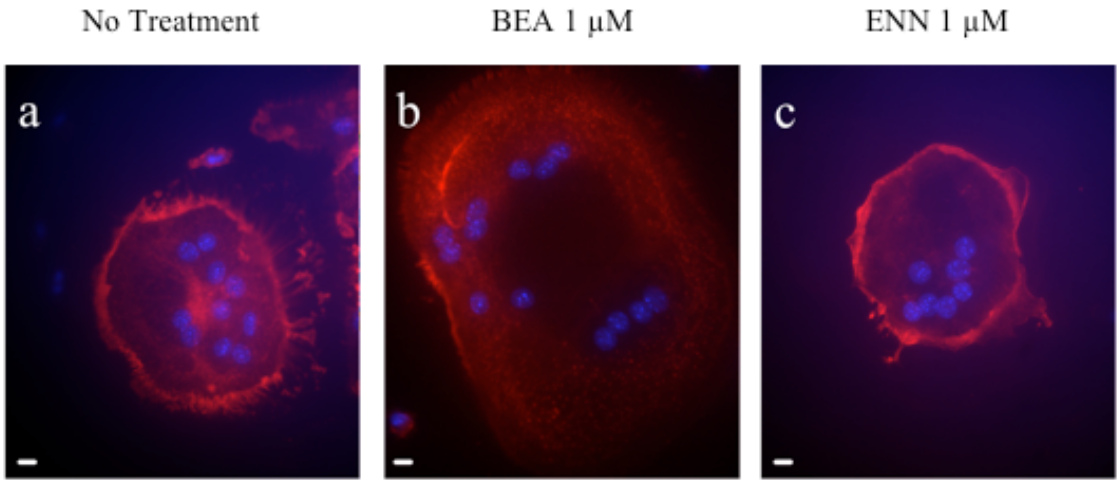

B

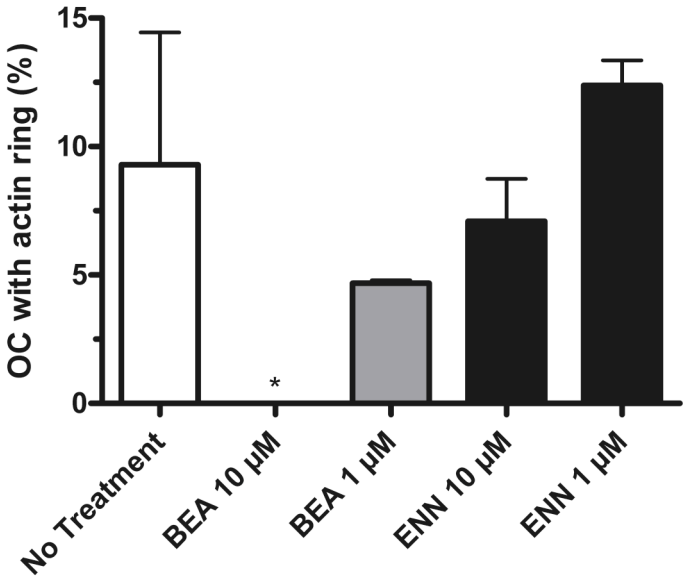

Fig. 5A and B. Effect of BEA and ENN on the cytoskeleton and apoptosis of OC. (A) Pre-fusion OC were treated with the vehicle (No treatment) or with BEA or ENN in increasing concentrations for 24 hours. Following treatment, cells were fixed with 3.7 % formaldehyde in PBS and stained with phalloidin/DAPI. The cytoskeleton was examined on the basis of cell shape and F-actin organization. (B) Quantitative representation of OC bearing an actin ring. *P<0.05 compared with the No treatment group, scale bars represent 10 µm.

C

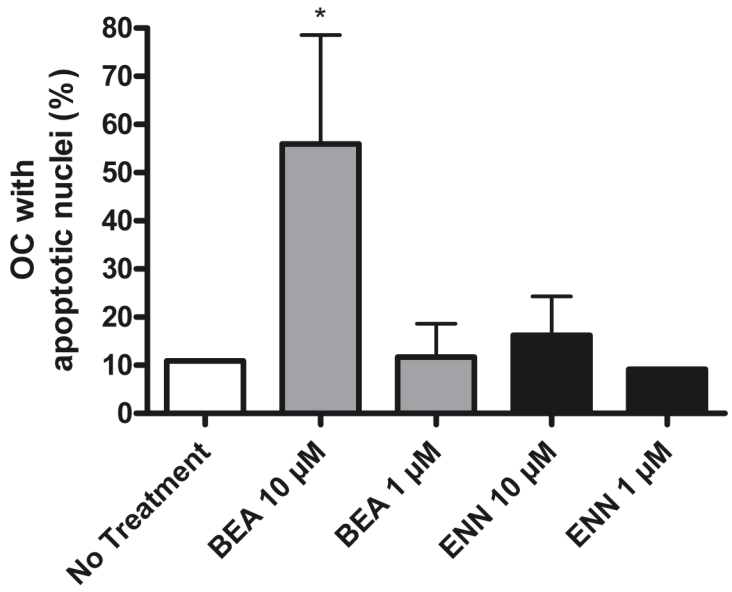

Fig. 5C. Effect of BEA and ENN on the cytoskeleton and apoptosis of OC. (C) Apoptotic cells were identified based on the fragmentation of nuclei and condensation of chromatin and shown here is the quantitative representation. Data are expressed as the mean ± SEM of 3 coverslips, *P<0.05 compared with the No treatment group.

A

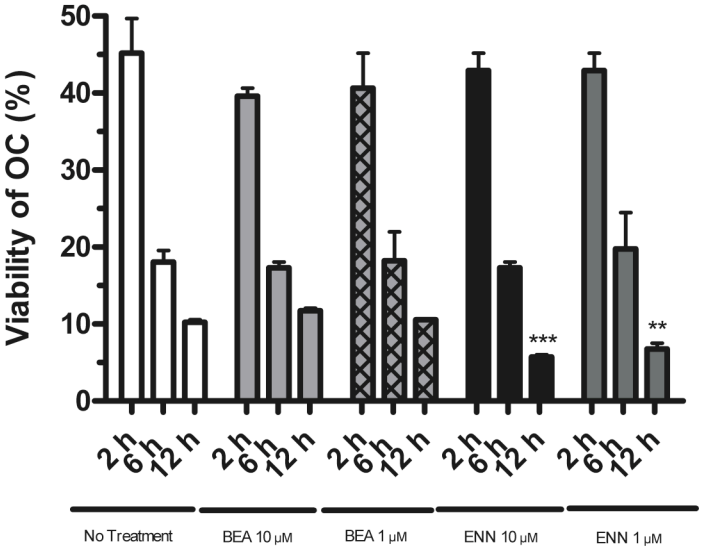

B

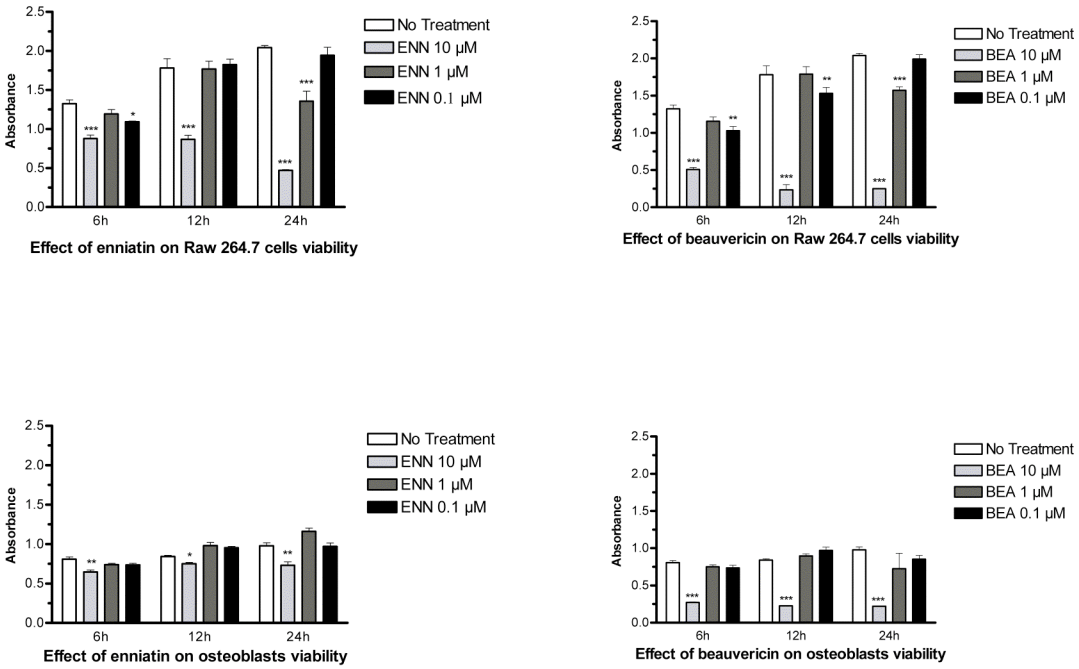

Fig. 6. Cell viability experiments. (A) OC obtained from coculture were treated with the vehicle (No treatment) or BEA or ENN in increasing concentrations for 2, 6 and 12 hours. After treatment, cells were fixed with 3.7 % formaldehyde in PBS and TRAP stained. TRAP-positive multinucleated cells with 3 or more nuclei were counted. (B) OB or RAW 264.7 cells were treated with the vehicle or BEA or ENN in increasing concentrations for 6, 12 and 24 hours. Following treatment, the MTS test was performed to determine the number of viable cells. Data are expressed as the mean ± SEM of at least 3 wells, *P<0.05; **P<0.01; ***P<0.001 compared with the No Treatment group.

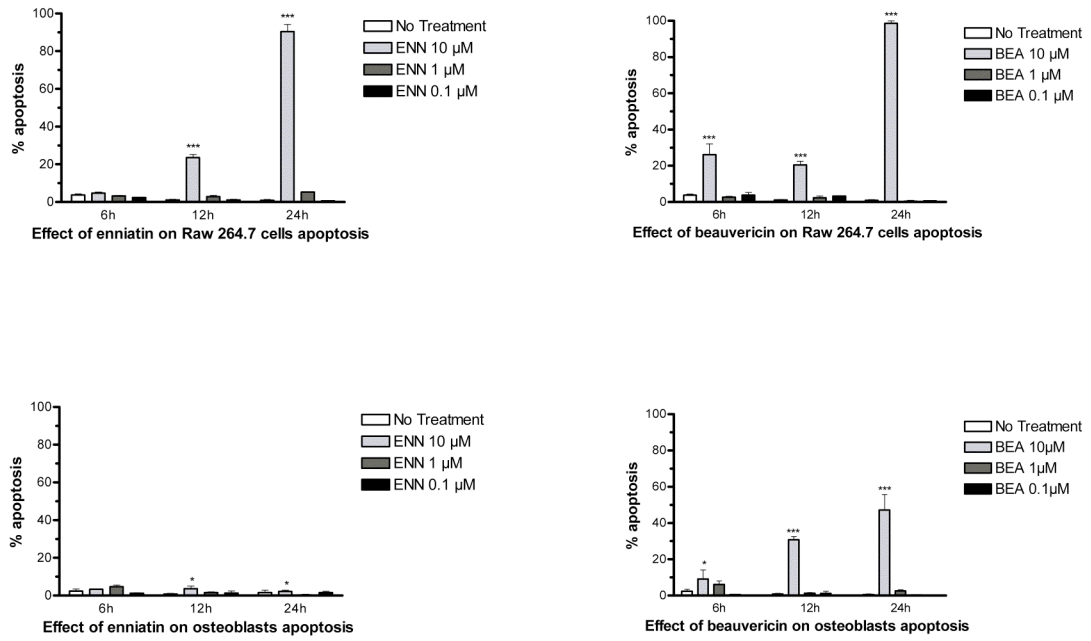

Fig. 7. Effects of BEA and ENN on OC precursors. OB or RAW 264.7 cells were treated with the vehicle or BEA or ENN in increasing concentrations for 6, 12 and 24 hours. Following treatment, the DAPI staining was performed and apoptotic cells were identified based on the fragmentation of nuclei and condensation of chromatin. Shown here is the quantitative representation. Data are expressed as the mean ± SEM of at least 3 wells, *P<0.05; **P<0.01; ***P<0.001 compared with the No Treatment group.

A

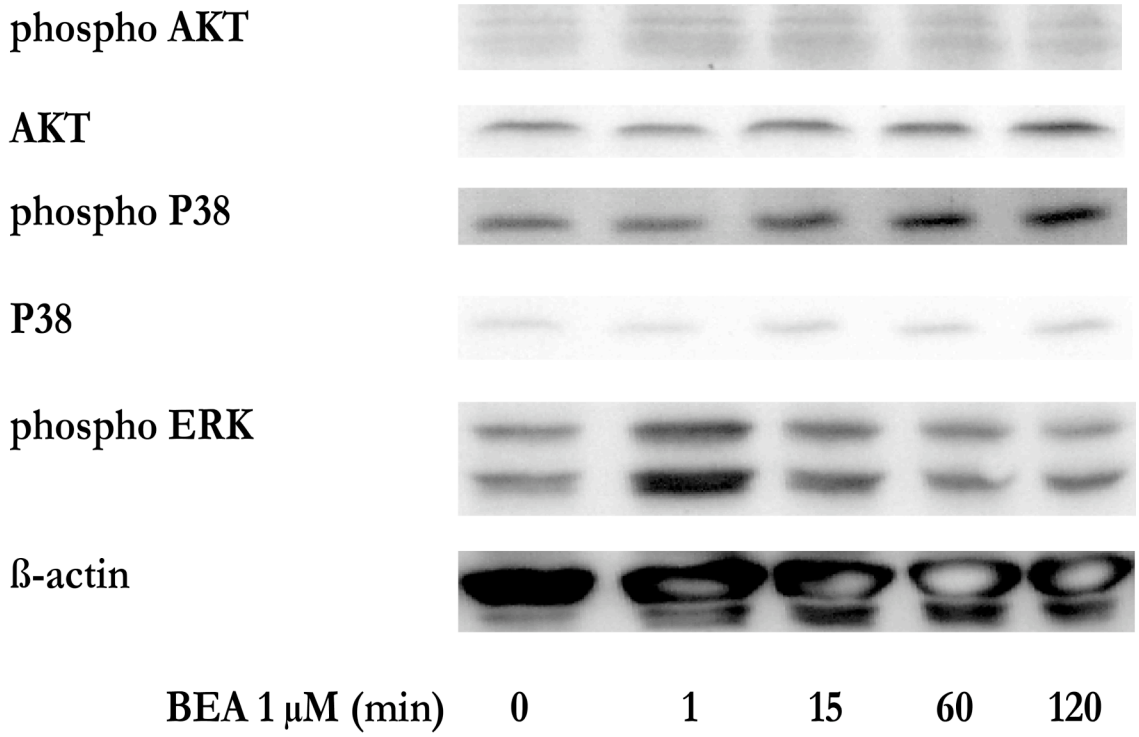

Fig. 8A. Signal transduction of BEA in RAW 264.7-derived OC. RAW 264.7 were stimulated with rmRANKL at 50 ng/ml to allow differentiation in OC. After culture, cells were treated with BEA 1 µM for 1, 15, 60 and 120 min. Cells were then lysed, elctrophoresed and the western blot was carried out to determine the level of indicated proteins. All experiments were carried out at least in triplicate and representative radiographs are shown.

B

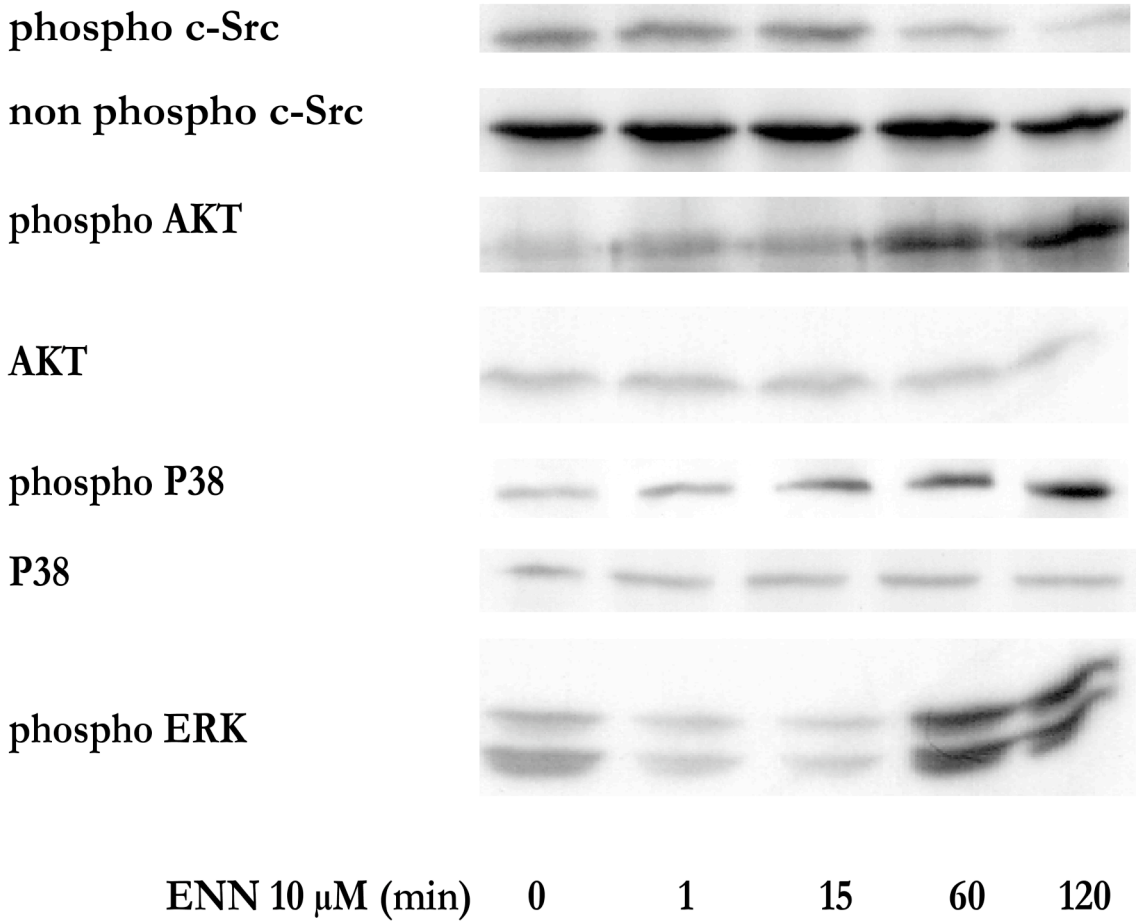

Fig. 8B. Signal transduction of ENN in RAW 264.7 derived OC. RAW 264.7 were stimulated with rmRANKL at 50 ng/ml to allow differentiation in OC. After culture, cells were treated with ENN 10 μM for 1, 15, 60 and 120 min. Cells were then lysed, elctrophoresed and the western blot was carried out to determine the level of indicated proteins. All experiments were carried out at least in triplicate and representative radiographs are shown.

A

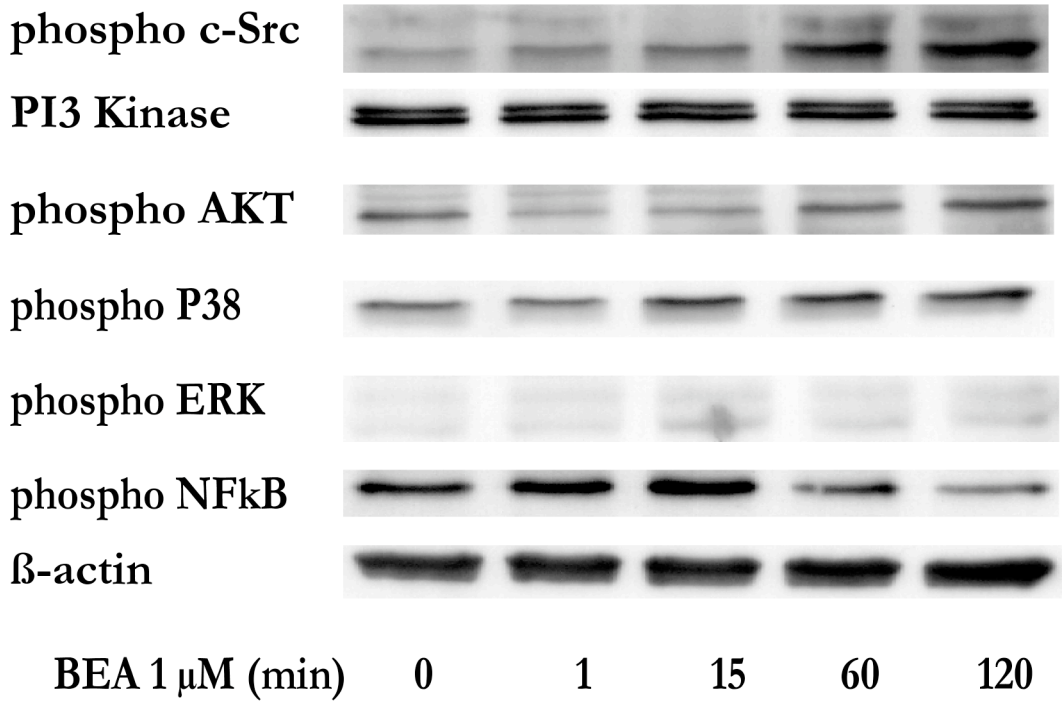

B

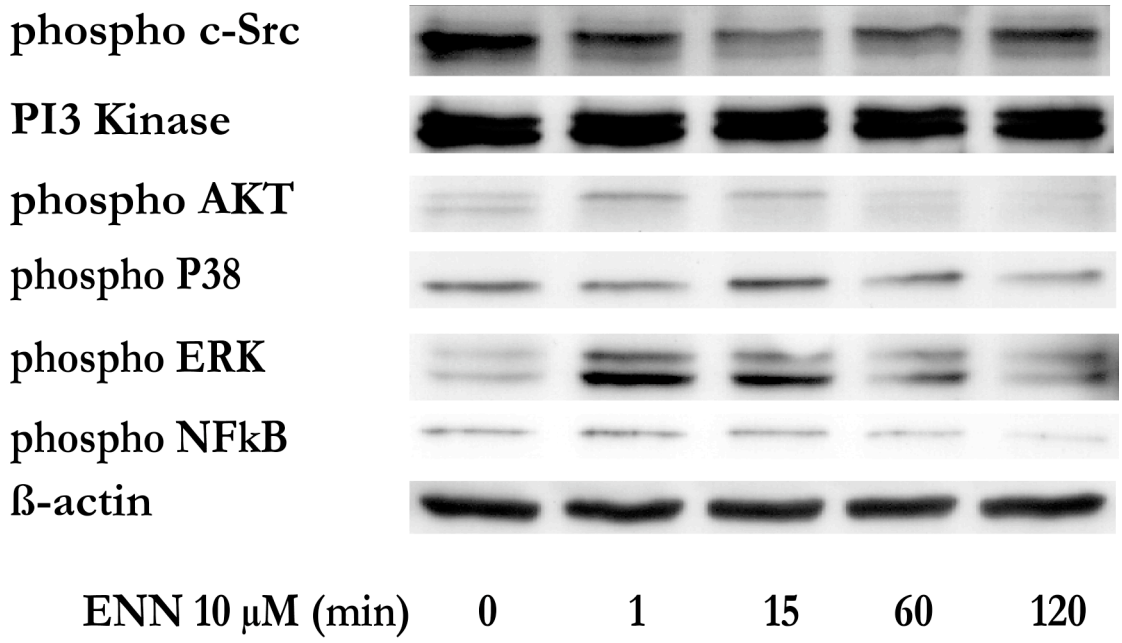

Fig. 9A and B. Signal transduction of BEA and ENN in coculture-derived OC. Mouse bone marrow cells were cocultured with primary OB from newborn mice for 5 days in presence of 1 nM vitamin D3 and 1 µM PGE2 to generate OC. Afterwards, OC were starved in medium containing 0.5 % FCS for 15 min, then treated with BEA 1 µM (A) or ENN 10 µM (B) for 1, 15, 60 and 120 min. Following treatment, cells were lysed, elctrophoresed and the western blot was performed to determine the level of indicated proteins. All experiments were carried out at least in triplicate and representative radiographs are shown.

C

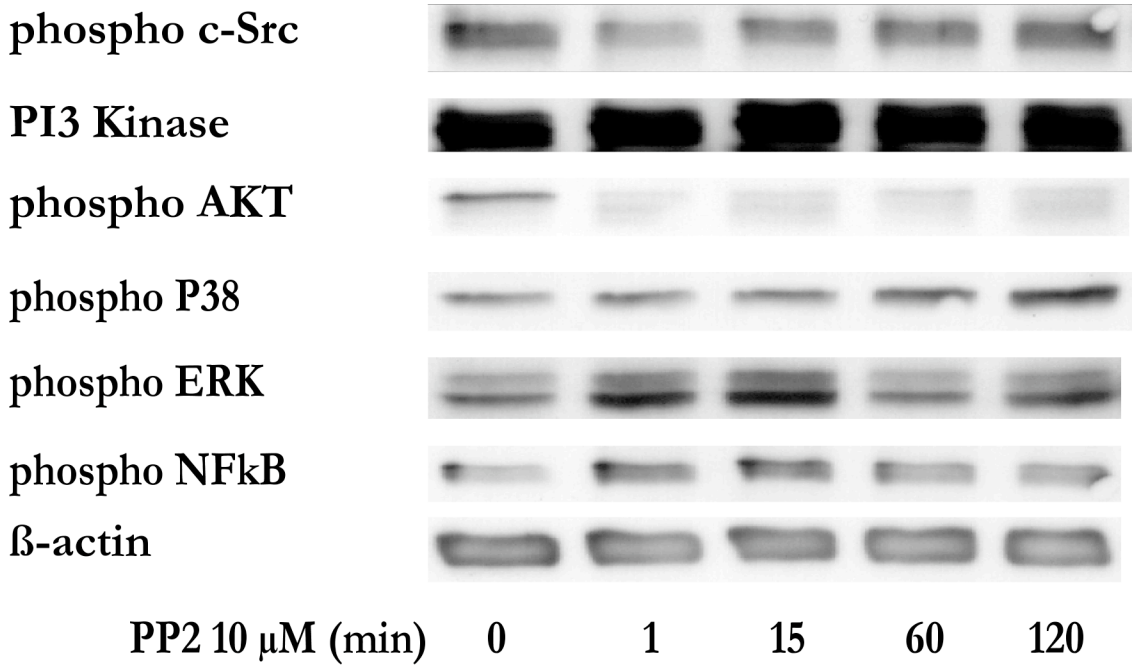

Fig. 9C. Signal transduction of PP2 in coculture-derived OC. (C) Mouse bone marrow cells were cocultured with primary OB from newborn mice for 5 days in presence of 1 nM vitamin D3 and 1 µM PGE2 to generate OC. Afterwards, OC were starved in medium containing 0.5 % FCS for 15 min, then treated with PP2 10 µM for 1, 15, 60 and 120 min. Following treatment, cells were lysed, elctrophoresed and the western blot was performed to determine the level of indicated proteins. All experiments were carried out at least in triplicate and representative radiographs are shown.

D

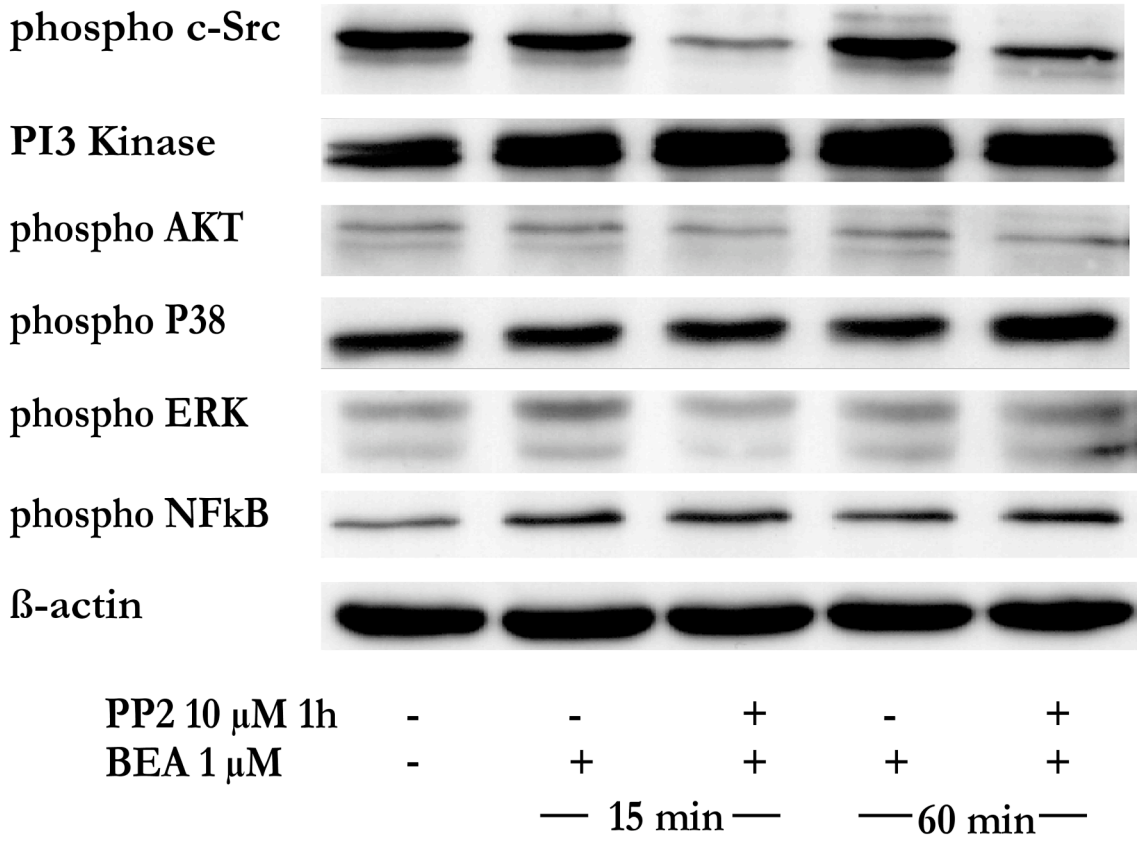

Fig. 9D. Signal transduction of BEA and PP2 in coculture derived OC. Mouse bone marrow cells were cocultured with primary OB from newborn mice for 5 days in presence of 1 nM vitamin D3 and 1 µM PGE2 to generate OC. Afterwards, OC were starved in medium containing 0.5 % FCS for 15 min, pretreated with PP2 (10 µM) 1 hour before addition of BEA 1 µM for 15 or 60 min. Following treatment, cells were lysed, elctrophoresed and the western blot was performed to determine the level of indicated proteins. All experiments were carried out at least in triplicate and representative radiographs are shown.

E

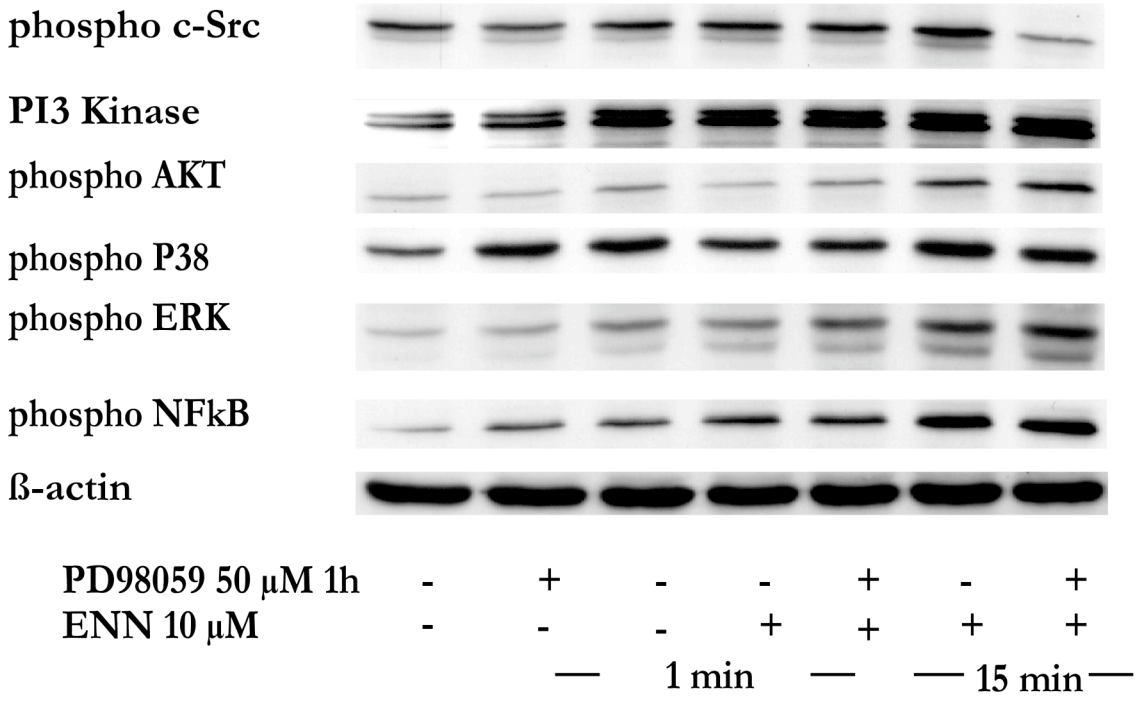

Fig. 9E. Signal transduction of ENN and PD98059 in coculture derived-OC. Mouse bone marrow cells were cocultured with primary OB from newborn mice for 5 days in presence of 1 nM vitamin D3 and 1 µM PGE2 to generate OC. Afterwards, OC were starved in medium containing 0.5 % FCS for 15 min, pretreated with PD98059 (50 µM) 1 hour before addition of ENN 10 µM for 1 or 15 min. Following treatment, cells were lysed, elctrophoresed and the western blot was performed to determine the level of indicated proteins. All experiments were carried out at least in triplicate and representative radiographs are shown.

References

[1] Zaidi M, Blair HC, Moonga BS, Abe E, Huang CL. Osteoclastogenesis, bone resorption, and osteoclast-based therapeutics. J Bone Miner Res 2003;18:599-609.

[2] Zaidi M. Skeletal remodeling in health and disease. Nat Med 2007;13:791-801.

[3] Hofbauer LC, Brueck CC, Singh SK, Dobnig H. Osteoporosis in patients with diabetes mellitus. J Bone Miner Res 2007;22:1317-28.

[4] Audhya TK, Russell DW. Production of enniatins by Fusarium sambucinum: selection of high-yield conditions from liquid surface cultures. J Gen Microbiol 1974;82:181-90.

[5] Doel BD, Ridley DD, Singh P. Isolation of cyclodepsipeptides from plant pathogenic fungi. Aust J Chem 1978;31:1397-9.

[6] Gupta S, Krasnoff SB, Underwood NL, Renwick JA, Roberts DW. Isolation of beauvericin as an insect toxin from Fusarium semitectum and Fusarium moniliforme var. subglutinans. Mycopathologia 1991;115:185-9.

[7] Logrieco A, Moretti A, Castella G, Kostecki M, Golinski P, Ritieni A, et al. Beauvericin production by Fusarium species. Appl Environ Microbiol 1998;64:3084-8.

[8] Logrieco A, Rizzo A, Ferracane R, Ritieni A. Occurrence of beauvericin and enniatins in wheat affected by Fusarium avenaceum head blight. Appl Environ Microbiol 2002;68:82-5.

[9] Hamill RL, Higgens CE, Boaz HE, Gorman M. The structure of beauvericin, a new depsipeptide antibiotic toxic to *Artemia salina*. Tetrahedron Lett 1969;1969:4255-8.

[10] Suzuki A, Kanoaka M, Isogai A, Murakoshi S, Ichinoe M, Tamura S. Bassianolide, a new insecticidal cyclodepsipeptide from *Beauveria bassiana* and *Verticillium lecanii*. Tetrahedron Lett 1977;1977:2167-70.

[11] Bernardini M, Carilli A, Pacioni G, Santurbano B. Isolation of beauvericin from *Paecilomyces fumoso-roseus*. Phytochemistry 1975;14:1865.

[12] Jestoi M, Rokka M, Yli-Mattila T, Parikka P, Rizzo A, Peltonen K. Presence and concentrations of the Fusarium-related mycotoxins beauvericin, enniatins and moniliformin in finnish grain samples. Food Addit Contam 2004;21:794-802.

[13] Uhlig S, Torp M, Heier BT. Beauvericin and enniatins A, A1, B and B1 in Norwegian grain: a survey. Food Chemistry 2004;94:193-201.

[14] Castlebury LA, Sutherland JB, Tanner LA, Henderson AL, Cerniglia CE. Use of a bioassay to evaluate the toxicity of beauvericin to bacteria. World Journal of Microbiology & Biotechnology 1999;15:119-21.

[15] Fotso J, Smith JS. Evaluation of Beauvericin Toxicity with the Bacterial Bioluminescence Assay and the Ames Mutagenicity bioassay. JFS 2003;68:1938-41.

[16] Grove JF, Pople M. The insecticidal activity of beauvericin and the enniatin complex. Mycopathologia 1980;70:103-5.

[17] Guadet J, Julien J, Lafay JF, Brygoo Y. Phylogeny of some Fusarium species, as determined by large-subunit rRNA sequence comparison. Mol Biol Evol 1989;6:227-42.

[18] Tomoda H, Huang XH, Cao J, Nishida H, Nagao R, Okuda S, et al. Inhibition of acyl-CoA: cholesterol acyltransferase activity by cyclodepsipeptide antibiotics. J Antibiot (Tokyo) 1992;45:1626-32.

[19] Kamyar M, Rawnduzi P, Studenik CR, Kouri K, Lemmens-Gruber R. Investigation of the electrophysiological properties of enniatins. Arch Biochem Biophys 2004;429:215-23.

[20] Kouri K, Lemmens M, Lemmens-Gruber R. Beauvericin-induced channels in ventricular myocytes and liposomes. Biochim Biophys Acta 2003;1609:203-10.

[21] Kouri K, Duchen MR, Lemmens-Gruber R. Effects of beauvericin on the metabolic state and ionic homeostasis of ventricular myocytes of the guinea pig. Chem Res Toxicol 2005;18:1661-8.

[22] Behm C, Degen GH, Follmann W. The Fusarium toxin enniatin B exerts no genotoxic activity, but pronounced cytotoxicity in vitro. Mol Nutr Food Res 2009;53:423-30.

[23] Ojcius DM, Zychlinsky A, Zheng LM, Young JD. Ionophore-induced apoptosis: role of DNA fragmentation and calcium fluxes. Exp Cell Res 1991;197:43-9.

[24] Logrieco A, Moretti A, Ritieni A, Caiaffa MF, Macchia L. Beauvericin: chemistry biology and significance. In: Upadhyay R e, editor. Advances in microbial toxin research and its biotechnological exploitation. New York: Kluwer Academic, 2002. p. 23-30.

[25] Macchia L, Di Paola R, Fornelli F, Nenna S, Moretti A, Napoletano R, et al. Cytotoxicity of beauvericin to mammalian cells. In: Proceeding of the

International Seminar on *Fusarium* Mycotoxin, Taxonomy and Pathogenicity. Martina Franca, Bari, Italy, 1995. p. 72-3.

[26] Calo L, Fornelli F, Ramires R, Nenna S, Tursi A, Caiaffa MF, et al. Cytotoxic effects of the mycotoxin beauvericin to human cell lines of myeloid origin. Pharmacol Res 2004;49:73-7.

[27] Jow GM, Chou CJ, Chen BF, Tsai JH. Beauvericin induces cytotoxic effects in human acute lymphoblastic leukemia cells through cytochrome c release, caspase 3 activation: the causative role of calcium. Cancer Lett 2004;216:165-73.

[28] Klaric MS, Rumora L, Ljubanovic D, Pepeljnjak S. Cytotoxicity and apoptosis induced by fumonisin B(1), beauvericin and ochratoxin A in porcine kidney PK15 cells: effects of individual and combined treatment. Arch Toxicol 2008;82:247-55.

[29] Tang CY, Chen YW, Jow GM, Chou CJ, Jeng CJ. Beauvericin activates Ca2+-activated Cl- currents and induces cell deaths in Xenopus oocytes via influx of extracellular Ca2+. Chem Res Toxicol 2005;18:825-33.

[30] Dornetshuber R, Heffeter P, Kamyar MR, Peterbauer T, Berger W, Lemmens-Gruber R. Enniatin exerts p53-dependent cytostatic and p53-independent cytotoxic activities against human cancer cells. Chem Res Toxicol 2007;20:465-73.

[31] Firakova S, Proksa B, Sturdikova M. Biosynthesis and biological activity of enniatins. Pharmazie 2007;62:563-8.

[32] Lemmens-Gruber R, Kamyar MR, Dornetshuber R. Cyclodepsipeptides - potential drugs and lead compounds in the drug development process. Curr Med Chem 2009;16:1122-37.

[33] Nakagawa H, Takami M, Udagawa N, Sawae Y, Suda K, Sasaki T, et al. Destruxins, cyclodepsipeptides, block the formation of actin rings and prominent clear zones and ruffled borders in osteoclasts. Bone 2003;33:443-55.

[34] Recchia I, Rucci N, Festuccia C, Bologna M, MacKay AR, Migliaccio S, et al. Pyrrolopyrimidine c-Src inhibitors reduce growth, adhesion, motility and invasion of prostate cancer cells in vitro. Eur J Cancer 2003;39:1927-35.

[35] Body JJ. Calcitonin for the long-term prevention and treatment of postmenopausal osteoporosis. Bone 2002;30:75S-9S.

[36] Plotkin LI, Weinstein RS, Parfitt AM, Roberson PK, Manolagas SC, Bellido T. Prevention of osteocyte and osteoblast apoptosis by bisphosphonates and calcitonin. J Clin Invest 1999;104:1363-74.

[37] Naidu A, Dechow PC, Spears R, Wright JM, Kessler HP, Opperman LA. The effects of bisphosphonates on osteoblasts in vitro. Oral Surg Oral Med Oral Pathol Oral Radiol Endod 2008;106:5-13.

[38] Soriano P, Montgomery C, Geske R, Bradley A. Targeted disruption of the c-src proto-oncogene leads to osteopetrosis in mice. Cell 1991;64:693-702.

[39] Wong BR, Besser D, Kim N, Arron JR, Vologodskaia M, Hanafusa H, et al. TRANCE, a TNF family member, activates Akt/PKB through a signaling complex involving TRAF6 and c-Src. Mol Cell 1999;4:1041-9.

[40] Dougall WC, Glaccum M, Charrier K, Rohrbach K, Brasel K, De Smedt T, et al. RANK is essential for osteoclast and lymph node development. Genes Dev 1999;13:2412-24.

[41] Fuller K, Wong B, Fox S, Choi Y, Chambers TJ. TRANCE is necessary and sufficient for osteoblast-mediated activation of bone resorption in osteoclasts. J Exp Med 1998;188:997-1001.

[42] Li J, Sarosi I, Q. YX, Morony S, capparelli C, Tan HL, et al. RANK is the intrinsic hematopoietic cell surface receptor that controls osteoclastogenesis and regulation of bone mass and calcium metabolism. Proc Natl Acad Sci 2000;97:1566-71.

[43] Wong BR, Josien R, Choi Y. TRANCE is a TNF family member that regulates dendritic cell and osteoclast function. J Leukoc Biol 1999;65:715-24.

[44] Boyce BF, Yoneda T, Lowe C, Soriano P, Mundy GR. Requirement of pp60c-src expression for osteoclasts to form ruffled borders and resorb bone in mice. J Clin Invest 1992;90:1622-7.

[45] Xing L, Venegas AM, Chen A, Garrett-Beal L, Boyce BF, Varmus HE, et al. Genetic evidence for a role for Src family kinases in TNF family receptor signaling and cell survival. Genes Dev 2001;15:241-53.

[46] Li X, Udagawa N, Itoh K, Suda K, Murase Y, Nishihara T, et al. p38 MAPK-mediated signals are required for inducing osteoclast differentiation but not for osteoclast function. Endocrinology 2002;143:3105-13.

[47] Miyazaki T, Katagiri H, Kanegae Y, Takayanagi H, Sawada Y, Yamamoto A, et al. Reciprocal role of ERK and NF-kappaB pathways in survival and activation of osteoclasts. J Cell Biol 2000;148:333-42.

[48] Tang D, Wu D, Hirao A, Lahti JM, Liu L, Mazza B, et al. ERK activation mediates cell cycle arrest and apoptosis after DNA damage independently of p53. J Biol Chem 2002;277:12710-7.

3.2 Manuscript 2: Beauvericin and enniatins inhibit proliferation and induce apoptosis in metastatic and non metastatic carcinomas: Involvement of the MAPK signaling

F. Tedjiotsop Feudjio[a], R. Lemmens-Gruber[a], O. Hoffmann[a,*]

[a] Department of Pharmacology and Toxicology, University of Vienna, Althanstrasse 14, A-1090 Vienna, Austria

* Correspondence: Professor Oskar Hoffmann, Department of Pharmacology and Toxicology, University of Vienna, Althanstrasse 14, A-1090 Vienna, Austria
Tel.: +43-1-4277-55340; fax: +43-1-4277-55390
E-mail: oskar.hoffmann@univie.ac.at

Abstract

The skeleton is one of the most preferred locations in the body to which cancer, particularly from breast, lung and prostate metastasizes. Bone metastases therefore constitute a common cause of morbidity and mortality in cancer patients and to date, the treatment is primary palliative. We investigated the effects of 2 well-described cyclodepsipeptides beauvericin (BEA) and enniatins (ENN) on 2 highly tumorigenic, hormone-independent cell lines MDA-MB-231 and PC3, and on a non metastatic cell line U2OS with characteristics of primary tumor of bone. The drug concentrations used ranged from 0.1 to 10 μM and the incubation times from 2 to 48 h. Herein, we report inhibition of cell growth, cell viability and induction of apoptosis in the above mentioned cancer cell lines. At lower concentrations (0.1 and 1 μM), ENN time-dependently (24 to 48 h) and significantly (up to 50 % inhibition after 48 h treatment of PC3 with 1 μM ENN, $p<0.001$ vs. control) inhibited proliferation of metastatic cells (MDA-MB-231 and PC3) compared to BEA. However, BEA exerted more cell growth inhibitory effect at higher concentration (10 μM) in all 3 cell lines as compared to ENN. BEA and ENN similarly affected the metastatic and non metastatic cell viability, as early as 24 h, with a significant effect observed already with 5 μM drug ($p<0.001$ vs. control). Both inhibitors more potently induced apoptosis after 24 h in metastatic cells when compared to non metastatic, with ENN being more apoptotic than BEA. This apoptotic effect was significant with 5 μM BEA in MDA-MB-231 ($p<0.01$), 10 μM BEA in PC3 ($p<0.001$), 5 μM ENN in MDA-MB-231 ($p<0.001$), 5 μM ENN in PC3 ($p<0.01$) and 10 μM ENN in U2OS ($p<0.01$). Interestingly, the metastatic profile of the cells did not seem to confer any selective advantage for the effects of both inhibitors at the molecular level. Indeed, while the p38 MAPK pathway remained continuously activated (from 6 to 24 h) in all cell lines, BEA and ENN inactivated ERK in MDA-MB-231 as opposed to its upregulation in PC3 and U2OS. Moreover, BEA was able to induce PARP cleavage in all cell lines, whereas ENN did so only in PC3 cells. Finally, the cell-cell adhesion molecule E-cadherin, whose loss of expression and/or activity has been implicated in the progression of metastasis, was upregulated in all cell lines following BEA or ENN treatment. These data support the antitumoral effects of cyclodepsipeptides and their therapeutic value in the treatment of bone cancer and skeletal metastases.

Key words: apoptosis, cyclodepsipeptides, metastasis, MAPK pathway

1. Introduction

Metastatic cancer cells have the ability to break away from their primary site, enter lymphatic and blood vessels, circulate through the bloodstream, and invade other parts of the body (secondary organs) where they settle anew. Theoretically, any secondary organ is susceptible to metastasis; however, the three main organs usually affected are the lungs, liver and bone. Actually, the skeleton is the place of choice for metastasis to develop. Over 60 % of patients with nonosseous primary malignant neoplasms present abnormal bone scans [1] and particularly, breast, lung and prostate cancer constitute the major source of all metastases to bone [2,3]. It is well known that the Batson venous plexus, a network of valveless veins in the human body, directly connects primary tumor sites (breast or prostate) with the skeleton bypassing the liver and lungs [4]. Additionally, tumour cells are known to form emboli that can be easily trapped in capillary beds within the bone [5]. More importantly, once the tumor cells reach the skeleton, growth factors released in the bone microenvironment during the process of bone remodeling together with those released by the tumour cells provide a "fertile soil" that favors interaction of cancer cells with bone cells, stimulation of tumour cell growth and bone remodeling, and development of metastases [5,2].

BEA and ENN are structurally related cyclodepsipeptides mycotoxins produced by *Fusarium*, *Beauveria*, *Paecilomyces* and *Polypovirus* [6-13]. They exhibit antibiotic [14,15], hydrophobic [16], ionophoric [17-19], insecticidal [20,21,9], phytopathogenic and non mutagenic properties [22,15], and are cytotoxic to several mammalian and cancer cell line models [23-27]. Recently (unpublished), we demonstrated that these 2 mycotoxins inhibit bone resorption. BEA induced apoptosis in osteoclasts by mechanisms likely involving ERK1/2 phosphorylation while ENN affected their survival by downregulating the Src/Akt pathway. As bone resorption is likely to be the main mechanism in the early stages of bone metastasis, and probably the main mechanism by which osteolysis in breast and prostate cancer patient progresses [5,28,3], it is anticipated that the two cyclodepsipeptides might actually reduce or eventually inhibit metastasis in the bone microenvironment. However, whether or not they can directly inhibit tumour cell growth itself, in particular the breast or prostate cancer cells that are known to highly metastasize to the skeleton remains unclear. In previous reports, serratamolide (AT514), a cyclodepsipeptide isolated from *Serratia marcescens* induced cell cycle arrest and apoptosis in B-cell chronic lymphocytic leukemia [29] and breast cancer cells [30]. Therefore, we investigated the effects of the

two cyclodepsipeptides BEA and ENN on breast (MDA-MB-231), prostate (PC3) and osteosarcoma (U2OS) cell lines. Herein, we show that BEA and ENN inhibit cell growth, cell viability and induce apoptosis in these cell lines irrespective of their metastatic profile by mechanisms likely involving the MAPK signaling.

2. Materials and methods

2.1. Drugs

The substances used were 2 mycotoxins BEA (#B-7510) and ENN (#E-3643) both produced as a desiccate by Sigma-Aldrich Chemie (Taufkirchen, Germany). ENN had a purity of approximately 96 %, a molecular weight of 681.5 g/mol and was composed of 3 % enniatin A, 20 % enniatin A_1, 19 % enniatin B and 54 % enniatin B_1. BEA was of 99 % purity with a molecular weight of 784 g/mol. The concentrations used ranged from 0.1 μM to 10 μM. The substances were dissolved in absolute ethanol to make stock solutions at 1 mM, 5 mM and 10 mM.

2.2. Cell culture

The metastatic breast cancer MDA-MB-231, the metastatic prostate cancer PC3 and the osteosarcoma cell line U2OS were obtained from the American Type Culture Collection (ATCC). They were grown in α-modification of the minimal essential medium (α-MEM) supplemented with 10 % heat inactivated FCS (Sigma-Aldrich Chemie GmbH, Taufkirchen, Germany), 100 U/ml of penicillin (Life Technologies Inc. Grand Island, USA) and 100 μg/ml streptomycin (Life Technologies Inc. Grand Island, USA). Cell culture was performed at 37 °C in a humidified 5 % CO_2 atmosphere.

2.3. Growth inhibition assay

MDA-MB-231 ($15x10^4$ cells/well), PC3 ($23x10^4$ cells/well) and U2OS ($7x10^4$ cells/well) were seeded in triplicates in 6-well plates (Greiner Bio-One GmbH, Frickenhausen, Germany) and allowed to attach for 2 days. Cells were then treated with the vehicle (absolute ethanol, final concentration in cultures 1 ‰ v/v) or drug (BEA or ENN) in increasing concentrations for 24 and 48 hours. Before treatment, cells of 3 wells (each well handled separately) were enzymatically detached, collected and

counted using the Casy cell counter (Model DT, Schärfe system, Germany). The average count at this step was considered as the starting time 0 cell density for all vehicle and treated groups. At different time points, cells were enzymatically detached, collected, counted and the average cell density per treated group (n=3 wells/group) was compared to the average cell density of the vehicle group at that specific time point. The experiment was repeated 3 times and data are presented as mean ± SEM.

2.4. Cell Viability assay

The MTS-test was used to determine the number of viable cells in culture. This method involves the CellTiter 96®AQ_{ueous} One Solution Reagent (#G3580, Promega, Madison, WI, USA,) composed of 1.90 mg/ml MTS and 300 µM PES in Dulbecco's buffered saline, pH 6.0. MDA-MB-231 ($37x10^3$ cells/well), PC3 ($37x10^3$ cells/well) and U2OS ($25x10^3$) were seeded in 96-well plate (Iwaki, Asahi Techno Glass, Japan), 8 wells per groups, and allowed to attach for 24 hours. Thereafter, cells were submitted to the vehicle or drug in increasing concentrations for another 24 and 48 hours. Before termination, the cells were incubated with 20 µl of the CellTiter reagent for 2 hours and the absorbance was read at 490 nm with a Multiskan plate reader (Labsystems Mult 45139, Finland). The data were collected using Delta Soft3 software and the results are presented as a proportion of viable cells in the presence of BEA or ENN compared to the vehicle group.

2.5. Apoptosis assay

The DAPI staining was performed to assess apoptosis. MDA-MB-231 ($16x10^4$ cells/well), PC3 ($8x10^4$ cells/well) and U2OS ($8x10^4$ cells/well) were seeded on coverslips (Menzel-Glaser, Germany) in triplicate in 6-well plates and allowed to attach for 24 hours. Cells were then treated with the vehicle or drug in increasing concentrations for another 24 hours. After culture, cells were fixed for 13 min with 3.7 % formaldehyde (Sigma-Aldrich Chemie GmbH, Steinheim, Germany) in PBS at room temperature. Thereafter, cells were incubated with 0.1 µg/ml of the DAPI reagent (4',6-Diamidino-2-phenylindole, Sigma-Aldrich) in PBS for 15 min at 37 °C, 5 % CO_2. The coverslips were mounted onto microscopes glass slides (Menzel-Glaser, Germany) using fluorosave embedding medium (bioMérieux® sa, Mary l'Etoile-France), sealed with Fixogum rubber cement (Marabuwerke GmbH & Co.KG, Germany) and stored at

4 °C in the dark. Stained coverslips were examined under a fluorescence microscope (Nikon, Japan) using the DAPI filter and a 60x objective with immersion oil. Data were collected using Cell*F software (Cell Imaging System). Apoptotic cells were identified based on the shrinking and fragmentation of nuclei, as well as condensation of chromatin.

2.6. Western blotting experiments

MDA-MB-231 ($33x10^4$ cells/well), PC3 ($16x10^4$ cells/well) and U2OS ($16x10^4$ cells/well) were cultured in 6-well plates until confluency (2 to 3 days). Cells were then submitted to the vehicle or 5 μM of drug in starvation medium (containing only 0.5 % heat inactivated FCS) for 2, 6, 12 and 24 hours. After treatment, cells were washed several times with ice-cold PBS and lysed in lysis buffer (50 mM NaCl, 10 mM Tris-base, 1 % Triton X-100, pH 7.05) containing several inhibitors of proteases and phosphatases (50 mM NaF, 10 μg/ml Aprotinin, 10 μg/ml Leupeptin, 1 μg/ml Pepstatin, 2 mM Orthovanadate, 1mM PMSF). The Bio-Rad DC protein assay kit (Bio-Rad Laboratories, Hercules, CA, USA) was used to quantify the proteins in the samples. About 30 μg of proteins per sample were resolved on 10 % SDS-PAGE according to their molecular weight, electrotransferred onto a 0.45 μm nitrocellulose membrane (Whatman GmbH, Dassel, Germany), blocked for one hour in 5 % non fat dry milk in Tris Buffer Saline Tween (TBST 0.1%) and incubated overnight with the primary antibody in TBST 0.1 %. Afterwards, the proteins were incubated for one hour with the secondary antibody (HRP-conjugated anti-mouse or anti-rabbit) (1:5000 in TBST) and the detection was performed with an enhanced chemoluminescence detection kit (GE Healthcare, UK). The membranes were stripped and reprobed several times and ß-actin served as control for equal loading.

The primary antibodies used were anti phospho Src-Tyr416 (1:1000, rabbit polyclonal, #2101, 60 kDa), anti phospho Akt-Ser 473 (1:1000, rabbit monoclonal, #4060, 60 kDa), anti phospho NF-κB p65-Ser536 (1:1000, rabbit monoclonal, #3033, 65 kDa), anti phospho-p38 MAPK Thr180/Tyr182 (1:1000, rabbit polyclonal, #9211, 43 kDa), anti caspase 3 (1:1000, rabbit polyclonal, #9662, 35 kDa) and anti cleaved PARP (1:1000, rabbit polyclonal, #9544, 89 kDa) from Cell Signaling, Inc (Beverly, MA, USA). Anti phospho p-44/42 MAPK Thr202/Tyr204 (1:1000, mouse monoclonal, #9106, 44/42 kDa) was from New England Biolabs, Inc (Ipswich, MA, USA). Anti E-cadherin

(1:2500, mouse monoclonal, #C20820, 120 kDa), anti FAK (1:1000, mouse monoclonal, #F15020, 125 kDa) and anti STAT3 (1:2500, mouse monoclonal, #S21320, 92 kDa) were purchased from Transduction Laboratories (Lexington, KY, USA). Anti PI3 kinase α (333) (1:1000, rabbit polyclonal, #sc-423, 85 kDa) was from Santa Cruz Biotechnology, Inc (Santa Cruz, CA, USA) and anti ß-actin (1:2000, mouse monoclonal, #A-2228, 42 kDa) from Sigma (St. Louis, MO, USA). The secondary antibodies anti-mouse IgG HRP-conjugate (# W4021) and anti-rabbit IgG HRP-conjugate (#W4011) were from Promega (Madison, WI, USA).

2.7. Statistical analyses

All experiments were repeated at least 3 times. Data were analysed using one factor ANOVA (analysis of variance) incorporated in the StatView statistical program and are presented as mean ± SEM. Significant differences between groups are presented as * $p<0.05$; ** $p<0.01$; *** $p<0.001$ in the treatment group compared to the vehicle.

3. Results

3.1. BEA and ENN inhibit cell growth of MDA-MB-231, PC3 and U2OS

At first, we investigated the effects of cyclodepsipeptides BEA and ENN on the proliferation of MDA-MB-231, PC3 and U2OS cancer cell lines. We allowed these cells to grow in presence of drug in increasing concentrations (0.1 to 10 μM) for 24 and 48 h (Fig.1).

At higher concentration (10 μM), BEA and ENN significantly and time-dependently inhibited MDA-MB-231 cell growth ($P<0.001$), with however more effect of BEA than ENN (Fig. 1a). At lower concentrations (0.1 and 1 μM), BEA did not affect cell growth, whereas ENN dose and time-dependently inhibited cell proliferation. Indeed, the inhibition was observed already at 0.1 μM for 48 h ($p<0.01$), and increased with concentration and time ($p<0.001$ at 24 and 48 h for 1 and 10 μM). Therefore, ENN was more potent (at lower concentrations) at inhibiting MDA-MB-231 cell growth as compared to BEA.

At 10 μM, BEA and ENN similarly inhibited PC3 cell growth (Fig. 1b), in a significant and time-dependent pattern ($P<0.001$). Although both compounds exerted significant inhibition at lower concentration (BEA 1 μM, ENN 0.1 and 1 μM), ENN was proven to

be more potent than BEA, as 50 % inhibition was observed within 48 h (ENN 1 μM) incubation. Moreover, the inhibition was observed already at 0.1 μM (24 h, $p<0.05$) and increased with concentration and time ($p<0.001$ at 24 and 48 h for 1 and 10 μM).
BEA significantly inhibited U2OS cell growth at 1 μM (48 h, $p<0.01$) and 10 μM ($p<0.001$ at both time points) (Fig. 1c). ENN inhibited cell growth only at 10 μM ($p<0.01$ at 24 h, $p<0.001$ at 48 h). Therefore, in this specific cell line, BEA was more potent at inhibiting growth as compared to ENN.

3.2. BEA and ENN affect cell viability of MDA-MB-231, PC3 and U2OS

Viability is an unquestionable requirement for a cell to fulfill in order to proliferate. We next investigated the effect of both compounds on viability of MDA-MB-231, PC3 and U2OS by MTS test as described in the materials and methods section.
BEA and ENN similarly affected MDA-MB-231 viability after 24 h incubation, with a significant effect at 5 and 10 μM ($p<0.001$) (Fig. 2a). This effect was pronounced after 48 h, where an additional inhibition was observed at 1 μM ($p<0.001$). However, ENN was more potent as compared to BEA given that the viability was affected even at the lowest ENN concentration (0.1 μM, 48 h, $p<0.001$).
BEA and ENN similarly inhibited PC3 viability after 24 h incubation, with a significant effect at 5 and 10 μM ($p<0.001$) (Fig. 2b). This inhibition increased with time, with an additional effect at 1 μM ($p<0.05$) after 48 h.
BEA and ENN similarly and significantly affected U2OS viability at 5 and 10 μM after 24 and 48 h treatment ($p<0.001$) (Fig. 2c).

3.3. BEA and ENN induce apoptosis in MDA-MB-231, PC3 and U2OS

Apoptosis is a process of programmed cell death in multicellular organisms. We evaluated apoptosis induced after 24 h of BEA or ENN treatment in MDA-MB-231, PC3 and U2OS by DAPI staining. Features characteristic of apoptosis include shrinking, condensation of chromatin and fragmentation of nuclei (Fig. 3a).
BEA induced apoptosis in MDA-MB-231 cells with a significant effect at 5 μM ($p<0.01$) (Fig. 3b). ENN also induced apoptosis in these cells at 1 μM ($p<0.05$), 5 μM ($p<0.001$) and 10 μM ($p<0.05$). However, ENN was more apoptotic as compared to BEA although 5 μM remained the most apoptotic concentration for both compounds.

BEA and ENN dose-dependently induced apoptosis in PC3 cells (Fig. 3c). The effect of ENN was significant as early at 1 μM ($p<0.05$) and increased at 5 and 10 μM ($p<0.01$) whereas BEA's effect was significant only at 10 μM ($p<0.001$).
BEA induced apoptosis in U2OS although the effect was not significant (Fig. 3d). However, ENN more potently and dose-dependently induced apoptosis in these cells with a significant effect observed at 10 μM ($p<0.01$).

3.4. Molecular signaling experiments

We have demonstrated that BEA and ENN inhibit cell growth, cell viability and induce apoptosis in metastatic (MDA-MB-231 and PC3) and non metastatic (U2OS) cell lines. Next, we sought to determine the molecular events underlying such biological responses. Deregulation of kinase activities has emerged as a major mechanism by which cancer cells evade normal physiological constraints on growth and survival. Therefore, we screened the kinase activities altered following treatment with both inhibitors.
MDA-MB-231, PC3 and U2OS were first cultured in 6-well plates until confluency, and then treated with the vehicle or 5 μM of drug in starvation medium for 2 to 24 h. The drug concentration chosen was 5 μM, as this was the concentration where significant inhibition was observed with regard to cell viability and/or apoptosis.

3.4.1. MDA-MB-231

The c-Src non-receptor tyrosine kinase is overexpressed and activated in a large number of human malignancies, and has been associated to the development of cancer and progression to distant metastases. Herein, we report a downregulation of c-Src, Akt, ERK and NFκB after 12 h with BEA and after 24 h with BEA or ENN (Fig. 4a). PI3 kinase was downregulated after 12 h only with BEA, whereas p38 showed sustained activation from 6 to 24 h following exposure of cells to each of the 2 compounds. We next examined whether the intrinsic mitochondrial pathway leading to apoptosis was affected. The effector caspase 3 was not affected while PARP was cleaved after 2, 6 and 24 h following BEA treatment. Stat3 and E-cadherin have been associated with the development of metastases. BEA downregulated Stat3 after 12 and 24 h, while BEA and ENN showed sustained upregulation of E-cadherin from 2 to 24 h. FAK promotes cell adhesion, cell migration and thereby metastatic potential of cancer cells. Herein,

FAK was downregulated after 2 h (with ENN), 6 h (with BEA) and 24 h (with BEA or ENN).

3.4.2. PC3

c-Src, PI3 kinase and NFκB were downregulated after 24 h, unlike Akt that was activated after 12 and 24 h following BEA or ENN treatment (Fig. 4b). Upon treatment, the 2 components of the MAPK pathway showed early (p38 after 6 h and ERK after 12 h) and sustained activation over time. Caspase 3 was not affected, whereas PARP cleavage was observed after 2 to 24 h treatment with BEA or ENN. Stat3 showed slight activation following ENN treatment (2 and 12 h), E-cadherin was upregulated by BEA (2, 12 and 24 h) or ENN (2 and 12 h), and FAK was downregulated after 24 h treatment with ENN.

3.4.3. U2OS

c-Src was not affected by BEA and interestingly, was even activated following 24 h ENN treatment (Fig. 4c). PI3 kinase was downregulated (after 24 h), whereas Akt showed sustained activation from 2 to 24 h treatment with each of the 2 compounds. BEA or ENN induced upregulation of the MAPK pathway. NFκB was inactivated after 24 h exposure of cells to BEA or ENN whereas ENN, but not BEA slightly activated caspase 3 (24 h). Unlike BEA (6 to 12 h), ENN did not induce PARP cleavage. Moreover, BEA or ENN did not affect Stat3. BEA (2 and 12 h) or ENN (2 and 6 h) promoted a transient E-cadherin expression followed by return to basal levels. FAK was first activated by BEA (12 h) or ENN (2 h), and finally downregulated after 24 h.

4. Discussion

Bone metastases are a frequent cause of morbidity in cancer patients. They are associated with bone pain, pathological fractures, hypercalcaemia and spinal cord or nerve root compression, all of which may profoundly impair a patient's quality of life [31]. To date, treatment of bone metastases is primarily palliative, and despite remarkable advances in the field, there is an important need to target bone metastases by developing drugs that preferentially target cancer cells in bone in addition to bone stroma, given that skeletal metastases are more refractory to treatment, constitute the

highest load of tumour mass in the body, function as secondary site for tumour spread, and are associated with significant morbidity [5].

We have investigated the effects of 2 well-known mycotoxins (BEA and ENN), on 2 highly tumorigenic hormone-independent cell lines MDA-MB-231 and PC3, and on a primary tumor of bone cell line model U2OS. Herein, we report inhibition of cell growth, cell viability and induction of apoptosis in the above mentioned cancer cell lines. 1) ENN significantly inhibited cell growth and induced apoptosis in metastatic cells (MDA-MB-231 and PC3) as compared to BEA. 2) However, BEA was more potent at inhibiting the non metastatic U2OS cell growth as compared to ENN. 3) The 2 inhibitors affected cell viability and induced apoptosis more potently in metastatic cells as compared to the non metastatic one. These data suggest a cell type and tumorigenic specific effect of drug.

Several anti-cancer agents, including genistein [32,33], indole-3-carbinol [34], resveratrol [35], grifolin [36], protoapigenone [37] and ß-inone [38] exhibit inhibitory and proapoptotic effects, and this is consistent with our findings. Moreover, the compounds used here, namely BEA and ENN, have previously shown cytotoxic effects in other cancer cell models [23-25,39]. Serratamolide (AT514), a structurally related cyclodepsipeptide isolated from *Serratia marcescens* has been reported to induce cell cycle arrest and apoptosis in B-cell chronic lymphocytic leukemia [29] and breast cancer cells [30]. Our findings are in line with these previous works and support the anti-cancer effect of cyclodepsipeptides, as well as their therapeutic potential in the treatment of bone metastases.

The pathophysiology of cancer involves deregulation of a number of molecules at the molecular level that play critical roles in cell growth, migration, invasion and metastases. Considerable evidence implicates elevated expression and/or activity of Src in cancer development [40]. Src inhibition reduced growth, adhesion, motility and invasion of prostate cancer cells *in vitro* [41], and reduced incidence of breast cancer metastases *in vivo* [42]. More importantly, reduction of c-Src activity induced osteoclast apoptosis *in vivo* and *in vitro* [43], and since bone resorption is likely to be the main mechanism in the early stages of bone metastasis and probably the main mechanism by which osteolysis in breast and prostate cancer patient progresses [5,28,3], Src inhibition represents a valuable therapeutic target [44-46] and should be validated by any potential anti-cancer agent aimed at treating bone metastases. Accordingly, we observed an inhibition of c-Src following treatment of metastatic cell lines with BEA or ENN. However, BEA did not affect Src activity, whereas ENN even stimulated it in the non

metastatic U2OS cell line, suggesting that Src is not involved in the inhibitory effects of BEA and ENN in these particular cells. The signal transducer and activator of transcription 3 (Stat3) promotes metastatic progression of prostate cancer [47], and is a downstream target of Src-mediated inhibitory effects of the phytoalexin resveratrol in malignant cells [35]. In our context, BEA but not ENN inactivated Stat3 in MDA-MB-231 cells. However, Stat3 was not affected in U2OS, as opposed to its activation in PC3 following ENN treatment. Whether or not Stat3 mediates Src-dependent inhibition of MDA-MB-231 cells following BEA treatment is still unclear, although both proteins were downregulated. Additionally, our data suggest that Stat3 is not downstream of Src in BEA or ENN inhibitory effects in PC3 and U2OS.

The PI3 kinase/Akt pathway is known to promote cell survival by inhibiting apoptosis [36,48]. PI3 kinase was slightly inactivated in breast cells by BEA (12 h), and downregulated in prostate and osteosarcoma cells following BEA or ENN treatment (24 h). However, although Akt was inhibited as well in breast cells, it appeared to be continuously activated in prostate and osteosarcoma cells. So while the PI3 kinase/Akt pathway may contribute to the apoptotic effects of BEA and ENN in MDA-MB-231 cells, the involvement of this pathway in BEA or ENN induced apoptosis in PC3 and U2OS deserves further investigation.

The mitogen-activated protein kinase (MAPK) family of proteins regulates extracellular signals that lead to proliferation, differentiation and survival. The extracellular signal regulated kinase (ERK)/MAPK pathway primarily directs a program of proliferation and survival [49], while the p38 MAPK is activated upon cellular stress and engages pathways that can block proliferation or promote apoptosis [50-55]. There is increasing evidence that p38 MAPK negatively regulates tumorigenesis [56,57], and selectively mediates oxidative stress (reactive oxygen species)-induced cancer cell apoptosis [58]. In this study, BEA and ENN induced ERK activation in PC3 and U2OS, unlike in MDA-MB-231 where a downregulation was observed. Interestingly, p38 MAPK was continuously activated in all cell lines. Downregulation of ERK has been associated to growth inhibition in other cell types [59-61] and may contribute, at least in part, to the inhibitory effects of BEA and ENN in MDA-MB-231 cells, but not in PC3 and U2OS cells, whose proliferation was inhibited as well. However, ERK activation has been reported to mediate apoptosis following DNA damage in other studies [62-64], and this is consistent with our observations in PC3 and U2OS. Moreover, our findings that BEA and ENN inhibit proliferation, induce apoptosis in MDA-MB-231, PC3 and U2OS, and activate the p38 MAPK pathway are in line with previous reports [60,65]. Keeping in

mind that p38 MAPK selectively mediates reactive oxygen species (ROS)-induced apoptosis, it is still a matter of debate whether or not mycotoxins do actually produce ROS. Indeed, Dornetshuber *et al*. recently demonstrated that the mycotoxins BEA and ENN exert moderate antioxydative activities, and that generation of ROS is not involved in their apoptotic effects [66]. However, BEA was found to induce a 4 fold increase of ROS [67] that correlated with reduced cell viability, lipid peroxidation and glutathione depletion [67,68]. Taken together, these data suggest the involvement of the MAPK signaling in the BEA and ENN inhibitory and/or apoptotic effects in metastatic and non metastatic cell lines.

Chemotherapeutic agents are known to induce nuclear factor kappa B (NFκB) activity in tumour cells, resulting in lower cell death and drug resistance. The NFκB pathway is activated upon binding of the receptor activator of NFκB ligand (RANKL) to its receptor RANK expressed on cancer cells, and regulates cell migration and bone metastasis [69]. Moreover, inhibition of the Akt/NFκB survival pathway is important for apoptosis induced by indole-3-carbinol (common phytochemical in cruciferous vegetables) [70], serratamolide (cyclodepsipeptide) [29], 3,3'-diindolylmethane (major *in vivo* acid-catalyzed condensation product of indole-3-carbinol) [71] and genistein (soybean isoflavone) [72]. Herein, BEA and ENN inactivate the NFκB pathway in MDA-MB-231, PC3 and U2OS. However, Akt was downregulated only in MDA-MB-231 cells, and we have not provided evidence of any relation between Akt and NFκB in our setting. Yet, BEA or ENN-induced NFκB inactivation in our cancer cells is an undeniable benefit for these compounds and deserves further investigation.

DNA damage, ischemia and oxidative stress are apoptotic signals that lead to cell death through the intrinsic mitochondrial pathway, involving release of cytochrome c, activation of caspases, and cleavage of poly-ADP-ribose polymerase (PARP). BEA, but not ENN, induced PARP cleavage in MDA-MB-231 and U2OS cells. However, BEA and ENN did not affect caspase 3 activation, although they induced PARP cleavage in PC3 cells. These data suggest cell type specific effects of our compounds in mitochondrial-induced apoptosis, and so far, the mitochondrial pathway has been implicated in cyclodepsipeptides [24,29,25,26,39,30], as well as other anti-cancer agents [73,36,74,38]-induced apoptosis.

Loss of the cell-cell adhesion molecule E-cadherin expression or function is implicated in tumor invasion, progression and metastasis, and is associated with poor prognosis in breast and prostate cancer patients [75,76]. Interestingly, E-cadherin appeared to be

upregulated by BEA and ENN irrespective of the metastatic profile. Aberrant expression, activity and signaling of FAK can potentially promote the progression of several types of tumors *in vivo* [77], and alterations of the FAK/Src signal transduction pathway correlate with increased migratory capacity of prostate carcinoma cells [78]. In this study, BEA and ENN inactivated FAK in MDA-MB-231 and U2OS whereas in PC3 cells, only ENN induced FAK inactivation. These data suggest that BEA and ENN trigger cell type specific responses to growth and migration, and that these are independent of their metastatic profile.

To summarize, BEA and ENN affected cell viability and induced apoptosis more potently in metastatic cells (MDA-MB-231 and PC3) as compared to the non metastatic one (U2OS). Interestingly, the metastatic profile of the cells did not confer any selective advantage for the effects of our inhibitors at the molecular level. While BEA more commonly interfered with the MAPK and the mitochondrial apoptotic pathways in all cell lines, ENN interacted predominantly with the MAPK signaling.

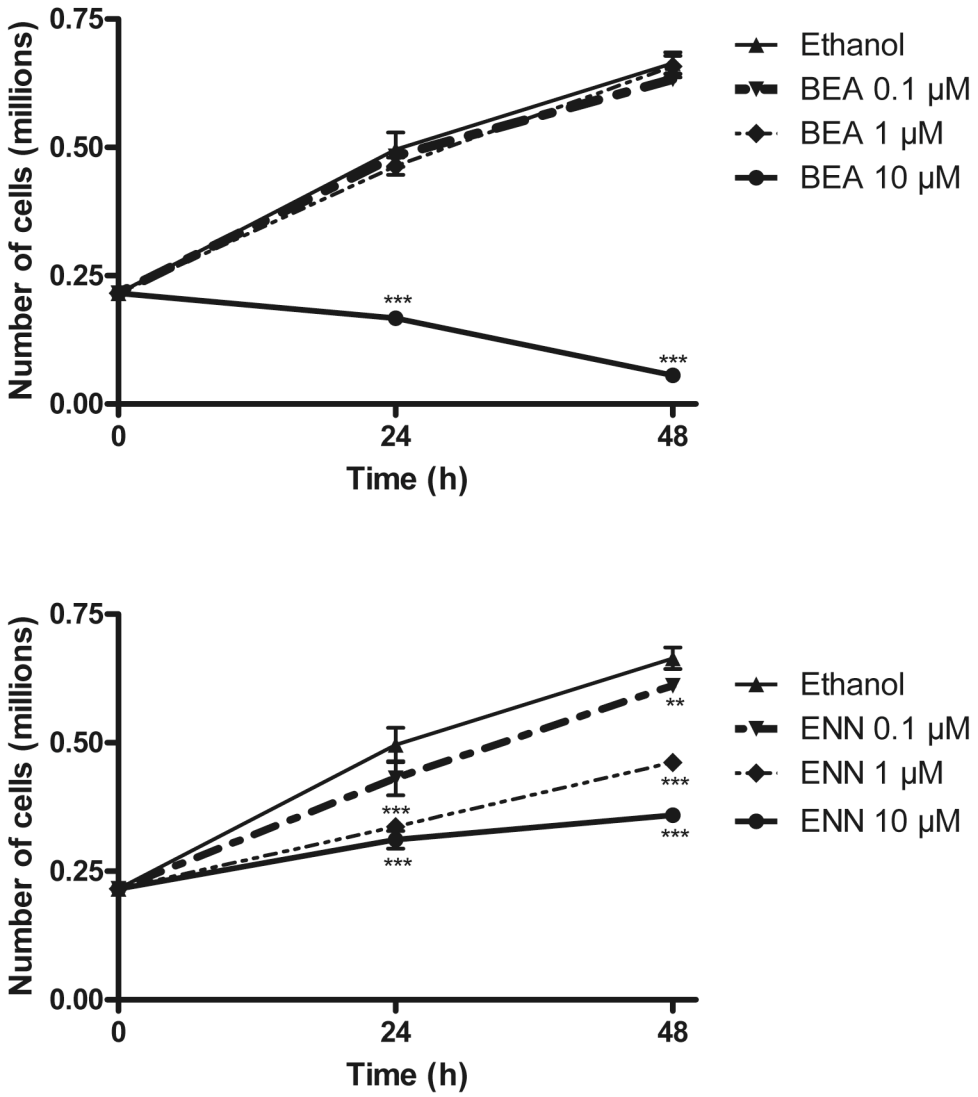

Fig. 1a. Growth inhibition assay: MDA-MB-231 ($15x10^4$ cells/well) were seeded in triplicates in 6-well plates and allowed to attach for 2 days. The cells were then treated with the vehicle (absolute ethanol) or drug (BEA or ENN) in increasing concentrations for 24 and 48 hours. After treatment, cells were enzymatically detached, collected, counted and the average cell density per treated group (n=3 wells/group) was compared to the average cell density of the vehicle group at that specific time point. The experiment was repeated 3 times and data are presented as mean ± SEM.

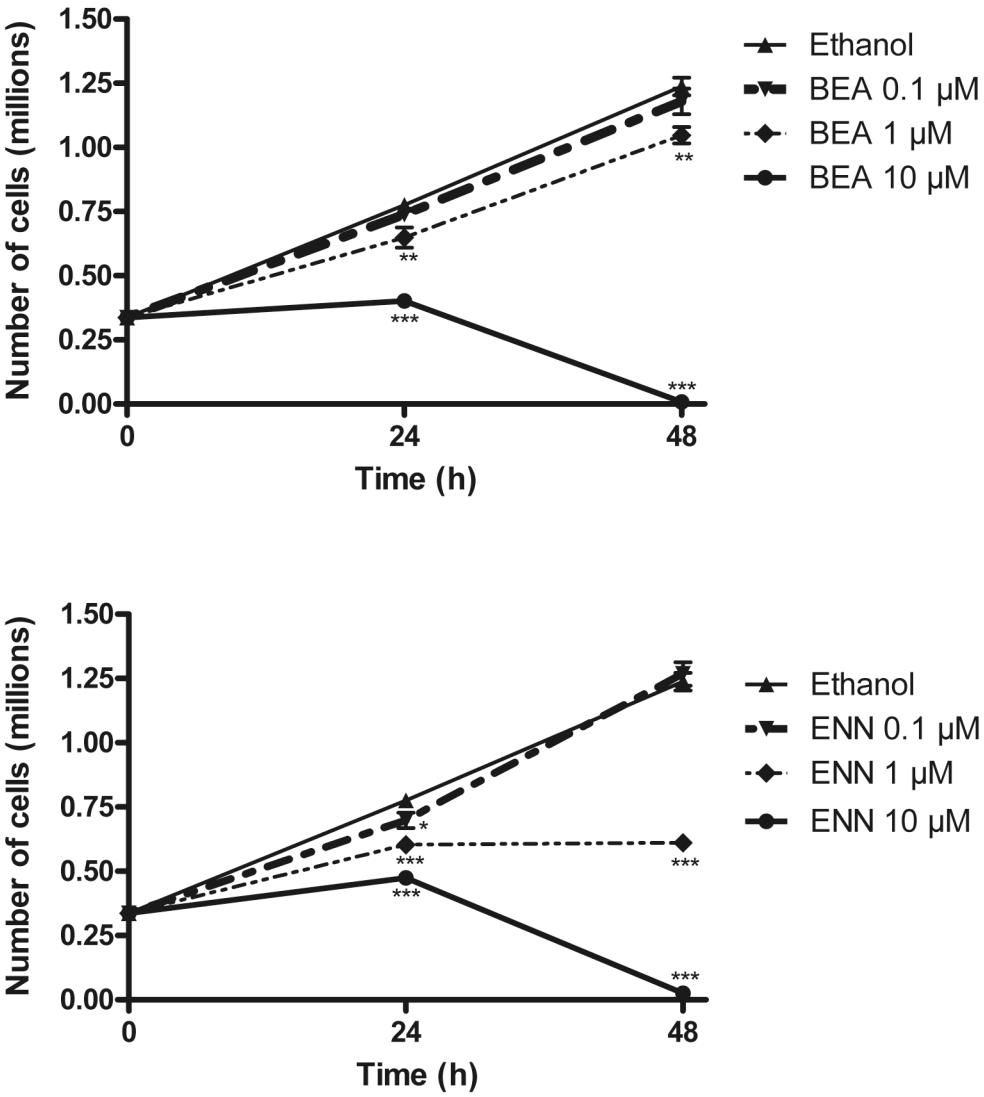

Fig. 1b. Growth inhibition assay: PC3 ($23x10^4$ cells/well) were seeded in triplicates in 6-well plates and allowed to attach for 2 days. The cells were then treated with the vehicle (absolute ethanol) or drug (BEA or ENN) in increasing concentrations for 24 and 48 hours. After treatment, cells were enzymatically detached, collected, counted and the average cell density per treated group (n=3 wells/group) was compared to the average cell density of the vehicle group at that specific time point. The experiment was repeated 3 times and data are presented as mean ± SEM.

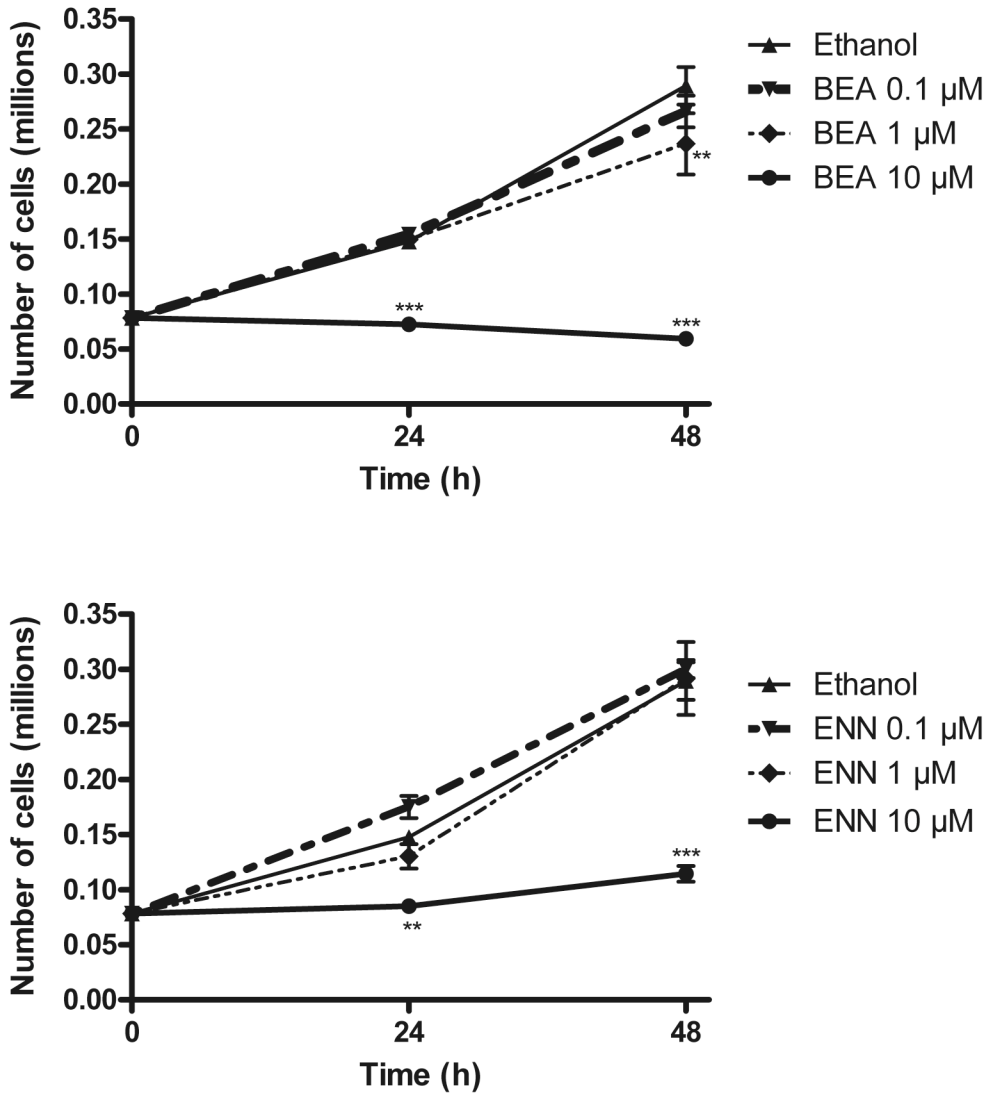

Fig. 1c. Growth inhibition assay: U2OS ($7x10^4$ cells/well) were seeded in triplicates in 6-well plates and allowed to attach for 2 days. The cells were then treated with the vehicle (absolute ethanol) or drug (BEA or ENN) in increasing concentrations for 24 and 48 hours. After treatment, cells were enzymatically detached, collected, counted and the average cell density per treated group (n=3 wells/group) was compared to the average cell density of the vehicle group at that specific time point. The experiment was repeated 3 times and data are presented as mean ± SEM.

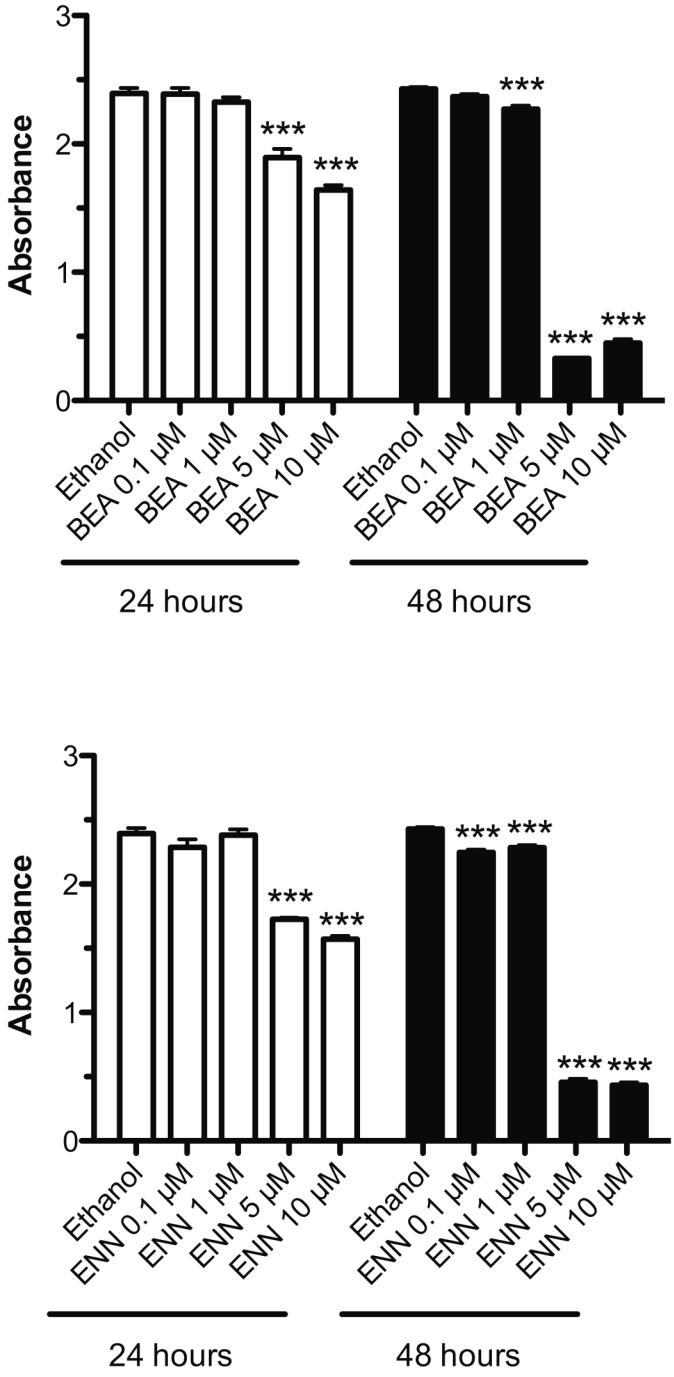

Fig. 2a. Cell viability assay: MDA-MB-231 ($37x10^3$ cells/well) were seeded in 96-well plate, 8 wells per group, and allowed to attach for 24 hours. Thereafter, cells were submitted to the vehicle or drug in increasing concentrations for another 24 and 48 hours. Before termination, cells were incubated with 20 µl of the CellTiter reagent for 2 hours and the absorbance was read at 490 nm with a Multiskan plate reader. The results are presented as the proportion of viable cells in the presence of BEA or ENN compared to the vehicle group. * $p<0.05$; ** $p<0.01$; *** $p<0.001$ in the treatment group compared to the vehicle.

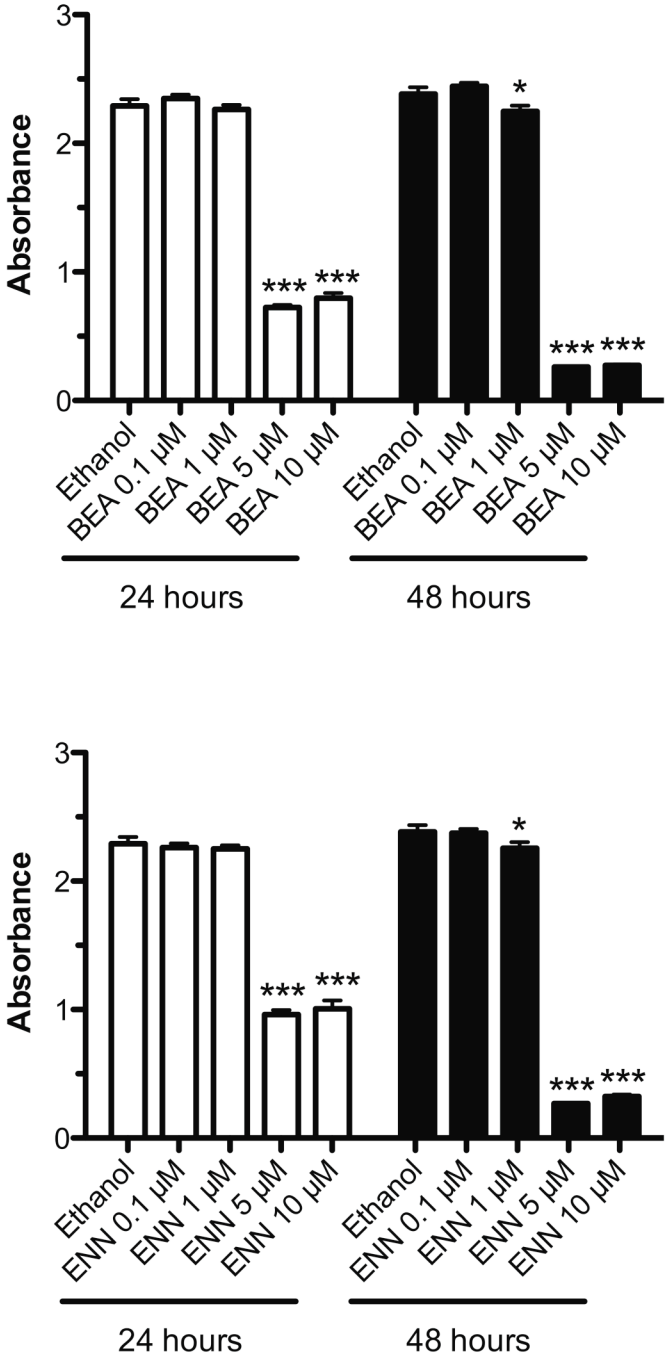

Fig. 2b. Cell viability assay: PC3 ($37x10^3$ cells/well) were seeded in 96-well plate, 8 wells per group, and allowed to attach for 24 hours. Thereafter, cells were submitted to the vehicle or drug in increasing concentrations for another 24 and 48 hours. Before termination, cells were incubated with 20 µl of the CellTiter reagent for 2 hours and the absorbance was read at 490 nm with a Multiskan plate reader. The results are presented as the proportion of viable cells in the presence of BEA or ENN compared to the vehicle group. * $p<0.05$; ** $p<0.01$; *** $p<0.001$ in the treatment group compared to the vehicle.

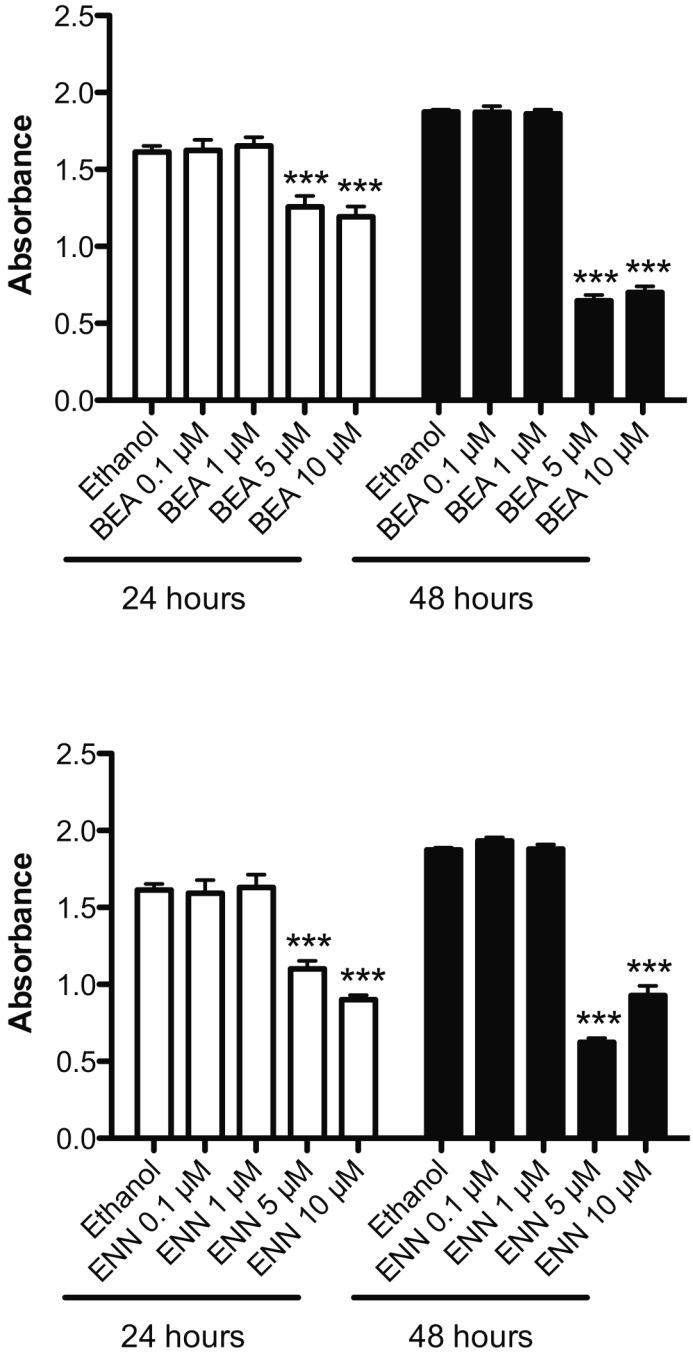

Fig. 2c. Cell viability assay: U2OS ($25x10^3$) were seeded in 96-well plate, 8 wells per group, and allowed to attach for 24 hours. Thereafter, cells were submitted to the vehicle or drug in increasing concentrations for another 24 and 48 hours. Before termination, cells were incubated with 20 µl of the CellTiter reagent for 2 hours and the absorbance was read at 490 nm with a Multiskan plate reader. The results are presented as the proportion of viable cells in the presence of BEA or ENN compared to the vehicle group. * $p<0.05$; ** $p<0.01$; *** $p<0.001$ in the treatment group compared to the vehicle.

A

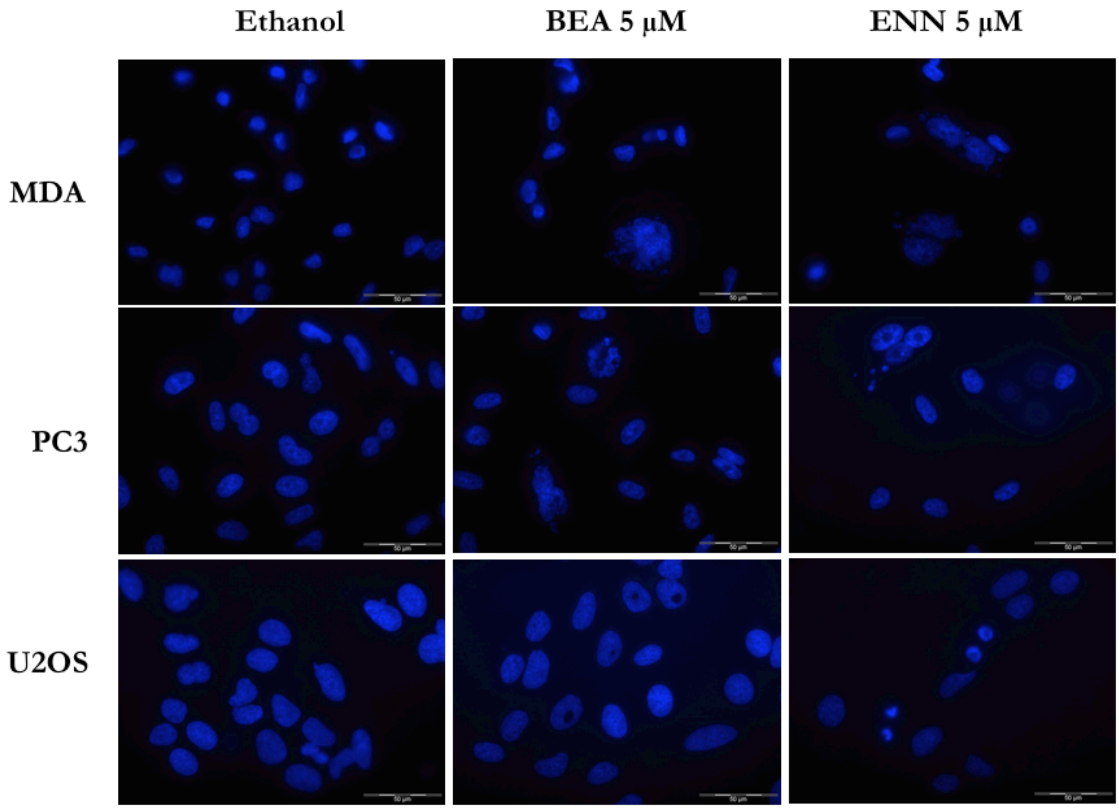

B

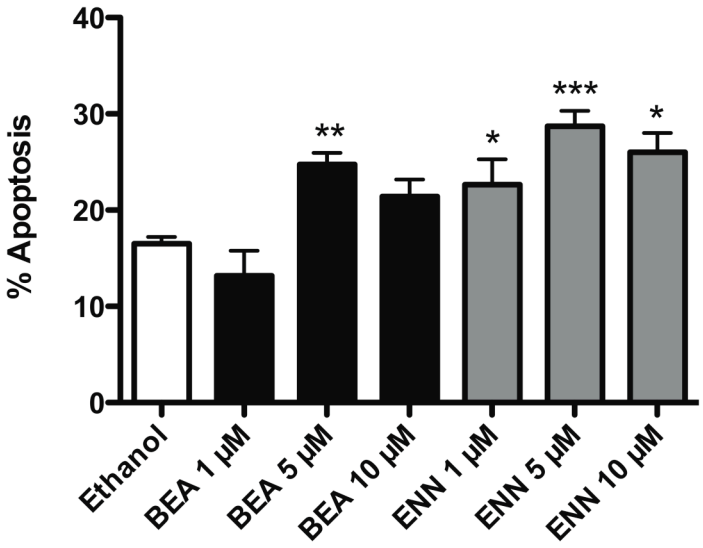

Fig. 3a and b. Apoptosis assay: MDA-MB-231 ($16x10^4$ cells/well), PC3 ($8x10^4$ cells/well) and U2OS ($8x10^4$ cells/well) were seeded on coverslips in triplicate in 6-well plates and allowed to attach for 24 hours. Cells were then treated with the vehicle or drug in increasing concentrations for another 24 hours. After treatment, cells were fixed with 3.7 % formaldehyde in PBS and nuclei were stained with DAPI. (A) is the qualitative representation of MDA-MB-231, PC3 and U2OS. (B) is the quantitative representation of MDA-MB-231. * $p<0.05$; ** $p<0.01$; *** $p<0.001$ in the treatment group compared to the vehicle.

C

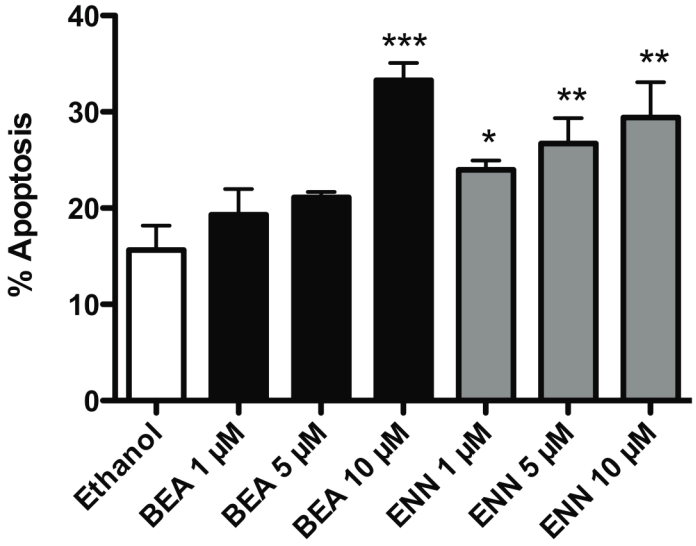

D

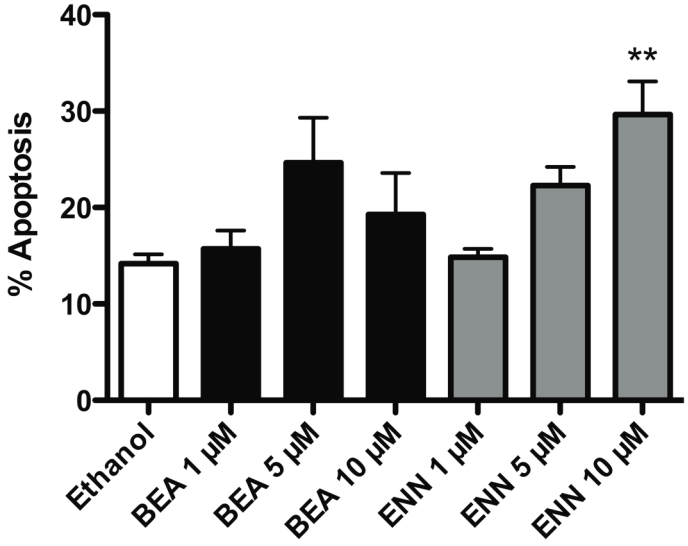

Fig. 3c and d. Apoptosis assay: (C) and (D) are respectively PC3 and U2OS quantitative representation. * $p<0.05$; ** $p<0.01$; *** $p<0.001$ in the treatment group compared to the vehicle.

A

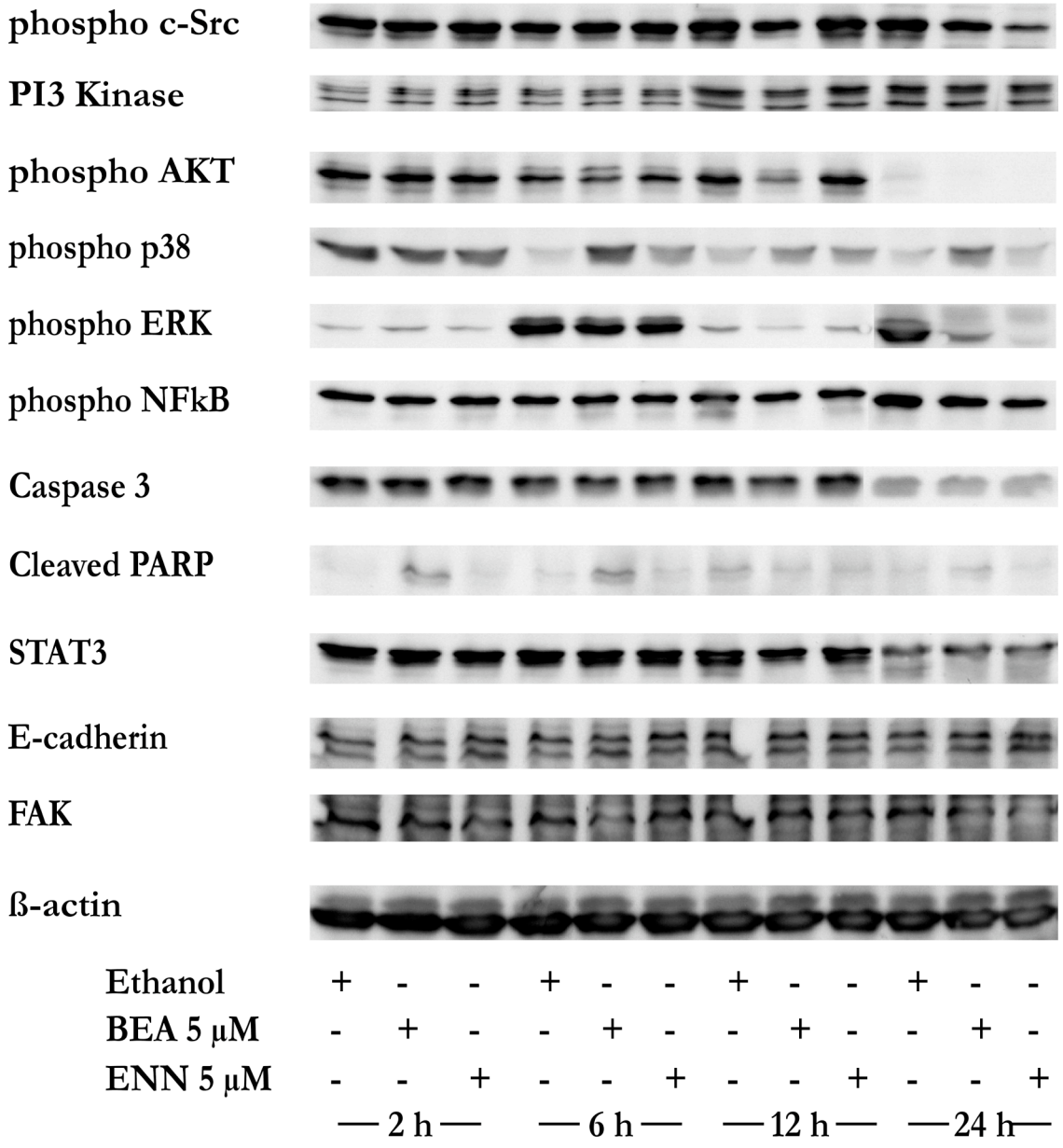

Fig. 4a. MDA-MB-231 were cultured in 6-well plates until cnfluency (2 to 3 days), and then treated with the vehicle or 5 µM of BEA or ENN in starvation medium for 2, 6, 12 and 24 h. Following treatment, the cells were lysed, proteins separated by SDS-Electrophoresis and the western blot carried out to determine phosphorylation of proteins. All experiments were carried out at least in triplicate and representative radiographs are shown.

B

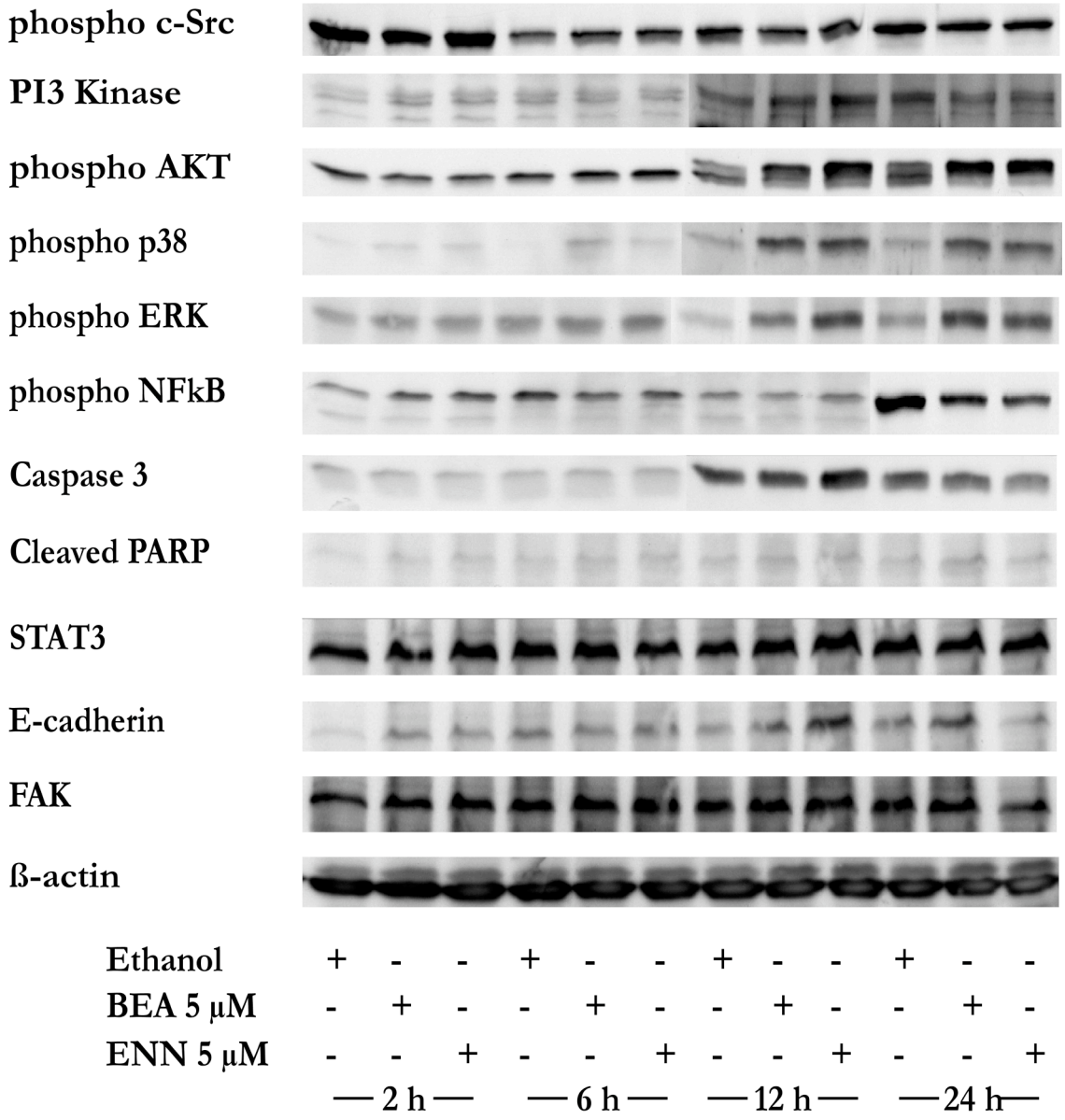

Fig. 4b. PC3 were cultured in 6-well plates until cnfluency (2 to 3 days), and then treated with the vehicle or 5 µM of BEA or ENN in starvation medium for 2, 6, 12 and 24 h. Following treatment, the cells were lysed, proteins separated by SDS-Electrophoresis and the western blot carried out to determine phosphorylation of proteins. All experiments were carried out at least in triplicate and representative radiographs are shown.

C

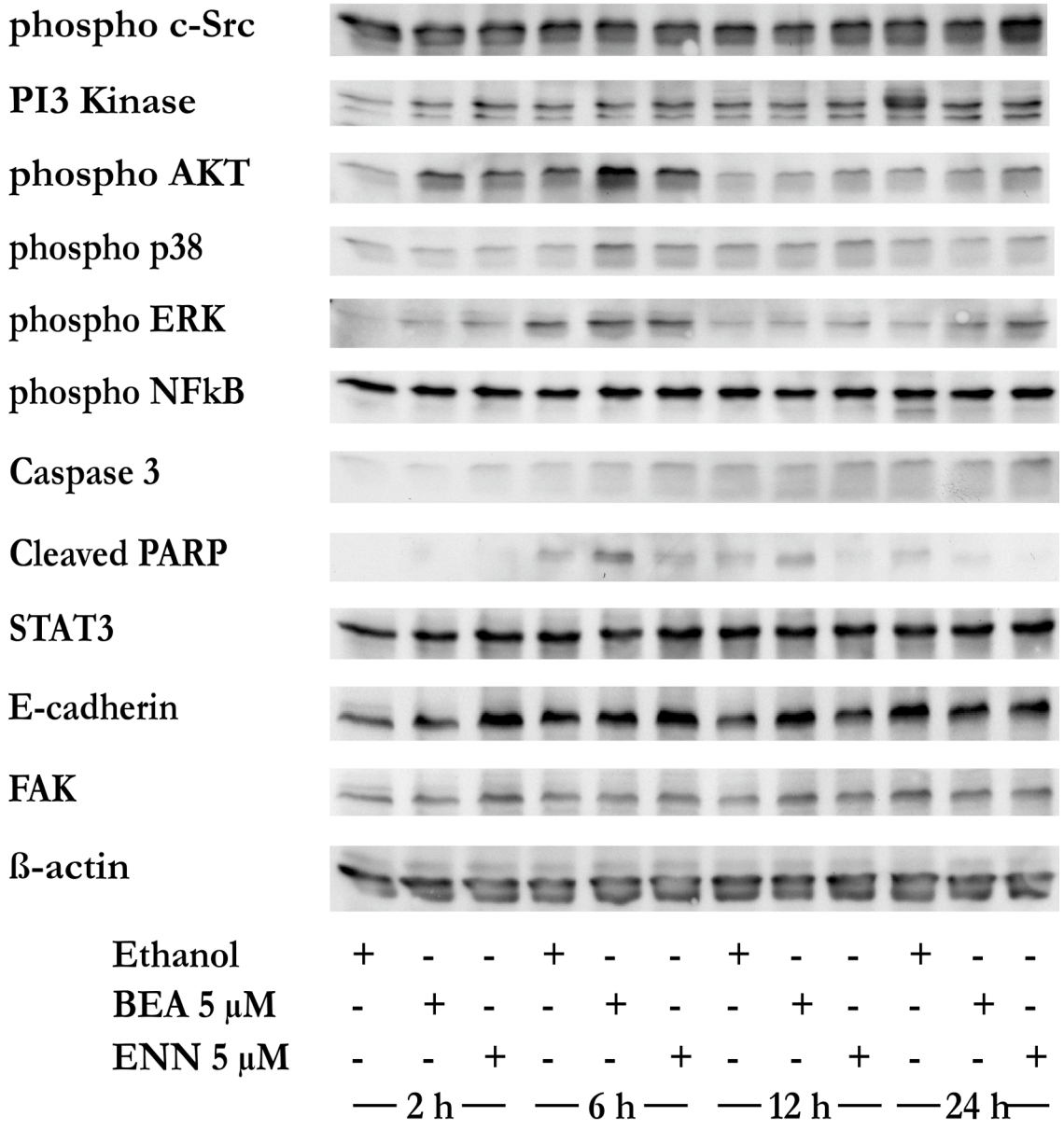

Fig. 4c. U2OS were cultured in 6-well plates until cnfluency (2 to 3 days), and then treated with the vehicle or 5 µM of BEA or ENN in starvation medium for 2, 6, 12 and 24 h. Following treatment, the cells were lysed, proteins separated by SDS-Electrophoresis and the western blot carried out to determine phosphorylation of proteins. All experiments were carried out at least in triplicate and representative radiographs are shown.

References

[1] Tofe AJ, Francis MD, Harvey WJ. Correlation of neoplasms with incidence and localization of skeletal metastases: An analysis of 1,355 diphosphonate bone scans. J Nucl Med 1975;16:986-9.

[2] Mundy GR. Metastasis to bone: causes, consequences and therapeutic opportunities. Nat Rev Cancer 2002;2:584-93.

[3] Tomita A, Kasaoka T, Inui T, Toyoshima M, Nishiyama H, Saiki H, et al. Human breast adenocarcinoma (MDA-231) and human lung squamous cell carcinoma (Hara) do not have the ability to cause bone resorption by themselves during the establishment of bone metastasis. Clin Exp Metastasis 2008;25:437-44.

[4] Batson OV. The function of the vertebral veins and their role in the spread of metastases. 1940. Clin Orthop Relat Res 1995:4-9.

[5] Bagi CM. Targeting of therapeutic agents to bone to treat metastatic cancer. Adv Drug Deliv Rev 2005;57:995-1010.

[6] Audhya TK, Russell DW. Production of enniatins by Fusarium sambucinum: selection of high-yield conditions from liquid surface cultures. J Gen Microbiol 1974;82:181-90.

[7] Bernardini M, Carilli A, Pacioni G, Santurbano B. Isolation of beauvericin from *Paecilomyces fumoso-roseus*. Phytochemistry 1975;14:1865.

[8] Doel BD, Ridley DD, Singh P. Isolation of cyclodepsipeptides from plant pathogenic fungi. Aust J Chem 1978;31:1397-9.

[9] Gupta S, Krasnoff SB, Underwood NL, Renwick JA, Roberts DW. Isolation of beauvericin as an insect toxin from Fusarium semitectum and Fusarium moniliforme var. subglutinans. Mycopathologia 1991;115:185-9.

[10] Hamill RL, Higgens CE, Boaz HE, Gorman M. The structure of beauvericin, a new depsipeptide antibiotic toxic to *Artemia salina*. Tetrahedron Lett 1969;1969:4255-8.

[11] Logrieco A, Moretti A, Castella G, Kostecki M, Golinski P, Ritieni A, et al. Beauvericin production by Fusarium species. Appl Environ Microbiol 1998;64:3084-8.

[12] Logrieco A, Rizzo A, Ferracane R, Ritieni A. Occurrence of beauvericin and enniatins in wheat affected by Fusarium avenaceum head blight. Appl Environ Microbiol 2002;68:82-5.

[13] Suzuki A, Kanoaka M, Isogai A, Murakoshi S, Ichinoe M, Tamura S. Bassianolide, a new insecticidal cyclodepsipeptide from *Beauveria bassiana* and *Verticillium lecanii*. Tetrahedron Lett 1977;1977:2167-70.

[14] Castlebury LA, Sutherland JB, Tanner LA, Henderson AL, Cerniglia CE. Use of a bioassay to evaluate the toxicity of beauvericin to bacteria. World Journal of Microbiology & Biotechnology 1999;15:119-21.

[15] Fotso J, Smith JS. Evaluation of Beauvericin Toxicity with the Bacterial Bioluminescence Assay and the Ames Mutagenicity bioassay. JFS 2003;68:1938-41.

[16] Tomoda H, Huang XH, Cao J, Nishida H, Nagao R, Okuda S, et al. Inhibition of acyl-CoA: cholesterol acyltransferase activity by cyclodepsipeptide antibiotics. J Antibiot (Tokyo) 1992;45:1626-32.

[17] Kamyar M, Rawnduzi P, Studenik CR, Kouri K, Lemmens-Gruber R. Investigation of the electrophysiological properties of enniatins. Arch Biochem Biophys 2004;429:215-23.

[18] Kouri K, Lemmens M, Lemmens-Gruber R. Beauvericin-induced channels in ventricular myocytes and liposomes. Biochim Biophys Acta 2003;1609:203-10.

[19] Kouri K, Duchen MR, Lemmens-Gruber R. Effects of beauvericin on the metabolic state and ionic homeostasis of ventricular myocytes of the guinea pig. Chem Res Toxicol 2005;18:1661-8.

[20] Grove JF, Pople M. The insecticidal activity of beauvericin and the enniatin complex. Mycopathologia 1980;70:103-5.

[21] Guadet J, Julien J, Lafay JF, Brygoo Y. Phylogeny of some Fusarium species, as determined by large-subunit rRNA sequence comparison. Mol Biol Evol 1989;6:227-42.

[22] Behm C, Degen GH, Follmann W. The Fusarium toxin enniatin B exerts no genotoxic activity, but pronounced cytotoxicity in vitro. Mol Nutr Food Res 2009;53:423-30.

[23] Calo L, Fornelli F, Ramires R, Nenna S, Tursi A, Caiaffa MF, et al. Cytotoxic effects of the mycotoxin beauvericin to human cell lines of myeloid origin. Pharmacol Res 2004;49:73-7.

[24] Dornetshuber R, Heffeter P, Kamyar MR, Peterbauer T, Berger W, Lemmens-Gruber R. Enniatin exerts p53-dependent cytostatic and p53-independent cytotoxic activities against human cancer cells. Chem Res Toxicol 2007;20:465-73.

[25] Jow GM, Chou CJ, Chen BF, Tsai JH. Beauvericin induces cytotoxic effects in human acute lymphoblastic leukemia cells through cytochrome c release, caspase 3 activation: the causative role of calcium. Cancer Lett 2004;216:165-73.

[26] Klaric MS, Rumora L, Ljubanovic D, Pepeljnjak S. Cytotoxicity and apoptosis induced by fumonisin B(1), beauvericin and ochratoxin A in porcine kidney PK15 cells: effects of individual and combined treatment. Arch Toxicol 2008;82:247-55.

[27] Ojcius DM, Zychlinsky A, Zheng LM, Young JD. Ionophore-induced apoptosis: role of DNA fragmentation and calcium fluxes. Exp Cell Res 1991;197:43-9.

[28] Grano M, Mori G, Minielli V, Cantatore FP, Colucci S, Zallone AZ. Breast cancer cell line MDA-231 stimulates osteoclastogenesis and bone resorption in human osteoclasts. Biochem Biophys Res Commun 2000;270:1097-100.

[29] Escobar-Diaz E, Lopez-Martin EM, Hernandez del Cerro M, Puig-Kroger A, Soto-Cerrato V, Montaner B, et al. AT514, a cyclic depsipeptide from Serratia marcescens, induces apoptosis of B-chronic lymphocytic leukemia cells: interference with the Akt/NF-kappaB survival pathway. Leukemia 2005;19:572-9.

[30] Soto-Cerrato V, Montaner B, Martinell M, Vilaseca M, Giralt E, Perez-Tomas R. Cell cycle arrest and proapoptotic effects of the anticancer cyclodepsipeptide serratamolide (AT514) are independent of p53 status in breast cancer cells. Biochem Pharmacol 2005;71:32-41.

[31] Coleman RE. Management of bone metastases. Oncologist 2000;5:463-70.

[32] Li Y, Upadhyay S, Bhuiyan M, Sarkar FH. Induction of apoptosis in breast cancer cells MDA-MB-231 by genistein. Oncogene 1999;18:3166-72.

[33] Li Y, Sarkar FH. Inhibition of nuclear factor kappaB activation in PC3 cells by genistein is mediated via Akt signaling pathway. Clin Cancer Res 2002;8:2369-77.

[34] Sarkar FH, Li Y. Indole-3-carbinol and prostate cancer. J Nutr 2004;134:3493S-8S.

[35] Kotha A, Sekharam M, Cilenti L, Siddiquee K, Khaled A, Zervos AS, et al. Resveratrol inhibits Src and Stat3 signaling and induces the apoptosis of malignant cells containing activated Stat3 protein. Mol Cancer Ther 2006;5:621-9.

[36] Jin S, Pang RP, Shen JN, Huang G, Wang J, Zhou JG. Grifolin induces apoptosis via inhibition of PI3K/AKT signalling pathway in human osteosarcoma cells. Apoptosis 2007;12:1317-26.

[37] Chang HL, Wu YC, Su JH, Yeh YT, Yuan SS. Protoapigenone, a novel flavonoid, induces apoptosis in human prostate cancer cells through activation of p38 mitogen-activated protein kinase and c-Jun NH2-terminal kinase 1/2. J Pharmacol Exp Ther 2008;325:841-9.

[38] Zhu J, Zhang L, Jin X, Han X, Sun C, Yan J. beta-Ionone-induced apoptosis in human osteosarcoma (U2os) cells occurs via a p53-dependent signaling pathway. Mol Biol Rep 2009.

[39] Lin HI, Lee YJ, Chen BF, Tsai MC, Lu JL, Chou CJ, et al. Involvement of Bcl-2 family, cytochrome c and caspase 3 in induction of apoptosis by beauvericin in human non-small cell lung cancer cells. Cancer Lett 2005;230:248-59.

[40] Frame MC. Src in cancer: deregulation and consequences for cell behaviour. Biochim Biophys Acta 2002;1602:114-30.

[41] Recchia I, Rucci N, Festuccia C, Bologna M, MacKay AR, Migliaccio S, et al. Pyrrolopyrimidine c-Src inhibitors reduce growth, adhesion, motility and invasion of prostate cancer cells in vitro. Eur J Cancer 2003;39:1927-35.

[42] Rucci N, Recchia I, Angelucci A, Alamanou M, Del Fattore A, Fortunati D, et al. Inhibition of protein kinase c-Src reduces the incidence of breast cancer metastases and increases survival in mice: implications for therapy. J Pharmacol Exp Ther 2006;318:161-72.

[43] Recchia I, Rucci N, Funari A, Migliaccio S, Taranta A, Longo M, et al. Reduction of c-Src activity by substituted 5,7-diphenyl-pyrrolo[2,3-d]-pyrimidines induces osteoclast apoptosis in vivo and in vitro. Involvement of ERK1/2 pathway. Bone 2004;34:65-79.

[44] Hiscox S, Nicholson RI. Src inhibitors in breast cancer therapy. Expert Opin Ther Targets 2008;12:757-67.

[45] Morgan L, Nicholson RI, Hiscox S. SRC as a therapeutic target in breast cancer. Endocr Metab Immune Disord Drug Targets 2008;8:273-8.

[46] Rucci N, Susa M, Teti A. Inhibition of protein kinase c-Src as a therapeutic approach for cancer and bone metastases. Anticancer Agents Med Chem 2008;8:342-9.

[47] Abdulghani J, Gu L, Dagvadorj A, Lutz J, Leiby B, Bonuccelli G, et al. Stat3 promotes metastatic progression of prostate cancer. Am J Pathol 2008;172:1717-28.

[48] LoPiccolo J, Granville CA, Gills JJ, Dennis PA. Targeting Akt in cancer therapy. Anticancer Drugs 2007;18:861-74.

[49] Price DT, Della Rocca G, Guo C, Ballo MS, Schwinn DA, Luttrell LM. Activation of extracellular signal-regulated kinase in human prostate cancer. J Urol 1999;162:1537-42.

[50] Bulavin DV, Demidov ON, Saito S, Kauraniemi P, Phillips C, Amundson SA, et al. Amplification of PPM1D in human tumors abrogates p53 tumor-suppressor activity. Nat Genet 2002;31:210-5.

[51] Bulavin DV, Fornace AJ, Jr. p38 MAP kinase's emerging role as a tumor suppressor. Adv Cancer Res 2004;92:95-118.

[52] Cocolakis E, Lemay S, Ali S, Lebrun JJ. The p38 MAPK pathway is required for cell growth inhibition of human breast cancer cells in response to activin. J Biol Chem 2001;276:18430-6.

[53] Lenassi M, Plemenitas A. The role of p38 MAP Kinase in cancer cell apoptosis. Radiol Oncol 2006;40:51-6.

[54] Thornton TM, Rincon M. Non-classical p38 map kinase functions: cell cycle checkpoints and survival. Int J Biol Sci 2009;5:44-51.

[55] Wood CD, Thornton TM, Sabio G, Davis RA, Rincon M. Nuclear localization of p38 MAPK in response to DNA damage. Int J Biol Sci 2009;5:428-37.

[56] Bradham C, McClay DR. p38 MAPK in development and cancer. Cell Cycle 2006;5:824-8.

[57] Kennedy NJ, Cellurale C, Davis RJ. A radical role for p38 MAPK in tumor initiation. Cancer Cell 2007;11:101-3.

[58] Dolado I, Swat A, Ajenjo N, De Vita G, Cuadrado A, Nebreda AR. p38alpha MAP kinase as a sensor of reactive oxygen species in tumorigenesis. Cancer Cell 2007;11:191-205.

[59] Bocca C, Bozzo F, Gabriel L, Miglietta A. Conjugated linoleic acid inhibits Caco-2 cell growth via ERK-MAPK signaling pathway. J Nutr Biochem 2007;18:332-40.

[60] Frey RS, Singletary KW. Genistein activates p38 mitogen-activated protein kinase, inactivates ERK1/ERK2 and decreases Cdc25C expression in immortalized human mammary epithelial cells. J Nutr 2003;133:226-31.

[61] Miglietta A, Bozzo F, Gabriel L, Bocca C, Canuto RA. Extracellular signal-regulated kinase 1/2 and protein phosphatase 2A are involved in the antiproliferative activity of conjugated linoleic acid in MCF-7 cells. Br J Nutr 2006;96:22-7.

[62] Kim YK, Kim HJ, Kwon CH, Kim JH, Woo JS, Jung JS, et al. Role of ERK activation in cisplatin-induced apoptosis in OK renal epithelial cells. J Appl Toxicol 2005;25:374-82.

[63] Jeon ES, Kang YJ, Song HY, Woo JS, Jung JS, Kim YK, et al. Role of MEK-ERK pathway in sphingosylphosphorylcholine-induced cell death in human adipose tissue-derived mesenchymal stem cells. Biochim Biophys Acta 2005;1734:25-33.

[64] Tang D, Wu D, Hirao A, Lahti JM, Liu L, Mazza B, et al. ERK activation mediates cell cycle arrest and apoptosis after DNA damage independently of p53. J Biol Chem 2002;277:12710-7.

[65] Seidman R, Gitelman I, Sagi O, Horwitz SB, Wolfson M. The role of ERK 1/2 and p38 MAP-kinase pathways in taxol-induced apoptosis in human ovarian carcinoma cells. Exp Cell Res 2001;268:84-92.

[66] Dornetshuber R, Heffeter P, Lemmens-Gruber R, Elbling L, Marko D, Micksche M, et al. Oxidative stress and DNA interactions are not involved in Enniatin- and Beauvericin-mediated apoptosis induction. Mol Nutr Food Res 2009;53:1112-22.

[67] Ferrer E, Juan-Garcia A, Font G, Ruiz MJ. Reactive oxygen species induced by beauvericin, patulin and zearalenone in CHO-K1 cells. Toxicol In Vitro 2009.

[68] Klaric MS, Pepeljnjak S, Domijan AM, Petrik J. Lipid peroxidation and glutathione levels in porcine kidney PK15 cells after individual and combined treatment with fumonisin B(1), beauvericin and ochratoxin A. Basic Clin Pharmacol Toxicol 2007;100:157-64.

[69] Jones DH, Nakashima T, Sanchez OH, Kozieradzki I, Komarova SV, Sarosi I, et al. Regulation of cancer cell migration and bone metastasis by RANKL. Nature 2006;440:692-6.

[70] Rahman KM, Li Y, Sarkar FH. Inactivation of akt and NF-kappaB play important roles during indole-3-carbinol-induced apoptosis in breast cancer cells. Nutr Cancer 2004;48:84-94.

[71] Rahman KW, Sarkar FH. Inhibition of nuclear translocation of nuclear factor-{kappa}B contributes to 3,3'-diindolylmethane-induced apoptosis in breast cancer cells. Cancer Res 2005;65:364-71.

[72] Li Y, Ahmed F, Ali S, Philip PA, Kucuk O, Sarkar FH. Inactivation of nuclear factor kappaB by soy isoflavone genistein contributes to increased apoptosis induced by chemotherapeutic agents in human cancer cells. Cancer Res 2005;65:6934-42.

[73] Hiraga T, Williams PJ, Mundy GR, Yoneda T. The bisphosphonate ibandronate promotes apoptosis in MDA-MB-231 human breast cancer cells in bone metastases. Cancer Res 2001;61:4418-24.

[74] Miglietta A, Bozzo F, Bocca C, Gabriel L, Trombetta A, Belotti S, et al. Conjugated linoleic acid induces apoptosis in MDA-MB-231 breast cancer cells through ERK/MAPK signalling and mitochondrial pathway. Cancer Lett 2006;234:149-57.

[75] Berx G, Van Roy F. The E-cadherin/catenin complex: an important gatekeeper in breast cancer tumorigenesis and malignant progression. Breast Cancer Res 2001;3:289-93.

[76] Umbas R, Isaacs WB, Bringuier PP, Schaafsma HE, Karthaus HF, Oosterhof GO, et al. Decreased E-cadherin expression is associated with poor prognosis in patients with prostate cancer. Cancer Res 1994;54:3929-33.

[77] Hecker TP, Gladson CL. Focal adhesion kinase in cancer. Front Biosci 2003;8:s705-14.

[78] Slack JK, Adams RB, Rovin JD, Bissonette EA, Stoker CE, Parsons JT. Alterations in the focal adhesion kinase/Src signal transduction pathway correlate with increased migratory capacity of prostate carcinoma cells. Oncogene 2001;20:1152-63.

4 Summary and conclusion

BEA and ENN are two secondary metabolites produced by several strains of the fungi genus *Fusarium*, *Beauveria*, *Polyporus* and *Paecilomyces* that are known to contaminate food and feed. Both mycotoxins belong to a group of cyclohexadepsipeptides, and exert ionophoric, antibiotic, insecticidal, phytotoxic, anthelminthic and cytotoxic properties. Yet, dextruxins, related cycodepsipeptides, have been shown to inhibit bone resorption without affecting osteoclast differentiation and survival, raising the need of screening BEA and ENN for their antiresorptives effects. Thus, in a first approach, this study aimed to characterize pharmacological and toxicological activities of BEA and ENN on bone cells, namely osteoblasts (OB) and osteoclasts (OC).

we: 1- cocultured murine bone marrow cells with primary calvarial OB to generate OC, 2- assessed OC differentiation and viability using TRAP staining, 3- performed pit analyses of bovine bone slices, and 4- stained the cytoskeleton with phalloidin. BEA and ENN dose-dependently inhibited OC differentiation and bone resorption from bone marrow precursors. At concentrations equal to 1 µM, BEA affected both OC differentiation from bone marrow precursors and bone resorption while ENN affected only OC differentiation from bone marrow precursors, but not bone resorption *per se*. At concentrations equal and lower than 1 µM, BEA and ENN had no effect on OC differentiation from pre-fusion OC. At 1 µM, BEA affected bone resorption from pre-fusion OC, but not OC differentiation while at the same concentration (1 µM), ENN had no effect both in bone resorption and OC differentiation from pre-fusion OC. Cytoskeleton staining of OC treated with BEA or ENN confirmed that BEA, likewise dextruxins, primarily affects bone resorption by disrupting the resorbing organelle (actin ring) of OC and later on due to the reduction of TRAP+ multinucleated cells, while ENN has no effect on the actin ring structure, and therefore affects bone resorption by directly reducing the number of TRAP multinucleated OC.

BEA induced apoptosis in pre-fusion OC with fragmentation and/or condensation of nuclei, but did not affect the viability of mature OC. Interestingly, ENN treated-pre-fusion OC presented no signs of apoptosis, but dose-dependently inhibited OC viability after 12 h. Both mycotoxins, particularly BEA, induced apoptosis and reduced cell viability in the monocyte-macrophage cell line RAW 264.7 compared to OB, suggesting an effect on OC precursors.

BEA and ENN both affected the MAPK and Akt pathways in RAW 264.7- derived OC. However, in coculture-derived OC, BEA acted as a Src activator, promoted a Src-dependent activation of Akt, up-regulated the MAPK pathway independently of Src and down-regulated the NFκB pathway independently of Src. Additionally, ENN that behaves like a Src kinase inhibitor, up-regulated the MAPK pathway independently of MEK and finally down-regulated the NFκB pathway in a MEK-independent manner.

In summary, the 2 mycotoxins BEA and ENN, although structurally related, differentially regulate OC life span. BEA specifically inhibits bone resorption and induces apoptosis in pre-fusion OC by a mechanism probably involving upregulation of ERK1/2 while ENN specifically inhibits OC viability in a Src/Akt dependent manner. Interestingly, the reference MAPK inhibitor PD98059 failed to prevent upregulation of ERK1/2 when applied before ENN and thus, further analyses are necessary to fully characterize the origin of this upregulation of ERK1/2 in ENN treated OC. Both cyclodepsipeptides could therefore be potential candidates for osteoporotic therapies where they could be used alone or in combination.

The skeleton is one of the most common locations in the body to which cancer, particularly from breast, lung and prostate metastasizes. Bone metastases therefore constitute a common cause of morbidity and mortality in cancer patients and to date, the treatment is primary palliative. As bone resorption seems to be the main mechanism in the early phases of bone metastasis, and probably the main mechanism by which osteolysis, particularly from breast and prostate cancer patient progresses, an effect of BEA and ENN on OC is therefore likely to impact on the tumour cell itself in the local bone milieu. However, it was interesting to examine the direct effect of BEA and ENN on tumour cells that have the ability to metastasize to the bone. Therefore, we investigated the pharmacological and toxicological effects of BEA and ENN on 2 highly tumorigenic, hormone-independent cell lines MDA-MB-231 and PC3, and on a non metastatic cell line U2OS with characteristics of primary tumor of bone.

At lower concentrations (0.1 and 1 μM), ENN time dependently (24 to 48 h) and significantly (up to 50 % inhibition after 48 h treatment of PC3 with 1 μM ENN, $p<0.001$ vs. control) inhibited proliferation of metastatic cells (MDA-MB-231 and PC3) as compared to BEA. However, BEA exerted more cell growth inhibitory effect at higher concentration (10 μM) in all 3 cell lines compared to ENN. BEA and ENN similarly affected the metastatic and non metastatic cell viability, as early as 24 h, with a significant effect observed already with 5 μM drug ($p<0.001$ vs. control). Both

inhibitors more potently induced apoptosis after 24 h in metastatic cells as compared to non metastatic, with ENN being more apoptotic as compared to BEA.

We analyzed the signal transduction pathways leading to proliferation, survival, apoptosis and motility. Interestingly, the metastatic profile of the cells did not seem to confer any selective advantage for the effects of our inhibitors at the molecular level. Indeed, while the p38 MAPK pathway remained continuously activated (from 6 to 24 h) in all cell lines, BEA and ENN inactivated ERK in MDA-MB-231 as opposed to its upregulation in PC3 and U2OS. Moreover, BEA was able to induce PARP cleavage in all cell lines, although ENN did so only in PC3 cells. Finally, the cell-cell adhesion molecule E-cadherin, whose loss of expression and/or activity has been implicated in the progression of metastasis, was upregulated in all cell lines following BEA or ENN treatment.

To summarize, BEA and ENN affected cell viability and induced apoptosis more potently in metastatic cells (MDA-MB-231 and PC3) as compared to the non metastatic one (U2OS). Interestingly, the metastatic profile of the cells did not seem to confer any selective advantage for the effects of our inhibitors at the molecular level. While BEA more commonly interfered with the MAPK and the mitochondrial apoptotic pathways in all cell lines, ENN interacted predominantly with the MAPK signaling. These data support the antitumoral effects of BEA and ENN, and their therapeutic potential in the treatment of OC-induced bone loss, bone cancer and skeletal metastases.

5 Bibliography

Akiyama H, Chaboissier MC, Martin JF, Schedl A, de Crombrugghe B 2002 The transcription factor Sox9 has essential roles in successive steps of the chondrocyte differentiation pathway and is required for expression of Sox5 and Sox6. Genes Dev **16**(21)**:**2813-28.

Aubin JE, Bonnelye E 2000 Osteoprotegerin and its ligand: a new paradigm for regulation of osteoclastogenesis and bone resorption. Osteoporos Int **11**(11)**:**905-13.

Audhya TK, Russell DW 1974 Production of enniatins by Fusarium sambucinum: selection of high-yield conditions from liquid surface cultures. J Gen Microbiol **82**(1)**:**181-90.

Bagi CM 2005 Targeting of therapeutic agents to bone to treat metastatic cancer. Adv Drug Deliv Rev **57**(7)**:**995-1010.

Balemans W, Ebeling M, Patel N, Van Hul E, Olson P, Dioszegi M, Lacza C, Wuyts W, Van Den Ende J, Willems P, Paes-Alves AF, Hill S, Bueno M, Ramos FJ, Tacconi P, Dikkers FG, Stratakis C, Lindpaintner K, Vickery B, Foernzler D, Van Hul W 2001 Increased bone density in sclerosteosis is due to the deficiency of a novel secreted protein (SOST). Hum Mol Genet **10**(5)**:**537-43.

Behm C, Degen GH, Follmann W 2009 The Fusarium toxin enniatin B exerts no genotoxic activity, but pronounced cytotoxicity in vitro. Mol Nutr Food Res **53**(4)**:**423-30.

Bernardini M, Carilli A, Pacioni G, Santurbano B 1975 Isolation of beauvericin from *Paecilomyces fumoso-roseus*. Phytochemistry **14:**1865.

Bi W, Deng JM, Zhang Z, Behringer RR, de Crombrugghe B 1999 Sox9 is required for cartilage formation. Nat Genet **22**(1)**:**85-9.

Bialek P, Kern B, Yang X, Schrock M, Sosic D, Hong N, Wu H, Yu K, Ornitz DM, Olson EN, Justice MJ, Karsenty G 2004 A twist code determines the onset of osteoblast differentiation. Dev Cell **6**(3)**:**423-35.

Brennan FM, McInnes IB 2008 Evidence that cytokines play a role in rheumatoid arthritis. J Clin Invest **118**(11)**:**3537-45.

Brunkow ME, Gardner JC, Van Ness J, Paeper BW, Kovacevich BR, Proll S, Skonier JE, Zhao L, Sabo PJ, Fu Y, Alisch RS, Gillett L, Colbert T, Tacconi P, Galas D, Hamersma H, Beighton P, Mulligan J 2001 Bone dysplasia sclerosteosis results from loss of the SOST gene product, a novel cystine knot-containing protein. Am J Hum Genet **68**(3)**:**577-89.

Bruzzaniti A, Baron R 2006 Molecular regulation of osteoclast activity. Rev Endocr Metab Disord **7**(1-2)**:**123-39.

Bussard KM, Gay CV, Mastro AM 2008 The bone microenvironment in metastasis; what is special about bone? Cancer Metastasis Rev **27**(1)**:**41-55.

Calo L, Fornelli F, Ramires R, Nenna S, Tursi A, Caiaffa MF, Macchia L 2004 Cytotoxic effects of the mycotoxin beauvericin to human cell lines of myeloid origin. Pharmacol Res **49**(1)**:**73-7.

Castlebury LA, Sutherland JB, Tanner LA, Henderson AL, Cerniglia CE 1999 Use of a bioassay to evaluate the toxicity of beauvericin to bacteria. World Journal of Microbiology & Biotechnology **15:**119-21.

Christodoulou C, Choy EH 2006 Joint inflammation and cytokine inhibition in rheumatoid arthritis. Clin Exp Med **6**(1)**:**13-9.

Coccia PF, Krivit W, Cervenka J, Clawson C, Kersey JH, Kim TH, Nesbit ME, Ramsay NK, Warkentin PI, Teitelbaum SL, Kahn AJ, Brown DM 1980 Successful bone-marrow transplantation for infantile malignant osteopetrosis. N Engl J Med **302**(13)**:**701-8.

Doel BD, Ridley DD, Singh P 1978 Isolation of cyclodepsipeptides from plant pathogenic fungi. Aust J Chem **31:**1397-9.

Dornetshuber R, Heffeter P, Kamyar MR, Peterbauer T, Berger W, Lemmens-Gruber R 2007 Enniatin exerts p53-dependent cytostatic and p53-independent cytotoxic activities against human cancer cells. Chem Res Toxicol **20**(3)**:**465-73.

Ducy P, Karsenty G 1995 Two distinct osteoblast-specific cis-acting elements control expression of a mouse osteocalcin gene. Mol Cell Biol **15**(4)**:**1858-69.

Ducy P, Zhang R, Geoffroy V, Ridall AL, Karsenty G 1997 Osf2/Cbfa1: a transcriptional activator of osteoblast differentiation. Cell **89**(5)**:**747-54.

Fidler IJ, Poste G 2008 The "seed and soil" hypothesis revisited. Lancet Oncol **9**(8)**:**808.

Firakova S, Proksa B, Sturdikova M 2007 Biosynthesis and biological activity of enniatins. Pharmazie **62**(8)**:**563-8.

Fotso J, Smith JS 2003 Evaluation of Beauvericin Toxicity with the Bacterial Bioluminescence Assay and the Ames Mutagenicity bioassay. JFS **68**(6)**:**1938-41.

Franzoso G, Carlson L, Xing L, Poljak L, Shores EW, Brown KD, Leonardi A, Tran T, Boyce BF, Siebenlist U 1997 Requirement for NF-kappaB in osteoclast and B-cell development. Genes Dev **11**(24)**:**3482-96.

Frattini A, Orchard PJ, Sobacchi C, Giliani S, Abinun M, Mattsson JP, Keeling DJ, Andersson AK, Wallbrandt P, Zecca L, Notarangelo LD, Vezzoni P, Villa A 2000 Defects in TCIRG1 subunit of the vacuolar proton pump are responsible for a subset of human autosomal recessive osteopetrosis. Nat Genet **25**(3)**:**343-6.

Garcia-Moreno C, Catalan MP, Ortiz A, Alvarez L, De la Piedra C 2004 Modulation of survival in osteoblasts from postmenopausal women. Bone **35**(1)**:**170-7.

Gelb BD, Shi GP, Chapman HA, Desnick RJ 1996 Pycnodysostosis, a lysosomal disease caused by cathepsin K deficiency. Science **273**(5279)**:**1236-8.

Girotra M, Rubin MR, Bilezikian JP 2006 Anabolic skeletal therapy for osteoporosis. Arq Bras Endocrinol Metabol **50**(4)**:**745-54.

Goldring SR 2003 Pathogenesis of bone and cartilage destruction in rheumatoid arthritis. Rheumatology (Oxford) **42 Suppl 2:**ii11-6.

Grove JF, Pople M 1980 The insecticidal activity of beauvericin and the enniatin complex. Mycopathologia **70**(2)**:**103-5.

Guadet J, Julien J, Lafay JF, Brygoo Y 1989 Phylogeny of some Fusarium species, as determined by large-subunit rRNA sequence comparison. Mol Biol Evol **6**(3)**:**227-42.

Gupta S, Krasnoff SB, Underwood NL, Renwick JA, Roberts DW 1991 Isolation of beauvericin as an insect toxin from Fusarium semitectum and Fusarium moniliforme var. subglutinans. Mycopathologia **115**(3)**:**185-9.

Hamill RL, Higgens CE, Boaz HE, Gorman M 1969 The structure of beauvericin, a new depsipeptide antibiotic toxic to *Artemia salina*. Tetrahedron Lett **1969:**4255-8.

Han Y, Cowin SC, Schaffler MB, Weinbaum S 2004 Mechanotransduction and strain amplification in osteocyte cell processes. Proc Natl Acad Sci U S A **101**(47)**:**16689-94.

Hartmann C, Tabin CJ 2000 Dual roles of Wnt signaling during chondrogenesis in the chicken limb. Development **127**(14)**:**3141-59.

Hay E, Lemonnier J, Fromigue O, Marie PJ 2001 Bone morphogenetic protein-2 promotes osteoblast apoptosis through a Smad-independent, protein kinase C-dependent signaling pathway. J Biol Chem **276**(31)**:**29028-36.

Hershey CL, Fisher DE 2004 Mitf and Tfe3: members of a b-HLH-ZIP transcription factor family essential for osteoclast development and function. Bone **34**(4)**:**689-96.

Hill TP, Spater D, Taketo MM, Birchmeier W, Hartmann C 2005 Canonical Wnt/beta-catenin signaling prevents osteoblasts from differentiating into chondrocytes. Dev Cell **8**(5)**:**727-38.

Inada M, Yasui T, Nomura S, Miyake S, Deguchi K, Himeno M, Sato M, Yamagiwa H, Kimura T, Yasui N, Ochi T, Endo N, Kitamura Y, Kishimoto T, Komori T 1999 Maturational disturbance of chondrocytes in Cbfa1-deficient mice. Dev Dyn **214**(4)**:**279-90.

Jestoi M, Rokka M, Yli-Mattila T, Parikka P, Rizzo A, Peltonen K 2004 Presence and concentrations of the Fusarium-related mycotoxins beauvericin, enniatins and moniliformin in finnish grain samples. Food Addit Contam **21**(8)**:**794-802.

Johnson RS, Spiegelman BM, Papaioannou V 1992 Pleiotropic effects of a null mutation in the c-fos proto-oncogene. Cell **71**(4)**:**577-86.

Jow GM, Chou CJ, Chen BF, Tsai JH 2004 Beauvericin induces cytotoxic effects in human acute lymphoblastic leukemia cells through cytochrome c release, caspase 3 activation: the causative role of calcium. Cancer Lett **216**(2)**:**165-73.

Kamyar M, Rawnduzi P, Studenik CR, Kouri K, Lemmens-Gruber R 2004 Investigation of the electrophysiological properties of enniatins. Arch Biochem Biophys **429**(2)**:**215-23.

Karsenty G 2001 Minireview: transcriptional control of osteoblast differentiation. Endocrinology **142**(7)**:**2731-3.

Kim N, Kadono Y, Takami M, Lee J, Lee SH, Okada F, Kim JH, Kobayashi T, Odgren PR, Nakano H, Yeh WC, Lee SK, Lorenzo JA, Choi Y 2005 Osteoclast differentiation independent of the TRANCE-RANK-TRAF6 axis. J Exp Med **202**(5)**:**589-95.

Klaric MS, Rumora L, Ljubanovic D, Pepeljnjak S 2008 Cytotoxicity and apoptosis induced by fumonisin B(1), beauvericin and ochratoxin A in porcine kidney PK15 cells: effects of individual and combined treatment. Arch Toxicol **82**(4)**:**247-55.

Kobayashi T, Kronenberg H 2005 Minireview: transcriptional regulation in development of bone. Endocrinology **146**(3)**:**1012-7.

Koga T, Matsui Y, Asagiri M, Kodama T, de Crombrugghe B, Nakashima K, Takayanagi H 2005 NFAT and Osterix cooperatively regulate bone formation. Nat Med **11**(8)**:**880-5.

Kong YY, Feige U, Sarosi I, Bolon B, Tafuri A, Morony S, Capparelli C, Li J, Elliott R, McCabe S, Wong T, Campagnuolo G, Moran E, Bogoch ER, Van G, Nguyen LT, Ohashi PS, Lacey DL, Fish E, Boyle WJ, Penninger JM 1999 Activated T cells regulate bone loss and joint destruction in adjuvant arthritis through osteoprotegerin ligand. Nature **402**(6759)**:**304-9.

Kornak U, Kasper D, Bosl MR, Kaiser E, Schweizer M, Schulz A, Friedrich W, Delling G, Jentsch TJ 2001 Loss of the ClC-7 chloride channel leads to osteopetrosis in mice and man. Cell **104**(2)**:**205-15.

Kornak U, Schulz A, Friedrich W, Uhlhaas S, Kremens B, Voit T, Hasan C, Bode U, Jentsch TJ, Kubisch C 2000 Mutations in the a3 subunit of the vacuolar H(+)-ATPase cause infantile malignant osteopetrosis. Hum Mol Genet **9**(13)**:**2059-63.

Kouri K, Duchen MR, Lemmens-Gruber R 2005 Effects of beauvericin on the metabolic state and ionic homeostasis of ventricular myocytes of the guinea pig. Chem Res Toxicol **18**(11)**:**1661-8.

Kouri K, Lemmens M, Lemmens-Gruber R 2003 Beauvericin-induced channels in ventricular myocytes and liposomes. Biochim Biophys Acta **1609**(2)**:**203-10.

Lam J, Takeshita S, Barker JE, Kanagawa O, Ross FP, Teitelbaum SL 2000 TNF-alpha induces osteoclastogenesis by direct stimulation of macrophages exposed to permissive levels of RANK ligand. J Clin Invest **106**(12)**:**1481-8.

Lemmens-Gruber R, Kamyar MR, Dornetshuber R 2009 Cyclodepsipeptides - potential drugs and lead compounds in the drug development process. Curr Med Chem **16**(9)**:**1122-37.

Liotta LA 2001 An attractive force in metastasis. Nature **410**(6824)**:**24-5.

Liotta LA, Kohn EC 2001 The microenvironment of the tumour-host interface. Nature **411**(6835)**:**375-9.

Logrieco A, Moretti A, Castella G, Kostecki M, Golinski P, Ritieni A, Chelkowski J 1998 Beauvericin production by Fusarium species. Appl Environ Microbiol **64**(8)**:**3084-8.

Logrieco A, Moretti A, Ritieni A, Caiaffa MF, Macchia L 2002a Beauvericin: chemistry biology and significance. In: Upadhyay R e (ed.) Advances in microbial toxin research and its biotechnological exploitation. Kluwer Academic, New York, pp 23-30.

Logrieco A, Rizzo A, Ferracane R, Ritieni A 2002b Occurrence of beauvericin and enniatins in wheat affected by Fusarium avenaceum head blight. Appl Environ Microbiol **68**(1)**:**82-5.

Loots GG, Kneissel M, Keller H, Baptist M, Chang J, Collette NM, Ovcharenko D, Plajzer-Frick I, Rubin EM 2005 Genomic deletion of a long-range bone enhancer misregulates sclerostin in Van Buchem disease. Genome Res **15**(7)**:**928-35.

Macchia L, Di Paola R, Fornelli F, Nenna S, Moretti A, Napoletano R, Logrieco A, Caiaffa MF, Tursi A, Bottalico A 1995 Cytotoxicity of beauvericin to mammalian cells. In: Proceedings of the International Seminar on *Fusarium* Mycotoxin, Taxonomy and Pathogenicity, Martina Franca, Bari, Italy, pp 72-3.

Manelli F, Giustina A 2000 Glucocorticoid-induced osteoporosis. Trends Endocrinol Metab **11**(3)**:**79-85.

Matsuo K, Galson DL, Zhao C, Peng L, Laplace C, Wang KZ, Bachler MA, Amano H, Aburatani H, Ishikawa H, Wagner EF 2004 Nuclear factor of activated T-cells (NFAT) rescues osteoclastogenesis in precursors lacking c-Fos. J Biol Chem **279**(25)**:**26475-80.

Milat F, Ng KW 2009 Is Wnt signalling the final common pathway leading to bone formation? Mol Cell Endocrinol **310**(1-2)**:**52-62.

Miyazaki T, Katagiri H, Kanegae Y, Takayanagi H, Sawada Y, Yamamoto A, Pando MP, Asano T, Verma IM, Oda H, Nakamura K, Tanaka S 2000 Reciprocal role of ERK and NF-kappaB pathways in survival and activation of osteoclasts. J Cell Biol **148**(2)**:**333-42.

Miyazawa K, Shinozaki M, Hara T, Furuya T, Miyazono K 2002 Two major Smad pathways in TGF-beta superfamily signalling. Genes Cells **7**(12)**:**1191-204.

Muller A, Homey B, Soto H, Ge N, Catron D, Buchanan ME, McClanahan T, Murphy E, Yuan W, Wagner SN, Barrera JL, Mohar A, Verastegui E, Zlotnik A 2001 Involvement of chemokine receptors in breast cancer metastasis. Nature **410**(6824)**:**50-6.

Mundy GR 2002 Metastasis to bone: causes, consequences and therapeutic opportunities. Nat Rev Cancer **2**(8)**:**584-93.

Nakashima K, Zhou X, Kunkel G, Zhang Z, Deng JM, Behringer RR, de Crombrugghe B 2002 The novel zinc finger-containing transcription factor osterix is required for osteoblast differentiation and bone formation. Cell **108**(1)**:**17-29.

Ojcius DM, Zychlinsky A, Zheng LM, Young JD 1991 Ionophore-induced apoptosis: role of DNA fragmentation and calcium fluxes. Exp Cell Res **197**(1)**:**43-9.

Ralston SH, Langston AL, Reid IR 2008 Pathogenesis and management of Paget's disease of bone. Lancet **372**(9633)**:**155-63.

Recchia I, Rucci N, Funari A, Migliaccio S, Taranta A, Longo M, Kneissel M, Susa M, Fabbro D, Teti A 2004 Reduction of c-Src activity by substituted 5,7-diphenyl-pyrrolo[2,3-d]-pyrimidines induces osteoclast apoptosis in vivo and in vitro. Involvement of ERK1/2 pathway. Bone **34**(1)**:**65-79.

Roodman GD 2004 Mechanisms of bone metastasis. N Engl J Med **350**(16)**:**1655-64.

Schett G, Hayer S, Zwerina J, Redlich K, Smolen JS 2005 Mechanisms of Disease: the link between RANKL and arthritic bone disease. Nat Clin Pract Rheumatol **1**(1)**:**47-54.

Schlesinger PH, Blair HC, Teitelbaum SL, Edwards JC 1997 Characterization of the osteoclast ruffled border chloride channel and its role in bone resorption. J Biol Chem **272**(30)**:**18636-43.

Scimeca JC, Franchi A, Trojani C, Parrinello H, Grosgeorge J, Robert C, Jaillon O, Poirier C, Gaudray P, Carle GF 2000 The gene encoding the mouse homologue of the human osteoclast-specific 116-kDa V-ATPase subunit bears a deletion in osteosclerotic (oc/oc) mutants. Bone **26**(3)**:**207-13.

Semenov M, Tamai K, He X 2005 SOST is a ligand for LRP5/LRP6 and a Wnt signaling inhibitor. J Biol Chem **280**(29)**:**26770-5.

Simonet WS, Lacey DL, Dunstan CR, Kelley M, Chang MS, Luthy R, Nguyen HQ, Wooden S, Bennett L, Boone T, Shimamoto G, DeRose M, Elliott R, Colombero A, Tan HL, Trail G, Sullivan J, Davy E, Bucay N, Renshaw-Gegg L, Hughes TM, Hill D, Pattison W, Campbell P, Sander S, Van G, Tarpley J, Derby P, Lee R, Boyle WJ 1997 Osteoprotegerin: a novel secreted protein involved in the regulation of bone density. Cell **89**(2)**:**309-19.

Sly WS, Hewett-Emmett D, Whyte MP, Yu YS, Tashian RE 1983 Carbonic anhydrase II deficiency identified as the primary defect in the autosomal recessive

syndrome of osteopetrosis with renal tubular acidosis and cerebral calcification. Proc Natl Acad Sci U S A **80**(9)**:**2752-6.

Smits P, Li P, Mandel J, Zhang Z, Deng JM, Behringer RR, de Crombrugghe B, Lefebvre V 2001 The transcription factors L-Sox5 and Sox6 are essential for cartilage formation. Dev Cell **1**(2)**:**277-90.

St-Jacques B, Hammerschmidt M, McMahon AP 1999 Indian hedgehog signaling regulates proliferation and differentiation of chondrocytes and is essential for bone formation. Genes Dev **13**(16)**:**2072-86.

Stepan JJ, Alenfeld F, Boivin G, Feyen JH, Lakatos P 2003 Mechanisms of action of antiresorptive therapies of postmenopausal osteoporosis. Endocr Regul **37**(4)**:**225-38.

Suda T, Takahashi N, Udagawa N, Jimi E, Gillespie MT, Martin TJ 1999 Modulation of osteoclast differentiation and function by the new members of the tumor necrosis factor receptor and ligand families. Endocr Rev **20**(3)**:**345-57.

Suzuki A, Kanoaka M, Isogai A, Murakoshi S, Ichinoe M, Tamura S 1977 Bassianolide, a new insecticidal cyclodepsipeptide from *Beauveria bassiana* and *Verticillium lecanii*. Tetrahedron Lett **1977:**2167-70.

Takeda S, Bonnamy JP, Owen MJ, Ducy P, Karsenty G 2001 Continuous expression of Cbfa1 in nonhypertrophic chondrocytes uncovers its ability to induce hypertrophic chondrocyte differentiation and partially rescues Cbfa1-deficient mice. Genes Dev **15**(4)**:**467-81.

Tamura Y, Okinaga H, Takami H 2004 Glucocorticoid-induced osteoporosis. Biomed Pharmacother **58**(9)**:**500-4.

Tang CY, Chen YW, Jow GM, Chou CJ, Jeng CJ 2005 Beauvericin activates Ca2+-activated Cl- currents and induces cell deaths in Xenopus oocytes via influx of extracellular Ca2+. Chem Res Toxicol **18**(5)**:**825-33.

Teitelbaum SL 2007 Osteoclasts: what do they do and how do they do it? Am J Pathol **170**(2)**:**427-35.

Tofe AJ, Francis MD, Harvey WJ 1975 Correlation of neoplasms with incidence and localization of skeletal metastases: An analysis of 1,355 diphosphonate bone scans. J Nucl Med **16**(11)**:**986-9.

Tomita A, Kasaoka T, Inui T, Toyoshima M, Nishiyama H, Saiki H, Iguchi H, Nakajima M 2008 Human breast adenocarcinoma (MDA-231) and human lung squamous cell carcinoma (Hara) do not have the ability to cause bone resorption by themselves during the establishment of bone metastasis. Clin Exp Metastasis **25**(4)**:**437-44.

Tomoda H, Huang XH, Cao J, Nishida H, Nagao R, Okuda S, Tanaka H, Omura S, Arai H, Inoue K 1992 Inhibition of acyl-CoA: cholesterol acyltransferase activity by cyclodepsipeptide antibiotics. J Antibiot (Tokyo) **45**(10)**:**1626-32.

Tondravi MM, McKercher SR, Anderson K, Erdmann JM, Quiroz M, Maki R, Teitelbaum SL 1997 Osteopetrosis in mice lacking haematopoietic transcription factor PU.1. Nature **386**(6620)**:**81-4.

Udagawa N, Takahashi N, Akatsu T, Tanaka H, Sasaki T, Nishihara T, Koga T, Martin TJ, Suda T 1990 Origin of osteoclasts: mature monocytes and macrophages are capable of differentiating into osteoclasts under a suitable microenvironment prepared by bone marrow-derived stromal cells. Proc Natl Acad Sci U S A **87**(18)**:**7260-4.

Uhlig S, Torp M, Heier BT 2004 Beauvericin and enniatins A, A1, B and B1 in Norwegian grain: a survey. Food Chemistry **94**(2006)**:**193-201.

Van Antwerp DJ, Martin SJ, Kafri T, Green DR, Verma IM 1996 Suppression of TNF-alpha-induced apoptosis by NF-kappaB. Science **274**(5288)**:**787-9.

Vestergaard P 2005 Anti-resorptive therapy for the prevention of postmenopausal osteoporosis : when should treatment begin? Treat Endocrinol **4**(5)**:**263-77.

Wang ZQ, Ovitt C, Grigoriadis AE, Mohle-Steinlein U, Ruther U, Wagner EF 1992 Bone and haematopoietic defects in mice lacking c-fos. Nature **360**(6406)**:**741-5.

Wei S, Kitaura H, Zhou P, Ross FP, Teitelbaum SL 2005 IL-1 mediates TNF-induced osteoclastogenesis. J Clin Invest **115**(2)**:**282-90.

Westendorf JJ, Kahler RA, Schroeder TM 2004 Wnt signaling in osteoblasts and bone diseases. Gene **341:**19-39.

Woo KM, Kim HM, Ko JS 2002 Macrophage colony-stimulating factor promotes the survival of osteoclast precursors by up-regulating Bcl-X(L). Exp Mol Med **34**(5)**:**340-6.

Xing L, Boyce BF 2005 Regulation of apoptosis in osteoclasts and osteoblastic cells. Biochem Biophys Res Commun **328**(3)**:**709-20.

Xing L, Venegas AM, Chen A, Garrett-Beal L, Boyce BF, Varmus HE, Schwartzberg PL 2001 Genetic evidence for a role for Src family kinases in TNF family receptor signaling and cell survival. Genes Dev **15**(2)**:**241-53.

Yasuda H, Shima N, Nakagawa N, Yamaguchi K, Kinosaki M, Mochizuki S, Tomoyasu A, Yano K, Goto M, Murakami A, Tsuda E, Morinaga T, Higashio K, Udagawa N, Takahashi N, Suda T 1998 Osteoclast differentiation factor is a ligand for osteoprotegerin/osteoclastogenesis-inhibitory factor and is identical to TRANCE/RANKL. Proc Natl Acad Sci U S A **95**(7)**:**3597-602.

Yoneda T, Hiraga T 2005 Crosstalk between cancer cells and bone microenvironment in bone metastasis. Biochem Biophys Res Commun **328**(3)**:**679-87.

Yoshida CA, Yamamoto H, Fujita T, Furuichi T, Ito K, Inoue K, Yamana K, Zanma A, Takada K, Ito Y, Komori T 2004 Runx2 and Runx3 are essential for chondrocyte maturation, and Runx2 regulates limb growth through induction of Indian hedgehog. Genes Dev **18**(8)**:**952-63.

Yoshida H, Hayashi S, Kunisada T, Ogawa M, Nishikawa S, Okamura H, Sudo T, Shultz LD 1990 The murine mutation osteopetrosis is in the coding region of the macrophage colony stimulating factor gene. Nature **345**(6274)**:**442-4.

Zaidi M 2007 Skeletal remodeling in health and disease. Nat Med **13**(7)**:**791-801.

6 Curriculum vitae

Civil Status

Name and first name, Title: TEDJIOTSOP FEUDJIO Flora, MSc.

University of Vienna, Department of Pharmacology and Toxicology

Bone Research Group, Althanstrasse 14, 1090 Vienna, Austria

E. mail: ftedjiotsop@yahoo.com

Born on October 26, 1980 in Yaoundé, Cameroon

Nationality and marital status: Cameroonian, married, one daughter

Academic Profile

2007-2010: Doctoral studies in the Bone Research Group, Department of Pharmacology and Toxicology, University of Vienna, Austria, under the supervision of Univ.-Prof. Dr. Oskar Hoffmann; title of PhD thesis: "Pharmacological and Toxicological Activities of the two Cyclohexadepsipeptide Mycotoxins Beauvericin and Enniatins on Bone Cells and Bone Metastases"

2005: Master's Degree with thesis (**DEA,** Diplôme d'Études Approfondies) in Biochemistry, Faculty of Science, University State of Yaoundé I, Cameroon; title of master thesis: "Variation in Sodium, Potassium, Chloride and pH Levels in Severe Malaria"

2003: Master's degree (**Maîtrise**) in Biochemistry, Faculty of Science, University State of Yaoundé I, Cameroon

2001: Bachelor's Degree in Biochemistry, Faculty of Science, University State of Yaoundé I, Cameroon

1998: High school degree in "Mathematics and Natural Science", serie "D" and registration in first year Biochemistry at the University of Yaoundé I, Cameroon, Department of Biochemistry

Training and courses attended

2010: Annual seminar on the topic "Global Working Environment", 7^{th} – 10^{th} April, Hotel Europa Salzburg, Austria

2004: Training course at the "Gynaeco-Obstetric and Paediatric Hospital, Ngousso-Yaoundé - Cameroon, Topic: "Control of severe malaria in children of 0-5 years old", July – August 2004

Languages

French, mother tongue

English, very good

German, average

Computer knowledge

1) Ms-Word, 2) Ms-Excel, 3) Ms-PowerPoint, 4) SPSS for windows Version 11, 6) Prism version 5, 7) Endnote X1 Bld 2377, 8) Cell * F, 9) FreeHand MX version 10.4.9, 10) Photoshop version 7.0

Award

2007: Winner of the North-South Dialogue Scholarship Program for doctoral studies in Vienna, Austria

Published abstracts of congress contributions

F. Tedjiotsop Feudjio, R. Lemmens-Gruber, O. Hoffmann. The fungal secondary metabolites beauvericin and enniatin differentially regulate osteoclast inhibition during differentiation and bone resorption. 36th European Symposium on Calcified Tissues, Vienna, Bone, Volume 44, Supplement 2, June 2009, Page S327.

Publications

F. Tedjiotsop Feudjio, S. Forsdahl, J. Nguemo Djiometio, R. Lemmens-Gruber, O. Hoffmann. Structurally related cyclodepsipeptides beauvericin and enniatins differentially regulate bone resorption and osteoclast survival (Manuscript submitted).

F. Tedjiotsop Feudjio, R. Lemmens-Gruber, O. Hoffmann. Beauvericin and enniatins inhibit proliferation and induce apoptosis in metastatic and non metastatic carcinomas: Involvement of the MAPK signaling (Manuscript submitted).